

LOWER BOUND SOLUTIONS OF SOME STABILITY PROBLEMS IN GEOTECHNICAL ENGINEERING

*A Thesis Submitted
in Partial Fulfilment of the Requirements
for the Degree of
DOCTOR OF PHILOSOPHY*

By
DEVENDRA NARAIN SINGH

to the
DEPARTMENT OF CIVIL ENGINEERING
INDIAN INSTITUTE OF TECHNOLOGY KANPUR
NOVEMBER, 1992

पुराणमित्येव न साधु सर्वम्
न चापि कान्यम् नवमित्यवद्यम् ।
सन्तः परिक्षयान्यतरद्भजन्ते
मूढः परप्रत्यनेयबुद्धिः ॥
॥ कालिदासः मालविकार्णिनमित्र १,२ ॥

Just because it is old, it need not be good
nor a composition, because it is new, need be faulty
Accomplished persons select one of the two after proper examination
ignorant goes by the opinion of others

20 OCT 1992 CE

116561

CE-1992-D

26/11/92

CERTIFICATE

It is certified that the work contained in the thesis entitled LOWER BOUND SOLUTIONS OF SOME STABILITY PROBLEMS IN GEOTECHNICAL ENGINEERING by DEVENDRA NARAIN SINGH, has been carried out under my supervision and that this work has not been submitted elsewhere for a degree

P Basudhar

P K Basudhar
Professor
Dept of Civil Engineering
Indian Institute of Technology
Kanpur-208016, INDIA

November, 1992

ACKNOWLEDGEMENTS

It gives me immense pleasure to express my deep gratitude to Professor P K Basudhar for suggesting the present problem, giving constant guidance and attention at the various stages of this thesis. It is only through his critical comments and valuable suggestions that I could improve upon the various shortcomings associated with the present work. It was a nice experience to work under his guidance.

I express my indebtedness to my teachers for the help and continuous support they provided me during my stay in the Institute.

It gives me immense pleasure to express my sincere thanks for the help rendered by my friends and the laboratory staff as and when I approached them for the various purposes.

D N SINGH

SYNOPSIS

Devendra Narain Singh
Department of Civil Engineering
Indian Institute of Technology, Kanpur
India

LOWER BOUND SOLUTIONS OF SOME STABILITY PROBLEMS IN GEOTECHNICAL ENGINEERING

The thesis pertains to the application of modified Lysmer's approach (Lysmer-Basudhar) in determining the optimal lower bound solutions of some plane strain stability problems in geotechnical engineering. The soil mass under consideration is discretized into finite number of triangular elements. All nodal points, elements and element sides are then numbered in some arbitrary order. The material properties are specified for these elements. This is followed by choosing a linear stress field ensuring the element equilibrium. Interface equilibrium is satisfied by matching the normal and shear stresses at the element interfaces. This leads to a set of linear equality constraints. The boundary conditions also yield a set of linear equality constraints. The no-yield Mohr-Coulomb condition is incorporated directly in the analysis. In general, as many stress fields will satisfy the condition of static admissibility, the isolation of the stress field which optimizes the objective function is important. The problem is one of constrained nonlinear programming. The constrained optimization problem is converted to an unconstrained one using the extended penalty function method. Sequential Unconstrained Minimization of the composite function so developed is carried out using Powell's method along with quadratic interpolation technique for multidimensional and unidirectional search respectively. The

following problems have been studied considering the soil mass to be homogeneous and isotropic

- 1) Bearing capacity of both smooth and rough surface and embedded strip footings
- 2) Bearing capacity of smooth surface and embedded footings located above continuous voids
- 3) Pull out capacity of horizontal, vertical and inclined plate anchors embedded in sands
- 4) Stability of reinforced soil slopes and retaining walls
- 5) Stability of a vertical cut
- 6) Undrained stability of a trapdoor

Based on the study following generalized conclusions are drawn

- 1) Modified Lysmer approach using discrete element and nonlinear programming has been found to be successful in predicting the lower bound solutions of various stability problems considered
- 2) The mesh patterns have significant influence over the obtained optimal solutions. The suggested generalized mesh patterns pertinent to each problem can be used
- 3) Comparison of the obtained solutions with the available theoretical and experimental results shows a good agreement
- 4) Sequential unconstrained minimization of the composite function using Powell's technique for multivariable search and quadratic interpolation for unidirectional search is found to be efficient in isolating the optimal solutions
- 5) The approach is found to be very efficient in terms of economy of computations and takes only few seconds of CPU time to obtain a feasible solution

CONTENTS

	Page
LIST OF FIGURES	x
LIST OF TABLES	xii
NOTATIONS	xv
CHAPTER 1 INTRODUCTION	1
1 1 General	1
1 2 Review of Literature	2
1 3 Motivation and Scope of the Thesis	26
CHAPTER 2 GENERAL METHOD OF ANALYSIS	31
CHAPTER 3 CHOOSING A METHOD	40
3 1 General	40
3 2 Statement of the Problem	41
3 3 Boundary Conditions and the Objective function	42
3 4 Results and Discussions	42
3 5 Conclusions	47
CHAPTER 4 BEARING CAPACITY OF SURFACE AND EMBEDDED STRIP FOOTINGS	48
4 1 General	48
4 2 Surface Footings	49
4 2.1 Statement of the Problem	49
4 2 2 Boundary Conditions and the Objective function	49
4 2 3 Results and Discussions	50
4.3 Embedded Footings	58
4 3 1 Statement of the Problem	58
4 3 2 Boundary Conditions and the Objective function	60
4 3 3 Results and Discussions	60
4 4 Conclusions	66

CHAPTER 5	BEARING CAPACITY OF SURFACE AND EMBEDDED	
	FOOTINGS LOCATED ABOVE CONTINUOUS Voids	67
5 1	General	67
5 2	Statement of the Problem	67
5 3	Boundary Conditions and the Objective functions	70
5 3 1	Embedded Footings	70
5 3 2	Surface Footing	71
5 4	Results and Discussions	71
5 5	Conclusions	75
CHAPTER 6	PULL OUT CAPACITY OF STRIP ANCHORS IN SAND	76
6 1	General	76
6 2	Statement of the Problem	78
6 3	Boundary Conditions and the Objective functions	78
6 3 1	Horizontal Anchors	78
6 3 2	Vertical Anchors	79
6 3 3	Inclined Anchors	79
6.4	Results and Discussions	79
6 4 1	Horizontal Anchors	80
6 4 2	Vertical Anchors	87
6 4 3	Inclined Anchors	91
6 5	Conclusions	94
CHAPTER 7	BEARING CAPACITY OF REINFORCED SOIL	
	STRUCTURES	96
7 1	General	96
7 2	Statement of the Problem	97
7 3	Assumptions	98
7 4	Boundary Conditions and the Objective functions	99
7 4 1	Reinforced Cohesionless soil Retaining Wall	101
7 4 2	Reinforced Cohesive soil Slope	101
7 5	Results and Discussions	102
7 5 1	Reinforced Cohesionless soil Retaining Wall	102
7 5 2	Reinforced Cohesive soil Slope	108
7 6	Conclusions	111

CHAPTER 8	STABILITY OF VERTICAL CUTS IN HOMOGENEOUS SOILS	
		112
8 1	General	112
8 2	Statement of the Problem	112
8 3	Boundary Conditions and the Objective function	113
8 4	Results and Discussions	113
8 5	Conclusions	118
CHAPTER 9	STABILITY OF A TRAPDOOR IN COHESIVE SOILS	
		119
9 1	General	119
9 2	Statement of the Problem	119
9 3	Boundary Conditions and the Objective function	119
9 4	Results and Discussions	121
9 5	Conclusions	125
CHAPTER 10	GENERALIZED CONCLUSIONS AND SCOPE FOR FUTURE STUDIES	
10 1	Conclusions	127
10 2	Scope for Future Studies	128
REFERENCES		129
LIST OF PUBLICATIONS		137

LIST OF FIGURES

Figure		Page
2 1	Discretization of the soil mass for a typical problem	31
2 2	Definition sketch and body forces for nth element	31
2 3	Internal stresses at point i	32
2 4	Continuity of nodal stresses	34
3 1	Mesh pattern for earth pressure problem	41
3 2(a)	Variation of objective function with number of function evaluations	42
3 2(b)	Variation of objective function with penalty parameter	43
4 1	Mesh pattern for a surface strip footing	49
4 2(a)	Variation of objective function with penalty parameter for the rough surface footing	55
4 2(b)	Variation of objective function with number of function evaluations for the rough surface footing	55
4 3	Contours of stress-strength ratio	58
4 4	Mesh patterns for the embedded strip footing	59
4 5(a)	Variation of objective function with penalty parameter for mesh pattern E	66
4 5(b)	Variation of objective function with number of function evaluations for mesh pattern E	66
5 1	Details of a strip footing and a continuous void	68
5 2	Mesh patterns for the strip footing corresponding to the various locations of the void	69
5 3(a)	Variation of objective function with penalty parameter for Case A	74
5 3(b)	Variation of objective function with number of function evaluations for Case A	74
6 1(a)	Mesh pattern for shallow horizontal anchors	77
6 1(b)	Mesh pattern for deep horizontal anchors	77
6 2(a)	Mesh pattern for shallow vertical anchors	77
6 2(b)	Mesh pattern for deep vertical anchors	77
6 3	Mesh pattern for an anchor inclined at 45^0	78
6 4(a)	Variation of objective function with penalty parameter for smooth horizontal anchor ($H/B=L/B=5$)	82

6 4(b)	Variation of objective function with number of function evaluations for smooth horizontal anchor (H/B=L/B=5)	82
6 5	Breakout factor vs embedment ratio relationship for horizontal anchors(L/B=5)	83
6 6	Breakout factor vs Embedment ratio relationship for horizontal anchors(L/B=8 75)	83
6 7	Comparison of the obtained results with the results reported in the literature for horizontal anchors	84
6 8	Breakout factor vs embedment ratio relationship for vertical anchors(L/B=5)	87
6 9(a)	Variation of objective function with penalty parameter for vertical anchors	89
6 9(b)	Variation of objective function with number of function evaluations for vertical anchors	89
6 10(a)	Variation of objective function with penalty parameter for inclined anchor ($\alpha=45^0$)	94
6 10(b)	Variation of objective function with number of function evaluations for inclined anchor ($\alpha=45^0$)	94
7 1	Reinforced soil retaining wall	98
7 2	Reinforced soil slope	98
7 3(a)	Mesh pattern for the reinforced retaining wall with $a \neq b$	100
7 3(b)	Mesh pattern for the reinforced retaining wall with $a=b$	100
7 3(c)	Mesh pattern for the reinforced retaining wall extended beyond the footing for $a \neq b$	100
7 4(a)	Mesh pattern for the reinforced soil slope with $\beta=90^0$	101
7 4(b)	Mesh pattern for the reinforced retaining wall with $\beta=80^0$	101
7 5(a)	Variation of objective function with penalty Parameter for the reinforced retaining wall (Case C, weightless soil)	106
7 5(b)	Variation of objective function with number of function evaluations for the reinforced retaining wall (Case C, weightless soil)	106
7 6(a)	Variation of objective function with penalty parameter for the reinforced soil slope($\beta=90^0$)	109
7 6(b)	Variation of objective function with number of function evaluations reinforced soil slope($\beta=90^0$)	109
8 1	Mesh pattern for the vertical cut	113
8 2	Different zones for the vertical cut	116

8 3(a)	Variation of objective function with penalty parameter for a vertical cut ($\phi=0$)	117
8.3(b)	Variation of objective function with number of function evaluations for a vertical cut ($\phi=0$)	117
9 1(a)	Mesh pattern for a shallow trapdoor	120
9 1(b)	Mesh pattern for a deep trapdoor	120
9 2(a)	Variation of objective function with penalty parameter for a trapdoor ($H/B=2.5$)	125
9 2(b)	Variation of objective function with number of function evaluations for a trapdoor ($H/B=2.5$)	125

LIST OF TABLES

Table	Page
3.1(a) $(\sigma_z / \gamma H)$ values for the retaining wall	44
3.1(b) $(\sigma_x / \gamma H)$ values for the retaining wall	45
3.1(c) $(\tau_{zx} / \gamma H)$ values for the retaining wall	46
4.1 Bearing capacity factors for smooth surface footings	51
4.2 Bearing capacity factors for rough ($\delta=\phi$) surface footings	52
4.3 Initial design vector, sigma vector and constraints for rough surface footing ($G=1.0, \phi=30^\circ$)	53
4.4 Final design vector, sigma vector and constraints and objective function value for rough surface footing	54
4.5 Stress field and the stress-strength ratios at the nodal points for rough surface footing ($G=1.0, \phi=30^\circ$)	57
4.6 Effect of mesh pattern on the bearing capacity	61
4.7 Stress field and the stress-strength ratios at the nodal points for mesh pattern A	62
4.8 Stress field and the stress-strength ratios at the nodal points for mesh pattern C	62
4.9 Stress field and the stress-strength ratios at the nodal points for mesh pattern E	64
4.10 Bearing capacity factors for rough embedded footings	64
5.1 Material properties of foundation soils	68
5.2 Comparison of the bearing capacity solutions	72
5.3 Stress field and the stress-strength ratios at the nodal points for Case A ($T/B=2$)	73
5.4 Optimization details for the various cases studied	74
6.1 Present solution and its percentage differences from the results reported in the literature (for smooth horizontal anchors)	81
6.2 Stress field for smooth horizontal anchor ($H/B=L/B=5$)	82
6.3 Effect of roughness on the breakout factors for horizontal anchors	85
6.4 Final design vector, constraints and optimal function value for a smooth horizontal anchor ($H/B=L/B=5$)	86
6.5 Percentage differences of the present solutions from experimental and theoretical results for vertical anchors ($L/B=5$)	88

6 6	Stress field for smooth vertical anchor (H/B =2, L/B =5, ϕ =32°)	88
6 7	Final design vector,constraints and optimal function value for vertical anchor(H/B=2,L/B=5, ϕ =32°)	90
6 8	Comparative study of breakout factors and effect of roughness for vertical anchors (L/B=8, ϕ =32°)	90
6 9	Comparison of the present solution with the reported values	92
6 10	Stress field and stress-strength ratios at the nodal points for smooth anchor inclined at 45°	93
6 11	Final design vector,constraints and optimal objective function value for a smooth anchor inclined at 45°	93
7 1	Various cases considered for the present study	102
7 2	Comparison of present solutions with other experimental and theoretical results (weightless soil)	103
7 3	Comparison of the present solutions with other theoretical results (weighty soil)	104
7 4	Stress field and stress-strength ratios at the nodal points for Case C (weightless soil)	107
7 5	Final design vector,constraints and optimal objective function value for Case C (weightless soil)	107
7 6	Comparison of the present study with the reported values	108
7 7	Stress field and stress-strength ratios at the nodal points for 80° slope	110
7 8	Final design vector,constraints and optimal objective function value for 80° slope	110
8 1	Stress field and the stress-strength ratios at the nodal points for a vertical cut	114
8.2	Design vector, sigma vector, constraints and objective function value at the optimum for a vertical cut	115
8.3	Comparison of stress-strength ratios for different nodal points	117
9 1	Stability numbers for a trapdoor	121
9 2	Comparison of obtained stability numbers with the reported values	122
9 3	Final design and sigma vectors, constraints and optimal objective function values for trapdoor(H/B=2.5)	124

NOTATIONS

a_j	= Coefficient to σ_j in linear function to be optimized
$a_{i,j}$	= Coefficient to σ_j in linear constraint number i
$[A]$	= Coefficient matrix of the linear equality constraints
α	= Angle of inclination of the inclined anchor
$b_i, \{b\}$	= Coefficients
$[B]$	= 9×7 matrix, geometrical property of the element
β	= Angle of inclination of the slope
C_u	= Undrained cohesive strength of the soil
C	= Cohesion of the soil
$\{D\}$	= Design vector
D_m	= Optimum design vector
δ	= Angle of the surface friction
δ_t	= Transition term between two types of Penalty term
$F(D)$	= Objective function
$[G]$	= 9×7 matrix, geometrical property of the element
$\{g\}$	= 9 Component vector, related to body forces in n th element
g_j	= Inequality constraints
$\{h\}$	= 9 Component vector related to body forces in n th element
M	= Total number of inequality constraints
m, n	= Element numbers
r_k	= Penalty parameter
$[S]$	= 7×9 matrix, geometrical property of n th element
$\{\bar{s}_i\}$	= 3 Component internal stress vector at node i of element n
$\{s\}$	= 9 Component stress vector which defines internal stresses in n th element
$[T]$	= 6×9 matrix, geometrical property of n th element
x_i	= x Coordinate of nodal point i
z_j	= z Coordinate of nodal point j
γ_x, γ_z	= Body forces per unit volume in x and z directions
γ	= Density of the sand
θ_{ij}	= Slope of element side connecting nodal points i and j
μ, ζ, ε	= Known coefficients
$\sigma_{x,i}$	= Normal stress on vertical plane through nodal point i
$\sigma_{z,i}$	= Normal stress on horizontal plane through nodal point i
σ^n	= Normal stress at nodal point i on plane parallel to element side jk of element n

σ_{ij}^n = Normal stress at point i of element n on side ij
 $\{\sigma\}$ = Stress vector which defines the complete stress state
 $\{\sigma\}^n$ = 7 Component stress vector which defines external normal stress on n th element
 $\tau_{zx,i}$ = Shear stress on horizontal plane nodal point i
 τ_{ij} = Shear stress at node i on the side connecting points i and j
 $\{\tau\}^n$ = 6 Component stress vector which defines the external shear stresses on n th element
 ϕ = Angle of internal friction
 ϕ_{cv} = Angle of internal friction at constant volume

CHAPTER 1

INTRODUCTION

1.1 General

With the work of Drucker et al (1952) proving the validity of limit theorems to soils, lot of interest has been generated in applying the theory of plasticity to many problems of stability in soil mass. For the materials with an associated flow rule useful limit theorems (upper bound and lower bound) can be applied to approximate the critical load, even if it can not be determined exactly.

Many analytical and numerical studies have been carried out to find the upper bound solutions for bearing capacity, stability of slopes and earth pressure problems. But less attention has been paid to the lower bound solutions. It is due to the fact that it is considerably easier to construct a good kinematically admissible collapse mechanism than to construct a good statically admissible stress field. An upper bound is often a good estimate of the collapse load but a lower bound is more important as it results in a safe design. The construction of statically admissible stress field is a formidable task and except in few cases, it has not been possible to construct stress field for gravity loaded soil problems. Most often it is possible to build stress fields with one or two discontinuities and the lower bound falls short of the true value by a large amount.

As such, a great need had been felt to develop general methods by which critical loads could be obtained by either of the limit theorems. Since mid nineteen hundred and sixties determination of the upper bound collapse load by finite elements using appropriate constitutive relations has been developed with great

success. Efforts were also made to develop methods based on finite difference and linear programming to find the lower bound solutions. Later on in the beginning of nineteen hundred and seventies more generalized approaches combining the flexibility of the finite element method with the elegance of optimization techniques for isolating the optimal solution were developed. Subsequently, efforts were made to improve the computational efficiencies of these methods by using more and more sophisticated optimization algorithms in isolating the optimal stress field. These efforts are still being continued.

Till now the area of application of these methods has been limited only to the bearing capacity problems dealing with surface footings, earth pressures on retaining walls and stability of trapdoor problems. In the following section a brief literature review is presented to study the scope of extending these general methods to new problems in geotechnical engineering.

1.2 Review of Literature

Limit equilibrium methods (Chen, 1975), method of characteristics (Sokolovskı, 1965), finite elements method (Zienkiewicz, 1977) and limit analysis (Chen, 1968, 1975, Chen and Baladı, 1985) are the methods of analysis currently used to analyze the stability of soil mass and soil structures. Since it has been broadly decided to restrict the attention of the present study to determine limit loads, the literature concerning with the application of limit theorems to obtain the critical loads in geotechnical engineering has only been reviewed here. The review is concerned mainly with the techniques used by the earlier researchers and excludes the considerable amount of work on the various aspects of the problems.

under discussion

Coulomb first published his classic work on lateral earth pressures in 1776 but the foundations for an acceptable theory of plasticity were laid only after Tresca, Saint-Venant and Levy reported their works about a century later (Salencon, 1977) After another half a century von Karman, Harr, von Mises and Prandtl developed the theory into a useful tool The theoretical foundations of limit analysis were underlain by Drucker, Greenberg and Prager (1952) They demonstrated the application of limit theorems to a more general class of ideal materials including, in soil mechanics terms, a cohesive - frictional material (C- ϕ material) They also extended the Coulomb criterion to three-Dimensional soil problems

Drucker and Prager (1952) extended the study of Drucker et al (1952) for perfectly plastic materials which obey Mohr-Coulomb yield criterion to granular materials The theory and the limit theorems presented by them make it possible to establish definite upper and lower bounds for the ultimate load for a soil mass Drucker (1953) extended this work to asses the implications of assuming soil to be a perfectly plastic body and studied the stability of unbraced vertical cuts for a cohesive-frictional soil unable to take tension He has applied limit theorems to obtain the bearing capacity of slopes in inhomogeneous soils too He has concluded that although the results obtained are correct for the material postulated but may have no relevance to any actual material

Koopman and Lance (1965) have introduced a method of limit analysis whereby a continuous perfectly plastic material is

replaced by a discrete mathematical model. The stress analysis problem is then interpreted as a linear programming problem. They have obtained lower bound loads for a square plate, both clamped and simply supported at the edge, under uniform hydrostatic pressure. The method is general enough to be extended to the stability problems in geotechnical engineering.

Finn (1967) showed that for a slope to fail by rotational slip, the kinematically possible slip surface will be a logarithmic spiral and only when angle of internal friction of the soil is zero, the circular slip surface is kinematically possible.

Hayes and Marcal (1967) have developed a general finite element method for determining the upper bounds on the limit load for perfectly plastic plane stress problems, they have constructed a kinematically admissible velocity field and then obtained the optimum value by minimizing the associated load multiplier. The obtained results are in good agreement with those predicted by elasto-plastic finite element analysis. The method is having a good potential to be applied in analyzing stability problems in geotechnical engineering.

Davis (1968) has critically discussed the discrepancy between the plastic deformation properties of the ideal and real materials. He has obtained the lower and upper bound solutions in plain strain condition for materials with associated flow rules for ultimate bearing capacity of strip footings on purely cohesive soils, passive failure of cohesive-frictional soils and pressure on tunnel roofs overlain by clay by using discontinuous stress and velocity fields. The case of materials with non-associated flow rule has also been studied by taking a particular problem of

unconfined compression between rough end plates and it has been found that the use of limit theorems for such a material is not justified

Graham (1968) has extended the work of Sokolovski (1960) to predict an improved numerical solution for sands with self weight over finite sections of a plastic failure zone. The theory has been applied to study the failure of retaining walls, slopes and deep strip footings in non-homogeneous soils. Solutions obtained compare well with the existing theories and test results.

Chen (1969) has presented an excellent review of the application of the upper bound theorem to stability problems in geotechnical engineering.

Chen et al (1969) have used the upper bound theorem to obtain the complete numerical solutions for the critical height of an embankment by assuming a rotational discontinuity mechanism (log spiral). The results have been presented in the form of charts and are compared with the limit equilibrium solutions. A good agreement is reported.

Belytschko and Hodge (1970) have presented an interesting general approach for finding the lower bound on the limit load for plane stress problem. In this case, the finite element technique is used to construct a parametric family of stress field by representing the stress distribution in each element by a fourth order Airy stress function. Determination of the best lower bound then becomes a problem of mathematical programming which involves the maximization of the load multiplier subjected to the constraints that the yield condition is satisfied. Lower bounds are obtained for a number of weakened slabs and compared with the

upper bounds obtained by previously available methods. The bounds are in good agreement although a limited number of elements are used. The results are useful in checking the accuracy of finite element techniques for complete elasto-plastic solutions. The method is also of interest to the geotechnical engineers due to its potential to be extended in solving stability problems.

Chen and Scawthorn (1970) have presented a critical discussion for the significance of limit equilibrium and limit analysis solutions based on which it has been shown that the limit analysis approach is rigorous, competitive with limit equilibrium and is much simpler. They have investigated the earth pressure problem and bearing capacity of strip footings using the classical Coulomb plane failure mechanism and simple discontinuous stress field and have concluded that the assumption of perfect plasticity is sufficiently good for analyzing stability problems in soil mechanics.

Lysmer (1970) presented a generalized technique for the lower bound limit analysis of bearing capacity of surface strip footings and passive earth pressure on retaining walls. It was based on a simple three noded triangular element in which the stress distribution was assumed to be linear. By linearizing the no-yield Mohr-Coulomb criterion he formulated the problem as a linear programming one to isolate the optimal lower bound. The potential of the technique is yet to be fully utilized.

Assuming soil to be a perfectly plastic material obeying Coulomb's yield criterion with an associated flow rule, Chen and Giger (1971) have shown that the upper bound theorem of limit analysis may be applied to predict the critical height of embankments. They have compared the results with the existing limit

equilibrium solutions and have found a good agreement. Based on the study they have concluded that in many stability problems it is much more convenient to use upper bound method as it places the matter of slope stability analysis on a much more logical ground.

Anderheggen and Knopfel (1972) developed a numerical methods for the determination of the ultimate load of two and three-dimensional structures in general assuming an ideal rigid plastic material behavior. Determination of the ultimate load has been mathematically formulated as a problem of finding the maximum or minimum of a linear function whose independent variables are subjected to inequality constraints. The finite element analysis has been used to obtain the stress and displacement fields. They have assumed that the variation of the stress and displacement function within the triangular elements is either constant or linear. Numerical results for two plate bending models are presented and some possible plate-stretching models are described and discussed. A linear yield criterion is used. The work may be extended to the geotechnical engineering problems.

Booker and Davis (1972) have obtained plasticity solutions for an infinite slope in a purely cohesive soil whose cohesive strength increases linearly with depth using the method of characteristics. This strength corresponds to the undrained stability ($\phi_u = 0$) of normally consolidated soils. They have extended the work to study finite slopes and the results have been compared with the slip circle analysis. They have observed that the slip circle analysis gives a value of density to cause failure greater by 50% when the slope angle tends to zero than the plasticity solution, which with increasing slope angle decreases.

to less than 10% for the slopes steeper than 5^0

Sabzevari and Ghahramani (1972) have used the method of characteristics to derive the recurrence formulae and consequently the slip line field for non-homogeneous soil medium satisfying nonlinear yield criterion. This has been applied to the problems of bearing capacity and earth pressure. The obtained results have been compared with those predicted by the conventional theories of homogeneous soils. A significant difference between the two results indicates the inaccuracy of the conventional limit equilibrium approach of solving the bearing capacity and earth pressure problems in non-homogeneous soils with non-linear failure criterion.

Heyman (1973) has developed statically admissible stress fields for a vertical cut in a purely cohesive soil able to take tension. The problem is a plane strain one and the maximum shear stress criterion of failure has been assumed. He has given a lower bound of $2.83C/\gamma$ for the whole stress field along with a partial solution for $3.2C/\gamma$.

Chen and Davidson (1973) have reported the upper bound of limit loads for both surface and embedded footings with smooth and rough bases. The soil has been treated as a perfectly plastic material with the associated flow rule after Drucker. The upper bound solutions for smooth, surface footings are shown to compare well with the slip line solutions. Meyerhof's solutions (1951) and the upper bound solutions for rough sub surface footings are shown to agree reasonably well.

Davis and Booker (1973) have obtained the upper bound bearing capacity solutions for smooth and rough rigid strip footings

resting over a clay deposit which is inhomogeneous in the vertical direction only. They have shown that the rate of increase of undrained shear strength with depth plays the same role as density plays in the bearing capacity of homogeneous cohesive-frictional soils. The bearing capacity of rigid strip footings is shown to depend on the breadth and to a small extent on the roughness of the underside of the footings. A comparison with the slip circle solution has also been done and it has been reported that slip circle solutions overestimates the critical load when inhomogeneity dominates.

Chen and Rosenfarb (1973) have obtained the upper bound active and passive earth pressure solutions for a rigid retaining wall of varying roughness. The soil has been treated as a perfectly plastic cohesionless material obeying Mohr-Coulomb yield criterion. They have studied several failure mechanisms composed of rigid bodies and radial shearing zones. The obtained results compare well with those obtained by using slip line method. It is noticed that the values of passive pressures on rough walls have considerably improved.

Based on the upper bound limit analysis Purushothamaraj et al (1974) have developed a method to obtain bearing capacity of strip footings on two layered soils with varying cohesion, angle of internal friction and the unit weight. They have considered the failure mechanism similar to the Prandtl-Terzaghi but with different wedge angle. They have obtained the critical wedge angles and have presented the charts for the combination of the ratios of cohesion of the two layers, embedment ratio, friction angle and unit weight of soils.

Chen (1975) has presented stability factors for isotropic and homogeneous as well as anisotropic non-homogeneous slopes based on upper bound limit analysis approach for predicting the critical heights of slopes. He has also developed a closed form solution for determining passive earth pressure by using the theory of plasticity.

Giger and Krizek (1975) have determined the critical height of a vertical cut with a varying corner angle by using upper bound theorem of plasticity. A three dimensional collapse mechanism has been assumed. Results are presented graphically and the physical meaning and general implications of these results have been discussed. For a special case when corner angle of the cut is 180^0 , results are compared with those determined by limit analysis based on the conventional two dimensional plane strain solutions and are found to be identical.

Basudhar (1976) and Basudhar et al (1979, 1981) modified Lysmer's approach (1970) and incorporated the nonlinear no yield condition constraints directly in the analysis and obtained the lower bound solutions for bearing capacity and retaining wall problems. The constrained optimization problem is converted to an unconstrained one using the extended penalty function method as mentioned by Kavlie and Moe (1971) and Sequential Unconstrained Minimization of the composite function was carried out by using Powell's method along with quadratic interpolation technique for multidimensional and unidirectional search respectively (Fox, 1971 and Rao, 1984). The results so obtained are compared with that of Lysmer (1970) and are found to be in excellent agreement.

Rowe and Davis (1977) have shown the application of elasto-

plastic finite element method in predicting the collapse loads for a rigid footing resting on a deep homogeneous soil layer, and a rigid anchor buried at an infinite depth in a homogeneous soil mass. Two techniques, one based on simple extrapolation and the other one based on potential rupture lines have been presented. It has been observed that these two techniques when adopted improve estimates of collapse load particularly for buried structures like anchor plates, where the stress and velocity fields at collapse are more complex as compared to the other conventional problems of footing analyses.

Rowe and Booker (1978) have presented a general method of analysis of horizontal anchors in an elastic soil based on Fourier integral representation. Provisions for the considerations of anchor shape, layer depth, anchor soil interface condition, break away of the anchor from the underlying soil and interaction between groups of anchors has been made. The technique has been illustrated for strip and circular anchors and the solutions are presented in the form of influence charts which may be used directly for the prediction of elastic load deflection behavior of anchor plates for a wide variety of material and geometric conditions.

Snitbhan and Chen (1978) have used elasto-plastic finite element technique to obtain the limit load by studying the large deformation response of vertical cuts. They have assumed the Drucker-Prager loading criterion with an associated flow rule. It has been observed that the small displacement formulation results in a stiffer response.

Gioda and Donato (1979) have presented a numerical approach

based on finite elements and mathematical programming technique for the solution of geotechnical problems in elastic-plastic soils obeying any suitable yield condition taking into account, if necessary, work hardening behavior. The developed approach has been applied to three typical problems viz determination of a) surface settlement produced by a strip load acting on a layered soil deposit of finite thickness, b) horizontal and vertical displacement caused by an open excavation in a layered soil deposit and c) surface settlements and linear deformation and stress states after the completion of shallow tunnel excavation. The validation of the obtained results has been carried out by the in-situ measurements and other available results and a reasonable agreement is noticed.

Bottero et al (1980) have used elasto-plastic finite element formulation to obtain lower and upper bounds of plane strain problems in soil mechanics viz pull out and bearing capacity of strip footings and slope stability. They have assumed a linear variation of stress and velocity fields. Taking a linearized yield criterion for a standard Tresca material they have formulated the problem as a linear programming problem.

Davis et al (1980) have studied the stability of shallow circular tunnels and under ground opening for plane strain condition using the limit theorems of plasticity. The soil is idealized as a perfectly elasto-plastic material with a constant cohesion value with depth. The obtained results have been compared with the available experimental results and it has been concluded by the authors that the results obtained can be used with confidence for a depth of cover less than three times the diameter.

of the tunnel

Vijayan (1981) has used the elasto-plastic finite element analysis to study the response of strip and plate anchors subjected to static loading. Linear and parabolic isoparametric elements are used for continuum discretization and interface elements are used to model break away at anchor bottom. Also, conventional formulations for the determination of ultimate uplift capacity of horizontal strip and circular anchors have been carried out on the basis of assumed slip surfaces. The results have been presented in the form of break out factors for easy use and comparison from the results available in the literature. A good agreement between the results has been reported.

Kusakabe et al (1981) have obtained upper bound solutions for bearing capacity of slopes loaded on top surface and compared the results obtained with the conventional circular arc methods and by Kotter's stress characteristic equations. They have concluded that upper bound is useful from the engineering point of view because of the simplicity of the method. Model tests have also been conducted to check the validity of the upper bound solutions. Although the agreement between the solutions is generally good, the theory yields slightly higher values than those obtained experimentally. The Lysmer's (1970) method has also been used to obtain lower bound solutions to assess the validity of the upper bound analysis. It is observed that the upper bound solutions are good approximations of exact solutions for bearing capacity of loaded slopes. All computed results are presented in the form of charts.

Baus and Wang (1982) have studied the bearing capacity

behavior of strip footings located above a continuous void in silty clay soil using the finite element analysis. The foundation soil has been treated as an elastic-perfectly plastic material and the stress-strain relationship of the soil is described by Hooke's law within the elastic range. Beyond the elastic range, the soil is assumed to behave as perfectly plastic in accordance with von Mises yield criterion. The results have been presented in the graphical form. The validation of the analysis has been done based on the experimental studies. A good agreement has been reported.

Casciaro and Cascini (1982) have used a mixed variational principle for the limit analysis of perfectly plastic continuum in which the nonlinear yield criterion and the associated flow rule appear through 'penalty' function. They have used finite element formulation and Sequential Unconstrained Minimization technique to obtain lower and upper bound solutions for the problems like bearing capacity near to a vertical edge on a weight less material, rigid strip footing on a homogeneous and inhomogeneous semi infinite space and uniform strip loading on a variable layer. The results have been compared with the available exact and numerical solutions to show the validity of the formulation. A close agreement of the solutions is noticed.

Griffiths (1982) has predicted the collapse loads for deep foundations in plane strain and axisymmetric cases using finite elements in conjunction with elasto-viscoplastic material model and a close agreement with classical solutions has been observed. The computed collapse loads were found to be insensitive to the mesh size below footing level when Tresca material is used.

Naylor (1982) has used finite element analysis formulation

for the materials following associated flow rule to demonstrate the initiation and development of failure and the mechanism of collapse. The same has been used to determine the safety factor. The two methods a) direct limit analysis and b) the enhanced limit analysis, using Bishop's method of slices, have been used to check the computed safety factors. He has concluded that the direct method appears to have more potential.

Reddy and Rao (1982) have reported that the assumption of critical equilibrium at each and every point within the soil mass is not physically feasible while using the method of characteristics and it is reasonable to visualize that only the points along the failure surface are in critical equilibrium, and at other points above the failure surface, the mobilized shear strengths are less than those at critical equilibrium. They have studied the slope stability problem assuming the variation of mobilized shear strength with depth and treating the soil mass as a series of layers. They have noticed that the factors of safety obtained by this method is lower than those obtained by the friction circle method.

Rowe and Davis (1982a) have studied the behavior of strip anchor plates in clay, obeying Mohr-Coulomb failure criterion using an elasto-plastic finite element analysis. For a thin and perfectly rigid anchor the upper and lower bound solutions have been obtained and compared with the finite element analysis solutions. The same has been applied to sands with either an associated or a non-associated flow rule (Rowe and Davis, 1982b). The results obtained have been compared with the results of model and field tests and a good agreement has been noticed. The results

have been presented in the form of charts which may be used directly for the design purposes

Sloan and Randolph (1982) have investigated the ability of a displacement type finite element analysis to predict collapse loads for a smooth rigid strip and circular footings on a deep deposit of purely cohesive soil. They have shown the approach to be valid for any constitutive law such as critical state type soil models which attempt to enforce the constant volume condition (undrained) at failure. They have found that 15-noded cubic strain triangle is theoretically capable of accurate computations in the fully plastic range for such plane strain or axisymmetric geotechnical problems.

Turgeman and Pastor (1982) have formulated an upper bound limit analysis method based on finite element analysis for axisymmetric cases. The triaxial test problem and the stability of circular excavations have been studied by linearization of the yield (Tresca and von Mises) criteria formulating it as a linear programming problem.

Baker and Frydman (1983) studied the problem of finding the bearing capacity of a strip footing resting on the upper surface of a slope and have discussed the effects of non-linearity in the failure criterion of soil on the upper bound solution procedure. They have demonstrated that there is a fundamental difference in the procedure used for applying the theorem to materials with linear and non-linear failure envelopes, which they have concluded to be due to the different roles played by the normality criterion in these two cases.

Reddy and Rao (1983a) have studied the earth pressure problem

(active and passive) by the method of characteristics. The backfill is of $C-\phi-\gamma$ type with a horizontal free surface subjected to uniform surcharge. They have reported the results in the form of charts. It has been observed by them that the assumption of dependence of the coefficient of wall friction and adhesion on ϕ only is satisfactory as far as the coefficients of earth pressures are concerned. But when adhesion ratios are different from wall friction ratios, the adhesion ratio has considerable influence on the direction of resultant pressure.

Reddy and Rao (1983b) have obtained the upper bound bearing capacity of a strip footing on a two layer cohesive-frictional soil system exhibiting anisotropy and non-homogeneity in cohesion. They have assumed a Prandtl-Terzaghi failure mechanism with varying boundary wedge angles and have presented the results in the form of nondimensional charts. In order to compare the influence of soil strata on the bearing capacity, the obtained results have been compared with those obtained by extending the upper layer to the infinite depth. It is noticed that anisotropy and non-homogeneity in cohesion in each layer have considerable influence on the ultimate bearing capacity.

Mizuno and Chen (1983a) have used non associated flow rules, viz von Mises type and the Drucker-Prager criterion to investigate a problem previously studied by Smitbhan and Chen (1978) and have concluded that the non associated flow rule has a greater influence for materials with larger angle of internal friction resulting in a lower collapse loads.

Mizuno and Chen (1983b) have used finite element formulation adopting Drucker-Prager models, with the associated as well as non

associated flow rules, and cap models to obtain solutions for problems of flexible smooth, and rigid rough footings resting on a clay stratum. They have observed that velocity fields predicted by Drucker-Prager and elliptic cap models agree well with that of the Prandtl solution for both the cases.

Mizuno and Chen (1983c) have reviewed and discussed the advantages and the limitations of the plasticity and classical models applied to geotechnical engineering problems. They have also developed the computer implementations for Drucker-Prager and strain hardening cap models for solving slope stability problem under seismic loading conditions. The finite element solutions corresponding to different material models are compared to each other and with the limit analysis method.

DeBorst and Vermeer (1984) have examined the ability of the 15-noded displacement type finite element to obtain the critical loads of soil structures viz strip and circular footings, trap door problem and the cone penetration problem for soils with high friction angles and with non-associated flow rules. With reference to footing problems the accuracy and stability of obtained results has been assessed. It has been observed that the accuracy is high but some stability problems occur when non-associated flow rules are applied.

Tamura et al (1984) have obtained the upper bound limit loads for the bearing capacity of shallow footings and slope stability problems by using the rigid plastic finite element approach. A good agreement of the results with the existing solutions has been noticed.

Arai and Tagyo (1985) have presented a numerical procedure to

obtain lower bound solutions for different stability problems in geotechnical engineering viz bearing capacity of strip footings and slope stability. The procedure discretizes the stress field in a similar manner as in finite element approach. Formulating the problem as a nonlinear programming problem the optimal stress field giving the best lower bound has been achieved with the help of Sequential Unconstrained Minimization Technique. The comparison of results with the available results shows a good agreement. The short comings of the procedure is that it cannot represent arbitrary stress conditions at the boundary because a set of stresses is assumed to be constant within each element. As the procedure considers the stress as the independent variable and assumes the soil mass to be rigid-perfectly plastic material, it cannot also be applied to the problems of soil structure interaction like earth pressure problems. Through several case studies the validity of the procedure has been successfully demonstrated.

Vermeer and Sutjiadi (1985) have studied the behavior of shallow anchors by using elasto-plastic finite element analysis. The material model consists of an elastic shear modulus, Poisson's ratio, angle of internal friction and angle of dilatancy. They have suggested a truncated wedge like kinematically admissible failure mechanism and have presented an upper bound relationship for long strip anchors. The validation of the study has been made by comparing the obtained solutions with the available experimental data and a good agreement has been reported.

Tamura et al (1987) have obtained the finite element solutions for frictional materials using the stress-strain rate

relationship for rigid plastic materials of the Drucker-Prager type under the assumption of the associated flow rule. They have observed that materials with high friction angle values, show somewhat unreasonable velocity field due to the dilatancy effect affecting the bearing capacity solutions of the soil structures. As such, they have developed a numerical technique for the non-associated flow rule to reduce such effects.

In recent times the limit analysis has been extended to the reinforced soil retaining walls by Sawicki and Lesniewska (1987 and 1988). They have extended the Sokolovski's method of characteristics for predicting the lower bound bearing capacity of reinforced soil retaining walls and slopes. The soil has been treated as a rigid plastic macroscopically homogeneous material obeying Mohr-Coulomb yield criterion. Fairly good agreement between the experimental and theoretical predictions has been obtained.

Arai and Nakagawa (1988) have developed a numerical procedure for the slope stability analysis by combining the slice method in limit equilibrium method with the lower-bound limit analysis approach. The procedure provides an appropriate lower bound solution subject to the collapse mechanism represented by a potential slip surface. The problem has been formulated as an optimization problem for finding a stress field which minimizes the safety factor within the limitations of satisfying the lower bound considerations. The formulated problem has been solved by using the Sequential Unconstrained Minimization Technique using interior penalty function method as suggested by Fiacco and McCormick (1968). The obtained stress field is found to be physically

reasonable. With the help of several case studies they have shown that the simplified Janbu method based on the critical slip surface under estimates the safety factor as compared with the lower bound solution obtained by their method.

Britto and Kusakabe (1988) have used the upper bound limit analysis theorem and presented solutions for the stability numbers for unsupported and supported excavations. The soil has been treated as a perfectly plastic material satisfying the Tresca yield criterion. For unsupported excavations analysis was carried out considering both uniform and linear variation of undrained shear strengths with depth. A number of failure mechanisms have been considered. Comparison of the upper bound solutions is made with centrifuge tests and finite element analyses. It has been proved that the present solutions can be used with confidence to predict the stability number and the failure mechanisms for such problems. Stability charts are presented for both supported and unsupported axisymmetric excavations.

Sawicki (1988) has described the plastic behavior of reinforced earth from the view point of continuum mechanics. Both rigid plastic as well as elasto-plastic theory of reinforced earth which treat the composite material as macroscopically homogeneous have been presented. The lower and upper bounds for the bearing capacity of a strip footing and stability of a vertical cut have been presented and compared with the solutions available. A reasonably good agreement of the results is noticed.

Sloan (1988) has modified the method of Bottero et al (1980) to obtain the lower bound solutions for strip footings under the plane strain condition. A perfectly plastic soil model which may

either be purely cohesive or cohesive-frictional with an associated flow rule has been assumed. The Mohr-Coulomb yield criterion has been linearized and the procedure computes a statically admissible stress field with the help of finite elements and linear programming. Solutions have been obtained for a purely cohesive soil which has increasing strength with depth.

De Buhan et al (1989) have presented a method to study the stability of a reinforced earth wall in which the reinforced earth has been treated as a homogeneous material with anisotropic properties, due to the presence of the reinforcing strips. The strength criterion used for such an equivalent material has been shown to be of the anisotropic frictional type. The obtained lower and upper bound results are found to be in good agreement with those obtained experimentally than the values obtained from the classical design methods.

For analyzing the stability problems Koutsabeloulis and Griffiths (1989) have modeled the active and passive modes numerically using finite element method. The passive mode helps in computing the stress distribution and uplift force around buried structures like anchors while the active mode can be used to study the trapdoor problem. The results have been presented in the form of influence charts which may be used to provide failure loads for various geometries and a range of soil properties. The results obtained have been validated against the existing solutions and a good agreement has been obtained.

Seneviratne and Uthayakumar (1989) have shown the effectiveness of the limit theorems in obtaining the limit loads for a long rectangular tunnel (plane strain case) close to the ground surface.

in purely cohesive soils under undrained conditions. An elastic plastic total stress-strain model with a constant cohesion value is used for both weightless and weighty material. They have demonstrated the mechanics of deformation and load transfer by a trial problem. The solution obtained brackets the exact answers within $\pm 15\%$ in most of the cases studied.

Reddy et al (1989) have obtained bearing capacity factors for a circular footing placed at the interface of a two layered soil with top layer being weaker than the bottom layer using the method of characteristics and have presented the parametric studies.

Sloan (1989) has adopted the finite element formulation in conjunction with the upper bound limit theorem as suggested by Bottero et al (1980). This formulation leads to a linear programming problem which has been solved efficiently by applying active set algorithm. The method assumes a perfectly plastic soil model which is either purely cohesive or cohesive frictional. The upper bound solutions for strip footings and for a trapdoor in a purely cohesive soil have been presented and compared with the solutions available. A good agreement is noticed.

Drumm et al (1990) have obtained a lower bound solution using the theory of plasticity and the method of characteristics to evaluate the stability of C- ϕ soils adjacent to a cylindrical void. They have observed that for a given cavity diameter large overburden thickness are more stable than small thickness which is contrary to conventional slope stability where stability generally decreases with increasing height. This study has significance in soil stability analyses in Karst terrain and in the construction

of deep foundations such as drilled shafts

Reddy and Sridevi (1990) have derived the equations of method of characteristics for analyzing axisymmetric slopes. They have deleted the assumption that each and every point in the soil medium is at failure and have satisfied the equations of equilibrium. They have reported the results in the form of a stability chart giving stability numbers for different slope angles.

Reddy et al (1990) have used the method of characteristics for bearing capacity estimation of strip footing placed at the interface of two layered soil with the bottom layer stronger than the top layer. The ground has an upward slope at a distance from the footing. They have concluded that the presence of an upward slope just adjacent to the footing and presence of a stronger layer below the base of the footing increases the bearing capacity considerably.

Using the finite element method in conjunction with the linear programming technique Sloan et al (1990) have obtained the upper and lower bounds on stability number for undrained stability of a plane strain trapdoor problem assuming a perfectly plastic soil model with a Tresca yield criterion. The bound techniques are shown to be efficient computationally and the results have been verified by displacement type of finite element method. They have found that the upper and lower bounds derived bracket the exact collapse load to within 10% or better over the range of trapdoor geometries considered.

Assadi and Sloan (1991) have used the upper and lower bound theorems to examine the undrained stability of a shallow square tunnel in a purely cohesive soil under the plane strain condition.

of loading. They have also obtained rigorous bounds on the loads needed to support the tunnel against active or passive failures using the finite element analysis assuming a perfectly plastic soil model with a linearized Tresca yield criterion.

Azam et al. (1991) have studied the performance of strip footings on homogeneous and stratified soil deposits containing two soil layers both with and without a continuous void. The analysis involves a two-dimensional finite element method in which the reinforced concrete strip footing has been treated as a linear elastic material while the foundation soil has been idealized as an elastic perfectly plastic material obeying Drucker and Prager (1952) yield criterion. To accommodate the nonlinear stress-strain characteristics of the foundation soil in the finite element analysis the incremental footing load was applied. The obtained solutions have not been compared with the available results for homogeneous soils but for stratified soils the obtained results compare well with the solutions of Vesic (1975).

Sloan and Assadi (1991) have obtained the rigorous bounds on the internal pressure needed to support a square tunnel against active failure using finite element in conjunction with classical limit theorems assuming a perfectly plastic soil model with Tresca yield criterion, the problem is formulated as a linear programming problem to isolate the optimal solutions. The upper and lower bounds derived bracket the exact collapse load to within 15% or better over the a range of tunnel geometries considered.

1.3 Motivation and Scope of the Thesis

The literature review highlights that though lot of work has been undertaken to obtain the upper bound solutions of various stability problems in geotechnical engineering, very little attention has been paid to the lower bound solutions of these problems. In this context the general methods suggested by Lysmer (1970), Basudhar (1976) and Sloan (1988) are worth considering.

The methods given by Lysmer and Sloan are based on linear programming whereas the one proposed by Basudhar is based on nonlinear programming. Sloan has recognized the merit of Lysmer's approach in dealing with lesser number of design variables vis a vis his approach, however, he has pointed out that Lysmer's approach may become ill conditioned due to widely varying magnitudes of the elements of the constraint matrix especially when thin elements are used. The original Lysmer's method was constrained more by the use of Simplex method and non availability of high speed super computers in isolating the optimal solution and not by any drawback in the methodology of constructing a statically admissible stress field, however, Sloan demonstrated the capability of his method to incorporate more number of elements using the active set algorithm to solve bearing capacity of footings in nonhomogeneous cohesive materials.

The number of elements to be considered in any such analysis depends on various factors like the nature of soil deposit, problem geometry, boundary loading conditions, zone of significant influence and stability of the numerical scheme leading to a meaningful solution without any convergence problem. A single mesh geometry and specified number of elements may not be the panacea

that would solve a problem to the last details As such, there is a necessity to study the effect of mesh geometry on the solutions when the method is applied to a new problem

Satisfying the nonlinear no-yield constraints directly in the analysis irrespective of the computational efforts involved, so long the cost is not prohibitive, instead of approximating it by successive linearization is better as otherwise the search domain in finding the maximum lower bound gets restricted and may result in lower predictions Another reason being the fact that this further results in reducing the number of design variables and the computational efforts involved This has been recognized by Basudhar who has modified Lysmer's original method by incorporating no-yield constraints directly in the analysis Even though, Lysmer's method has an excellent potential the method has not been explored to its full potential except in one additional case where it has been used in finding the bearing capacity of sloping ground by Kusakabe et al (1981) Modified Lysmer's method as proposed by Basudhar has also not been used except for bearing capacity and earth pressure problems in homogeneous soils In contrast, Sloan has demonstrated the applicability of his approach in dealing with the bearing capacity of homogeneous and nonhomogeneous soil deposits and trapdoors However, for the reasons stated earlier modified Lysmer's method (Lysmer,1970 and Basudhar,1976) using nonlinear programming is preferable in isolating the optimal stress field

With this in view the same has been adopted for the prediction of lower bound critical loads of the various stability problems in geotechnical engineering to demonstrate its wide

applicability in dealing with such problems. The method is validated by comparing the obtained results with the available experimental and theoretical results.

The scope and organization of the thesis is as follows.

For the sake of completeness the original approach of Lysmer modified by Basudhar has been described in Chapter 2 in details. The concept of extended penalty function along with the Sequential Unconstrained Minimization formulation has also been presented.

In Chapter 3, efficiency of various unconstrained minimization techniques has critically been studied in order to pick up an appropriate algorithm for unconstrained minimization. The same has been done with reference to the determination of passive earth pressure on a retaining wall. A comparative study of these methods namely, the conjugate direction (Powell, 1964), conjugate gradient (Fletcher and Reeves, 1964) and variable metric methods (Davidon, 1959) when applied to such stability problems in geotechnical engineering is presented and critically discussed and the best method for dealing with such problems has been recommended.

Chapter 4 deals with the prediction of lower bound bearing capacity of smooth and rough surface and embedded strip footings. For surface footings the mesh pattern as suggested by Lysmer has been adopted and for embedded footings the effect of mesh pattern on the solution is studied and a generalized mesh pattern has been proposed to obtain the bearing capacity solutions for the different values of dimensionless parameter G ($=\gamma B/2C$) and ϕ values. The results so obtained are compared with the reported limit analysis, limit equilibrium and finite element solutions.

Chapter 5 deals with the prediction of lower bound bearing

capacity of smooth surface and embedded strip footings on a homogeneous soil with and without a continuous void. Generalized mesh patterns have been proposed for different conditions of voids. The validation of the obtained results has been done with the available finite element and experimental results.

In Chapter 6, the breakout factors and pull out capacity of horizontal, vertical and inclined strip anchors have been studied. Both smooth and rough strips have been considered. The validity of the results obtained has been demonstrated by comparing the predicted values with experimental data and theoretical solutions available in literature.

In Chapter 7, application of modified Lysmer's approach has been extended to the estimation of lower bound bearing capacity of reinforced soil retaining walls and cohesive slopes. The analysis is based on the rigid-plastic model for reinforced soil treating it as a macroscopically homogeneous anisotropic material. The obtained results are compared with the theoretical and experimental data reported in literature for validation of the method.

In Chapter 8, the generalized method has been extended to the widely studied problem of finding the stability of a vertical cut in homogeneous purely cohesive and cohesive-frictional soils capable of taking tension. The obtained results have been compared with solutions available in the literature.

Chapter 9 deals with the prediction of lower bound stability numbers of a trapdoor embedded in a homogeneous purely cohesive soil. For various embedment ratios, the effect of mesh pattern on the results has been studied and generalized mesh patterns have been proposed for both shallow and deep trapdoors. The obtained

results have been compared with the available solutions for validation

In Chapter 10, generalized conclusions are drawn and scope of the future works has been listed

CHAPTER 2

GENERAL METHOD OF ANALYSIS

The method originally suggested by Lysmer (1970) and modified by Basudhar (1976) has been adopted to analyze the problems. For the sake of completeness the analysis method is presented herein in brief.

The first step in the analysis of a problem is the discretization of the soil mass under consideration into finite number of triangular elements as shown in Fig 2.1. In general, to get a good solution the zone of influence to be discretized should be based on the previous experimental and theoretical studies. For further discretization of this zone into number of elements the guidelines as suggested by Lysmer, in particular for the identification of singularity points, should be kept in mind as far as possible. All the nodal points, elements and element sides are then numbered.

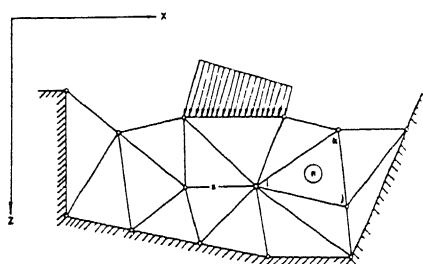


Fig 2.1 Discretization of the soil mass for a typical problem

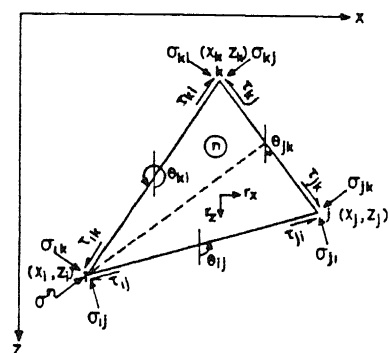


Fig 2.2 Definition sketch and body forces for nth element

in some arbitrary order. The forces acting on a typical element n are shown in Fig 2.2. It is sufficient to consider the stresses at the nodes only since the stresses are assumed to vary linearly within each element and in addition satisfy the equations of equilibrium for an elastic continuum. Also, one internal stress σ^n

is defined as the normal stress at node i acting on a plane having the same orientation as that of the plane represented by side jk . Hence, the normal stress vector for each element is obtained as

$$[\{\sigma\}^n]^T = \{\sigma^n \ \sigma_{ik} \ \sigma_{ij} \ \sigma_{ji} \ \sigma_{jk} \ \sigma_{kj} \ \sigma_{ki}\} \quad (1)$$

and the external shear stresses are collected in the matrix given by, $[\{\tau\}^n]^T = \{\tau_{ik} \ \tau_{ij} \ \tau_{ji} \ \tau_{jk} \ \tau_{kj} \ \tau_{ki}\}$ (2)

the internal stresses in each element are collected in a matrix as

$$\{s\}^T = \{\bar{s}_i \ \bar{s}_j \ \bar{s}_k\} \quad (3)$$

$$\text{with, } \{s_i\}^T = \{\sigma_{z,i} \ \sigma_{x,i} \ \tau_{zx,i}\} \text{ etc} \quad (4)$$

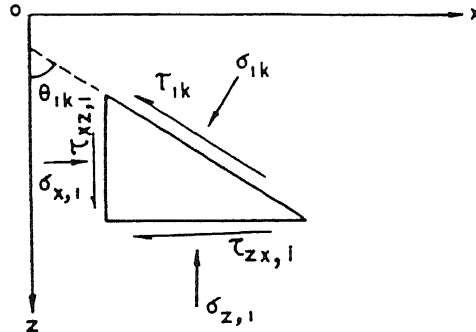


Fig 2.3 Internal stresses at point i

where, $\{\bar{s}_i\}$ are the internal stresses at node i . From the equilibrium of the infinitesimal element (Fig 2.3), σ_{ik} and τ_{ik} are expressed in terms of the internal stresses as

$$\sigma_{ik} = \sigma_{z,i} \sin^2 \theta_{ik} + \sigma_{x,i} \cos^2 \theta_{ik} - \tau_{zx,i} \sin 2\theta_{ik} \quad (5)$$

$$\tau_{ik} = 0.5(\sigma_{x,i} - \sigma_{z,i}) \sin 2\theta_{ik} + \tau_{zx,i} \cos 2\theta_{ik} \quad (6)$$

Similar equations when written for nodes j and k and substituted in equations (1) and (2) yield

$$\{\sigma\}^n = [S] \{s\} \quad (7)$$

$$\{\tau\}^n = [T] \{s\} \quad (8)$$

Matrices $[S]$ and $[T]$ consist of geometric properties of each element. The stress vector $\{\bar{s}_i\}$ is chosen satisfying the following conditions of internal equilibrium

$$\left. \begin{aligned} \frac{\partial \sigma_z}{\partial z} + \frac{\partial \tau_{zx}}{\partial x} &= \gamma_z \\ \frac{\partial \tau_{zx}}{\partial z} + \frac{\partial \sigma_x}{\partial x} &= \gamma_x \end{aligned} \right\} \quad (9)$$

The above equations are satisfied by assuming an appropriate linear stress field as follows

$$\left. \begin{aligned} \sigma_z &= c_1 z + c_2 x + c_3 + \gamma_z z \\ \sigma_x &= c_4 z + c_5 x + c_6 + \gamma_x x \\ \tau_{zx} &= -c_5 z - c_1 x + c_7 \end{aligned} \right\} \quad (10)$$

Using Eqns (3), (4) and (10) the stress vector $\{s\}$ can be written as

$$\{s\} = [G]\{c\} + \{g\} \quad (11)$$

where, $[G]$ is a matrix of the nodal coordinates and

$$\{c\}^T = \{c_1 \ c_2 \ c_3 \ c_4 \ c_5 \ c_6 \ c_7\}, \text{ and} \quad (12)$$

$$\{g\}^T = \{\gamma_z z_i, \gamma_x x_i, 0, \gamma_z z_j, \gamma_x x_j, 0, \gamma_z z_k, \gamma_x x_k, 0\} \quad (13)$$

using equations (7) and (11),

$$\{c\} = ([S] \ [G])^{-1} \{\sigma\}^n - ([S] \ [G])^{-1} [S] \{g\} \quad (14)$$

combining equations (8), (11) and (14),

$$\{\tau\}^n = [T] [B] \{\sigma\}^n + [T]\{h\} \quad (15)$$

$$\text{where, } [B] = [G]([S][G])^{-1} \text{ and } \{h\} = \{g\} - [B][S]\{g\} \quad (16)$$

The elements of $\{\sigma\}^n$ vectors for all the elements are collected into a general $\{\sigma\}$ vector. A system consisting of p elements connected at q nodal points will have $(3p+2q-2)$ stress variables in $\{\sigma\}$ vector, which are the principal unknowns.

The continuity of normal and shear stresses across any

interface as shown in Fig 2.4 requires

$$\sigma_{ij}^m = \sigma_{ij}^n \quad \text{and} \quad \tau_{ij}^m = \tau_{ji}^n \quad (17)$$

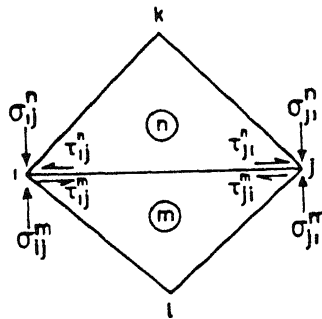


Fig 2.4 Continuity of nodal stresses

for all corresponding values of i , j , m and n . These conditions yield a set of linear equality constraints in terms of the principal unknowns. The boundary stresses on the external faces of the system may be expressed either as

$$\tau_{ij} \leq \mu \sigma_{ij} \quad (18)$$

$$\text{or, } \sigma_{ij} = \zeta \quad \text{and} \quad \tau_{ij} = \epsilon \sigma_{ij} \quad (19)$$

Equations (17), (18) and (19) can be transformed into the form

$$\sum_{j=1}^{(3p+2q-2)} a_{ij} \sigma_j = b_i \quad \text{and /or} \quad \sum_{j=1}^{(3p+2q-2)} a_{ij} \sigma_j \leq b_i \quad (20)$$

Also at any node i , the Mohr-Coulomb failure criterion

$$(\sigma_{z,i} - \sigma_{x,i})^2 + (2\tau_{zx,i})^2 \leq [(\sigma_{z,i} + \sigma_{x,i}) \sin\phi + 2C \cos\phi]^2 \quad (21)$$

must be satisfied. Eqn (21), is expressed in terms of the principal unknowns as follows

$$\sigma_{z,i} = Z_i(s), \quad \sigma_{x,i} = X_i(s) \quad \text{and} \quad \tau_{zx,i} = T_i(s) \quad (22)$$

where,

$$\left. \begin{array}{l} Z_i = (1, 0, 0, 0, 0, 0, 0, 0, 0, 0) \\ X_i = (0, 1, 0, 0, 0, 0, 0, 0, 0, 0) \\ T_i = (0, 0, 1, 0, 0, 0, 0, 0, 0, 0) \end{array} \right\} \quad (23)$$

similarly for nodes j and k ,

$$\left. \begin{array}{l} Z_j = (0, 0, 0, 1, 0, 0, 0, 0, 0, 0) \\ X_j = (0, 0, 0, 0, 1, 0, 0, 0, 0, 0) \\ T_j = (0, 0, 0, 0, 0, 1, 0, 0, 0, 0) \end{array} \right\} \quad (24)$$

and,

$$\left. \begin{array}{l} Z_k = (0, 0, 0, 0, 0, 0, 1, 0, 0, 0) \\ X_k = (0, 0, 0, 0, 0, 0, 0, 1, 0, 0) \\ T_k = (0, 0, 0, 0, 0, 0, 0, 0, 0, 1) \end{array} \right\} \quad (25)$$

Equations (21) and (22) yield

$$(A_i\{s\})^2 + (2 T_i\{s\})^2 - (B_i\{s\} \sin\phi + 2C \cos\phi)^2 \leq 0 \quad (26)$$

where,

$$\left. \begin{array}{l} A_i = (Z_i - X_i) \\ B_i = (Z_i + X_i) \end{array} \right\} \quad (27)$$

Now, equation (26) can be rewritten in terms of $\{\sigma\}^n$ as

$$\{[A_i([B]\{\sigma\}^n + \{h\})]^2 + [2 T_i([B]\{\sigma\}^n + \{h\})]^2 - [B_i([B]\{\sigma\}^n + \{h\}) \sin\phi + 2C \cos\phi]^2\} \leq 0 \quad (28)$$

Similar relations can be obtained for the nodes j and k . The elements of $\{\sigma\}^n$ vector can be picked up from the general stress vector $\{\sigma\}$. Since all stresses vary linearly within each element it is sufficient that the no-yield condition is not violated at the element corners. This leads to a set of 3p constraints.

In general many stress fields will satisfy the aforementioned condition of static admissibility. The isolation of the stress field which optimizes the objective function is important. The objective function and the various constraints can be represented in a general form as follows

$$\text{OPTIMIZE} \quad \sum a_j \sigma_j \quad (29)$$

Where, σ_j is the principal unknown. The design restrictions are interface equilibrium and the external boundary conditions (Eqn 20), along with the no yield criterion, (Eqn 28). As soil cannot take tension, the following constraints are also introduced,

$$-\sigma_j \leq 0 \quad (30)$$

the inequality constraints are designated as

$$g_j \leq 0 \quad (31)$$

The equality constraints (Eqn 20) can be rewritten in matrix notation as

$$[A] \{\sigma\} = \{b\} \quad (32)$$

Some of the elements of $\{\sigma\}$ vector are specified at the boundary

The following relation

$$[A^*] \{\sigma^*\} = \{b^*\} \quad (33)$$

can be arrived at by eliminating the columns of $[A]$ matrix corresponding to the known elements of the $\{\sigma\}$ vector. $\{\sigma^*\}$ is a vector which is achieved by eliminating the known elements of $\{\sigma\}$ vector. $\{b^*\}$ vector is calculated as follows

$$\{b^*\} = \{b\} - [A'] \{\sigma'\} \quad (34)$$

$[A']$ matrix contains the columns that are removed from $[A]$ matrix and $\{\sigma'\}$ contains those elements of $\{\sigma\}$ vector that are specified

The following steps are performed for the general rectangular matrix $[A^*]$

Step 1 The rank and the linearly dependent rows and columns if there be any of the given matrix, are determined

Step2 A sub matrix of maximal rank is expressed as product of triangular factors

Step3 The non basic rows are expressed in terms of the basic ones

Step4 The basic variables are expressed in terms of the free variables

By considering these free variables as design variables and expressing the remaining basic variables in terms of these design variables the equality constraints (Eqn 33) are implicitly satisfied Such a technique helps in reducing the complexity of the problem by eliminating the equality constraints and thereby reducing the dimensionality of the problem The independent design variables so obtained are collected in D vector

The rank(r) is determined using the standard Gaussian elimination technique with complete pivoting This implies that the rows and columns of the given $m' \times n'$ matrix $[A^*]$ are interchanged at each elimination step if necessary In general the following cases may arise

1 $r < m'$

$[A^*]$ is not row regular and the solution of Eqn (33) exists only if the remaining $(m' - r)$ equations are linearly dependent

2 $r < n'$

$[A^*]$ is not column regular and the system has no trivial solution

Cases (1) and (2) may occur combined The solution if it exists, can be uniquely determined if $r = n'$, otherwise, it contains $(n' - r)$ free parameters

The basic variables (σ^{**}) are expressed in terms of the free design variable (D) as follows

Once the steps 1,2 and 3 of the enunciated reduction process are

carried out the Eqn (33) is reduced to a form,

$$[A^*]^r \{\sigma^*\}^r = \{b^*\}^r \quad (35)$$

where, the superscript denotes the r th elimination step and

$$[A^*]^r = \begin{pmatrix} L \\ LR \end{pmatrix} (U, UR) \quad (36)$$

where, L is a unit lower triangular matrix of dimension $r \times r$

U is a unit upper triangular matrix of dimension $r \times r$

LR is of dimension $(m'-r) \times r$, if the matrix $[A^*]$ is row regular

that is $(m' = r)$, LR is absent in the final factorization

UR is of dimension $r \times (n'-r)$, if the matrix $[A^*]$ is column regular

that is $(n' = r)$, UR is absent in the final factorization

Let $\{\sigma^*\}^r$ and $\{b^*\}^r$ be partitioned into

$$\left\{ \begin{array}{c} \sigma^{**} \\ D \end{array} \right\} \text{ and } \left\{ \begin{array}{c} b_1^* \\ b_2^* \end{array} \right\}$$

Then for a consistent system of equations

$$\sigma^{**} = U^{-1} L^{-1} b_1^* + H D \quad (37)$$

where, $H = -U^{-1} UR \quad (38)$

and $b_1^* = L U \sigma^{**} + L UR D \quad (39)$

$$b_2^* = LR L^{-1} b_1^* \quad (40)$$

In the present thesis subroutine MFGR developed by IBM has been used to perform the calculations enunciated in steps 1 to 4 of the reduction process

The minimum value of the objective function subject to the inequality constraints as described above is found out by formulating the problem as a non linear programming problem as follows

Find D_m such that ,

$$F(D_m) = \sum a_j \sigma_j \text{ is minimum,} \quad (41)$$

subject to $g_j(D_m) \leq 0$

With the help of extended penalty function technique as suggested by Kavlie and Moe (1971) the constrained problem is converted to an unconstrained one. The Sequential Unconstrained Minimization of the developed composite function is carried out using Powell's conjugate direction algorithm (Powell, 1964) along with Quadratic interpolation technique for linear minimization to isolate the optimal solution. These methods are available in any standard text book on Optimization (Fox, 1971, Rao, 1984). The composite function $\phi(D, r_k)$ is developed by blending the objective function and constraints as follows

$$\phi(D, r_k) = F(D) + r_k \sum_{j=1}^M G_j [g_j(D)] \quad (42)$$

The function $G_j [g_j(D)]$ is chosen as

$$G_j [g_j(D)] = \begin{cases} 1/g_j(D) & g_j(D) \leq 0 \\ [2\lambda - g_j(D)]/\lambda^2, & g_j(D) > \lambda \end{cases} \quad (43)$$

where, $\lambda = -r_k/\delta t$

In this approach infeasible starting points are readily acceptable to the minimization algorithm, which makes it a powerful technique for solving various engineering problems even if an initial feasible design vector is difficult to guess.

Hence forth the method of analysis as described will be referred as Lysmer-Basudhar approach in the text

CHAPTER 3

CHOOSING A METHOD

3 1 General

Choosing an appropriate method for either minimizing or maximizing a function subjected to inequality constraints arising out of analysis of stability problems as described in Chapter 2 is an art Fox (1971) has provided guidelines for such an exercise. In such problems, it is extremely difficult to obtain an initial feasible vector and, as such, the interior penalty function method (Fiacco and McCormick, 1968) can not be used. In such cases the problem has to be solved by using either the exterior penalty function method or obtaining an initial feasible design vector following a procedure outlined by Fox and using the interior penalty function method. Even when the interior penalty function method is used, owing to the 'long step' nature of the unconstrained optimization algorithms the path may be diverted into infeasible regions. In such cases the function is set to an arbitrary high value and the minimization procedure is left to correct the situation on its own. Sometimes this approach presents numerical difficulties. Therefore, Basudhar (1976) has suggested the use of the extended penalty function method enunciated by Kavlie and Moe (1971). This readily accepts infeasible design points and needs no special treatment. Another reason for the choice made is the availability of well established unconstrained minimization techniques in the literature (Fox, 1971, Rao, 1984). As exact gradient of the function is not available in such an analysis, Basudhar was guided by the suggestion made by Fox and used the

nongradient technique viz Powell's method of conjugate direction for unconstrained minimization with Quadratic fit for linear minimization. But when the design variables and the constraints are too many arising out of consideration of more number of elements, adoption of a gradient based technique may be necessary. In this connection the Fletcher-Reeve's (FLRV) method of conjugate gradient and Davidon-Fletcher-Powell (DFP) variable metric method with finite difference derivatives are worth mentioning. However, the use of Conjugate gradient method has been discouraged by Fox unless the problem is very large and well conditioned. For ill conditioned problems variable metric method is likely to work better as compared to other gradient and nongradient methods. Like all other numerical methods the efficiency of these optimization algorithms is problem oriented. As such, it is necessary to make a detailed study of these methods in order to pick up the suitable algorithm. In the following sections such a study has been reported with reference to the stability analysis of a retaining wall previously studied by Lysmer (1970) and Basudhar (1976).

3 2 Statement of the Problem

Fig 3 1 shows a rough retaining wall ($\delta=20^0$) of 10 0ft (3.05m) height. The backfill consists of purely frictional

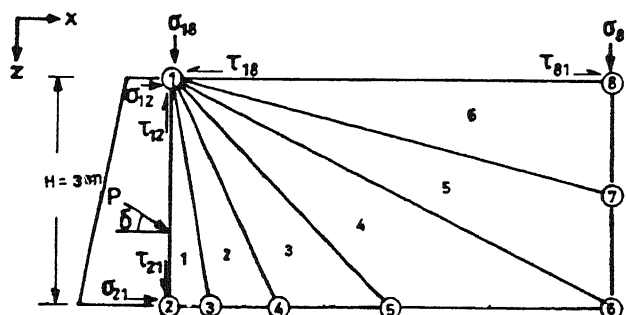


Fig 3 1 Mesh pattern for earth pressure problem

material ($C=0$ $\theta=0$) with the angle of internal resistance $\phi=40^0$ The unit weight of the material is 100pcf(16.018 KN/m³) The objective is to obtain the passive earth pressure acting on the wall

3.3 Boundary conditions and the Objective function

Boundary conditions

As shown in Fig 3.1 the following boundary conditions are imposed

$$\begin{array}{ll} 1) \sigma_{18} = \sigma_{81} = \tau_{18} = \tau_{81} = 0 & 2) \tau_{12} - \sigma_{12} \tan\delta \leq 0 \\ 3) \tau_{21} - \sigma_{21} \tan\delta \leq 0 & \end{array}$$

Objective function $-(\sigma_{12} + \sigma_{21})$

3.4 Results and Discussions

The results are obtained on HP-9000/850s computer system In Figs 3.2(a) and 3.2(b) the performance of the various algorithms used in analysis has been studied in terms of the number of function evaluations required to achieve the optimal objective function values (normalized with γH) and the penalty parameter

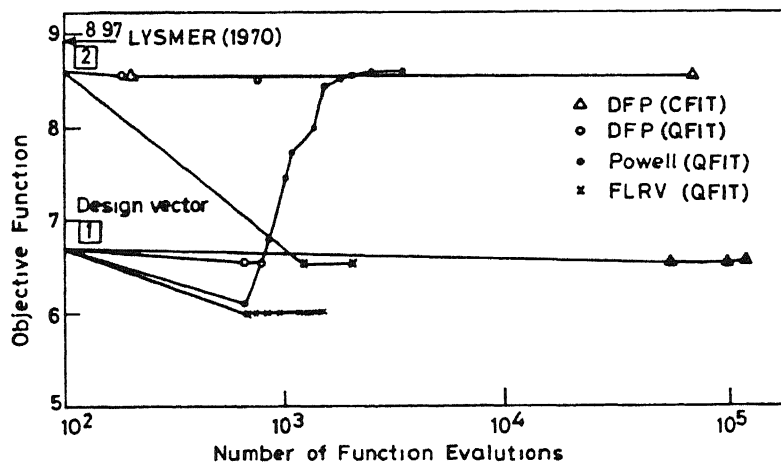


Fig 3.2(a) Variation of objective function with number of function evaluations

The effect of initial design vector on the final solution and efficiency of the technique has also been studied and presented in the figures Two initial design vectors designated by 1 and 2, in

the figure have been used. It can be seen from Fig 3 2(a) that for starting point 1, only POWELL algorithm converges to a solution which is close to that of Lysmer at about 2500 number of function evaluations and a corresponding penalty parameter equal to 1E-08

It can also be seen that DFP with QFIT and CFIT and FLRV with QFIT converge to feasible solutions quite far off from the Lysmers' values. It is clear from Fig 3 2(b) that the variation of penalty term has a great influence on POWELL as compared to DFP and FLRV beyond $r_k = 0.1$. From the optimal solution obtained by POWELL starting from initial design vector 1, a near optimal solution has been used as a starting point 2 for DFP and FLRV to check whether there is any improvement or not. The study as depicted in Figs 3 2(a) and 3 2(b) show that DFP with QFIT and CFIT converges almost to the same results as given by POWELL where as FLRV diverges.

Stress values at different nodal points are also presented and compared with those reported by Lysmer in Tables 3 1(a), 3 1(b) and 3 1(c) just for the sake of completeness. The study supports the conclusions as drawn regarding the relative efficiency of these methods.

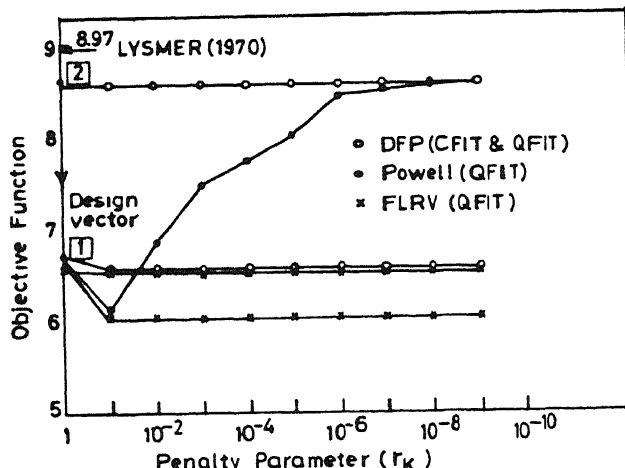


Fig 3 2(b) Variation of objective function with penalty parameter

TABLE 3 1(a)
 $(\sigma_z / \gamma H)$ values for the retaining wall

Element no	Nodal pt	Lysmer (1970)	Present Study			
			Powell	DFP		FLRV
				QFIT	CFIT	
1	1	0 000	0 000	0 000	0 000	0 000
	2	3 886	3 901	5 632	5 626	4 583
	3	3 200	3 227	(3 881)	(3 894)	(2 665)
2	1	0 000	0 000	0 000	0 000	0 000
	3	3 200	3 075	1 589	1 613	1 535
	4	2 333	2 385	(3 062)	(3 077)	(2 209)
3	1	0 000	0 000	0 000	0 000	0 000
	4	2 333	2 126	1 425	1 415	1 376
	5	1 410	1 535	(2 157)	(2 182)	(1 712)
4	1	0 000	0 000	0 000	0 000	0 000
	5	1 410	1 261	1 102	1 107	1 144
	6	0 937	0 964	(1 254)	(1 232)	(1 173)
5	1	0 000	0 000	0 000	0 000	0 000
	6	1 020	1 024	1 027	1 032	1 038
	7	0 459	0 490	(1 024)	(1 028)	(1 035)
6	1	0 000	0 000	0 493	0 489	0 502
	7	0 500	0 500	(0 490)	(0 488)	(0 503)
	8	0 000	0 000	0 000	0 000	0 000

Note Values in the parentheses correspond to design vector 2

TABLE 3 1(b)
 $(\sigma_x / \gamma H)$ values for the retaining wall

Element no	Nodal pt	Lysmer (1970)	Present Study			
			Powell	DFP		FLRV
				QFIT	CFIT	
1	1	0 000	0 000	0 000	0 000	0 000
	2	8 970	8 590	6 674 (8 566)	6 671 (8 553)	6 016 (6 555)
	3	8 320	7 970	6 188 (7 943)	6 185 (7 927)	5 617 (6 159)
2	1	0 000	0 000	0 000	0 000	0 000
	3	8 320	7 970	6 074 (7 937)	6 071 (7 923)	5 538 (6 155)
	4	7 340	7 060	5 755 (7 033)	5 748 (7 016)	5 237 (5 579)
3	1	0 000	0 000	0 000	0 000	0 000
	4	7 340	6 995	5 745 (6 978)	5 738 (6 964)	5 228 (5 552)
	5	5 860	5 752	5 271 (5 705)	5 270 (5 677)	4 757 (4 722)
4	1	0 000	0 000	0 000	0 000	0 000
	5	5 860	5 478	5 007 (5 449)	5 020 (5 397)	4 678 (4 528)
	6	4 260	4 426	4 609 (4 426)	4 631 (4 492)	4 017 (3 753)
5	1	0 000	0 000	0 000	0 000	0 000
	6	4 750	4 667	4 691 (4 642)	4 604 (4 595)	4 335 (3 973)
	7	2 070	2 141	2 165 (2 129)	2 108 (2 103)	1 858 (1 708)
6	1	0 000	0 000	0 000	0 000	0 000
	7	2 300	2 297	2 273 (2 282)	2 281 (2 291)	1 825 (1 659)
	8	0 000	0 000	0 075 (0 001)	0 117 (0 066)	0 000 (0 000)

Note Values in the parentheses correspond to design vector 2

TABLE 3 1(c)
 $(\tau_{xz}/\gamma H)$ values for the retaining wall.

Element no	Nodal pt	Lysmer (1970)	Present Study			
			Powell	DFP		FLRV
				QFIT	CFIT	
1	1	0 000	0 000	0 000	0 000	0 000
	2	3 250	3 128	2 429	2 429	1 994
	3	2 680	2 547	(3 115)	(3 122)	(1 979)
2	1	0 000	0 000	0 000	0 000	0 000
	3	2 680	2 517	0 928	0 935	0 879
	4	1 840	1 656	(2 509)	(2 514)	(1 626)
3	1	0 000	0 000	0 000	0 000	0 000
	4	1 840	1 627	0 706	0 699	0 676
	5	0 715	0 768	(1 643)	(1 649)	(1 131)
4	1	0 000	0 000	0 000	0 000	0 000
	5	0 715	0 494	0 200	0 214	0 332
	6	0 169	0 064	(0 486)	(0 443)	(0 408)
5	1	0 000	0 000	0 000	0 000	0 000
	6	0 040	0 057	0 044	0 024	0 163
	7	0 110	0 039	(0 057)	(0 034)	(0 151)
6	1	0 000	0 000	0 046	0 073	0 001
	7	0 000	0 000	(0 038)	(0 063)	(0 012)
	8	0 000	0 000	0 000	0 000	0 000

Note Values in the parentheses correspond to design vector 2

3 5 Conclusions

The following conclusions can be drawn based on the above presented results and discussion

- 1) The comparative study of the different unconstrained minimization algorithms reveals that POWELL (conjugate direction) method is the most suitable technique for such complex problems
- 2) Davidson-Fletcher-Powell variable metric method and Fletcher-Reeves conjugate gradient methods are not recommended for solving such problems where exclusive analytical expressions for gradients are not available
- 3) For such problems nongradient methods are superior and quite efficient in isolating the optimal lower bound than the gradient based techniques which may even diverge and terminate at points which are quite far off from the optimal value

CHAPTER 4

BEARING CAPACITY OF SURFACE AND EMBEDDED STRIP FOOTINGS

4 1 General

Bearing capacity of foundations under the condition of plain strain has been widely studied by various investigators. The methods of analyses are based on upper bound limit analysis, limit equilibrium and finite element techniques. Very often limit theorems of plasticity are used for predicting the bounds for the collapse load even if it can not be found exactly. A review of the literature pertaining to the subject has been presented by Chen (1975) and Bowles (1988). Chapter 1 of the thesis provides a brief account of the available upper and lower bound bearing capacity solutions. It is noticed that the literature to predict the collapse load from the upper bound approach is plenty but the same from lower bound approach is scanty. The lower bound bearing capacity solutions based on the method of characteristics and finite elements are available for smooth surface strip footings only (Cox, 1962, Sokolovskii, 1965, Lysmer, 1970, Basudhar, 1976, Basudhar et al, 1979, Sloan, 1988 and Reddy et al, 1990). But no lower bound solutions are available for the rough surface and embedded strip footings. The potential of the generalized numerical method as suggested by Lysmer based on finite element and linear programming using Simplex algorithm, had been recognized quite early (Chen and Davidson, 1973) to analyze the stability problems in geotechnical engineering. However, the original Lysmer's method as well as Basudhar's method have not

been explored any further. With this in view an attempt has been made in the following sections to extend the Lysmer-Basudhar approach for obtaining the bearing capacity solutions of smooth and rough surface and embedded strip footings.

4.2 Surface Footings

The mesh pattern identical to the one as suggested by Lysmer (1970) has been adopted for the surface footings. The study has been extended to the rough strip footing also in the thesis.

4.2.1 Statement of the problem

Fig 4.1 shows a strip surface footing. The objective is to find the bearing capacity of this footing for different values of angle of internal friction (ϕ) and the dimensionless parameter G ($=\gamma B/2C$). For rough footings the angle of base friction (δ) has been taken equal to the ϕ value.

4.2.2 Boundary conditions and the Objective function

Boundary conditions

With reference to Fig 4.1 the boundary conditions specified are as follows:

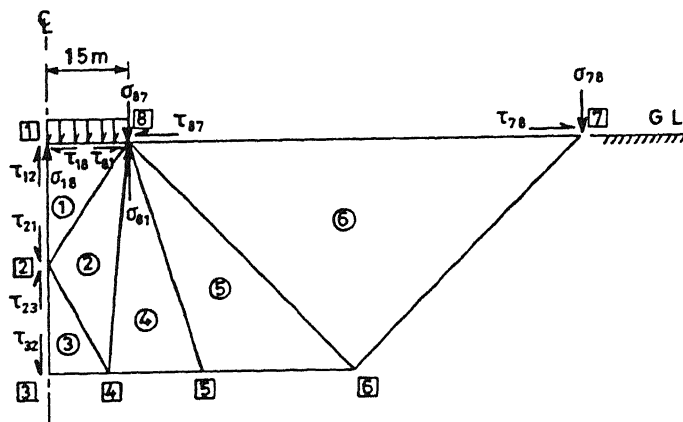


Fig. 4.1 Mesh pattern for a surface strip footing (Lysmer, 1970)

$$\sigma_{78} = \sigma_{87} = 0 \quad \text{and,}$$

$$\tau_{18} = \tau_{81} = \tau_{12} = \tau_{21} = \tau_{23} = \tau_{32} = \tau_{78} = \tau_{87} = 0 \quad (\text{for smooth footings})$$

$$\left. \begin{array}{l} 1) \tau_{12} = \tau_{21} = \tau_{23} = \tau_{32} = \tau_{78} = \tau_{87} = 0 \\ 2) \tau_{18} = C + \sigma_{18} \tan \delta, \quad 3) \tau_{81} = C + \sigma_{81} \tan \delta \end{array} \right\} \quad (\text{for rough footings})$$

$$\text{Objective function is } -(\sigma_{18} + \sigma_{81})$$

Bearing capacity (q_0) is equal to the half of the objective function value

4 2 3 Results and discussions

The results were obtained on HP-9000/850s computer system. For $\phi=0$, $G=0$ and $C=17.5 \text{ psi}$ (120.64 kN/m^2) the obtained bearing capacity value is 84.38 psi (581.7 kN/m^2) which is 6.24% on the safer side of the solution 90 psi (620.45 kN/m^2) given by Chen and Baladı (1985) using finite element elasto-plastic analysis. For a $C-\phi$ material with $\phi=20^\circ$, $G=0$ and $C=10 \text{ psi}$ (68.94 kN/m^2) the predicted bearing capacity value is 130.0 psi (896.22 kN/m^2) which is 8.45%, 9.09%, 14.47% and 25.71% on the safer side corresponding to the solutions 142 psi (978.92 kN/m^2), 143 psi (985.82 kN/m^2), 152 psi (1047.86 kN/m^2) and 175 psi (1206.42 kN/m^2) as predicted by Cap model, Prandtl, Coulomb and Terzaghi respectively (Chen and Baladı, 1985). It can be seen that the value predicted by the present analysis is very close (8.45-9.09%) to the solutions obtained by using refined theoretical predictive models based on constitutive relationships of the mathematical theory of plasticity. But the value is relatively lower (14.47-25.71%) from those obtained by using limit equilibrium methods.

The bearing capacity factors (q_0/C) are predicted for smooth surface footings with different values of ϕ and G and the obtained results are presented and compared with the solutions available in the literature (Chen and Davidson, 1973) as shown in Table 4 1. Values indicated in the parentheses are percentage differences of the present predictions from the corresponding solutions.

It is observed that as the value of ϕ increases from 0° to 30° the percent difference of the predicted solutions from those reported in the literature increases from 6.22% to 15.61% and from 4.47% to 40.53% for G equal to 0 and 1.0 respectively.

TABLE 4 1
Bearing capacity factors for smooth surface footings

See No. 116561

G	ϕ°	Spencer (1962)	Chen (1973)	Cox (1962)	Present study
0	0	5.14 (6.22)	5.14 (6.22)	5.14 (6.22)	4.82
	10	8.35 (11.86)	8.35 (11.86)	8.34 (11.86)	7.36
	20	14.80 (12.16)	14.80 (12.16)	14.80 (12.16)	13.00
	30	30.10 (15.61)	30.10 (15.61)	30.10 (15.61)	25.40
1.0	0	5.14 (4.47)	5.14 (4.47)	5.14 (4.47)	4.91
	10	9.07 (12.45)	9.05 (12.26)	9.02 (11.97)	7.94
	20	18.30 (26.55)	18.10 (25.75)	17.90 (24.92)	13.44
	30	45.30 (40.53)	44.30 (39.18)	42.90 (37.20)	26.94

The obtained bearing capacity factors for rough surface footings are presented and compared with the available limit analysis and limit equilibrium solutions (Chen and Davidson, 1973) as shown in Table 4 2 for different values of ϕ and G . It is

observed from the table that the present solution is only 7 82% lower than the upper bound limit analysis solution (Chen, 1973) for $\phi=10^0$ case but increases to 30 68% when ϕ is 30^0 . The present study predicts with a very small difference from that of the Terzaghi (1943) and Meyerhof (1951) solutions. These differences being 1 37% and 12 30% respectively, but the corresponding differences from the Hansen (1961) solution are 5 73% and 16 31%

TABLE 4 2
Bearing capacity factors for rough ($\delta=\phi$) surface footings

G	ϕ^0	Chen (1973)	Hansen (1961)	Terzaghi (1943)	Meyerhof (1951)	Present study
0 15	10	8 56 (7 82)	8 37 (5 73)	8 00 (1 37)	8 00 (1 37)	7 89
1 0	30	58 20 (30 68)	48 20 (16 31)	46 00 (12 30)	46 00 (12 30)	40 34

As no slip line solution is available for the rough surface footings bearing on a cohesive soil, the obtained solutions using the present analysis could not be compared with any lower bound solution. Chen and Davidson (1973) have observed that in case of upper bound solutions the difference between the limit analysis and slip line solutions may be of the order of 40%. In the present case it ranges from 6 22 to 39 18% for surface footing

As it is impossible to guess a feasible starting point design vector in such analytical problems, the iterations to obtain the optimal solutions were carried out starting from any chosen design vector whose all the elements are considered to be zero. Table 4 3 shows the initial stress vector along with the equality and inequality constraints corresponding to the rough surface footing

TABLE 4 3*

Initial design vector, sigma vector, and constraints for rough surface footing, ($G=1$ 0 and $\phi = 30^\circ$)

(D)Vector

0 0000	0 0000	0 0000	0 0000	0 0000	0 0000	0 0000
0 0000	0 0000	0 0000	0 0000	0 0000	0 0000	0 0000

(σ)Vector

0 0000	0 4348	0 0000	0 0000	0 0000	0 0000	0 0000
0 0000	0 3707	0 0000	-1 1033	0 0000	-1 1888	0 0000
0 2010	-0 3446	0 6219	0 0000	0 0000	0 5523	0 2666
0 0000	0 0000	0 0000	0 0000	0 0000	0 0000	1 4583
0 0000	-0 9442	0 0000	0 0000			

Interface shear equality constraints

-0 3576E-06	-0 1490E-06	0 0000	0 4685E-06	0 2384E-06
-0 1238E-06	-0 4923E-07	0 2384E-07	-0 8940E-07	0 2533E-06

Boundary shear equality constraints

0 0000	-0 3344E-07	0 0000	-0 8940E-07	0 9685E-07
0 2980E-07				

Yield Constraints(inequality)

-0 7500E 00	-0 2317E+01	-0 7500E 00	-0 1401E+01	0 1232E+01
-0 7499E+00	-0 9276E+00	-0 7500E+00	-0 1100E+00	-0 7500E+00
0 2319E+01	0 8394E+01	-0 7500E+00	0 8394E+01	0 7976E+02
-0 7500E 00	<u>0 2745E+02</u>	<u>0 3560E+01</u>		

No-tension constraints(inequality)

0 0000E+00	-0 4348E+00	0 0000	0 0000	0 0000
-0 2802E-07	0 0000	0 0000	-0 3707E 00	-0 4517E-07
0 1032E+01	0 2037E-06	<u>0 1888E+01</u>	0 5293E-07	-0 2010E 00
<u>0 3446E 00</u>	-0 6219E 00	0 0000	0 0000	-0 5523E 00
-0 2666E 00	0 0000	0 0000	0 0000	0 0000
0 0000	0 0000	-0 4583E+01	0 0000	<u>0 9442E+00</u>

*All values are normalized with 1000psf (47 9kN/m²)

TABLE 4 4 *

Final design vector, sigma vector, constraints and objective function value for rough surface footing, ($G=1$ 0 and $\phi=30^\circ$).

(D)Vector							
1 1186	6 4237	7 0289	18 4099	17 5263	9 6647	13 2888	
6 6411	10 5274	7 3531	5 0921	22 8167	3 8670	4 6501	
(σ)Vector							
11 4637	9 0451	18 4099	4 6501	1 1186	0 8659	22 8167	
17 5263	11 7815	3 5538	7 0027	2 0061	3 8649	0 8659	
9 4697	6 0546	16 0832	6 4237	7 0289	10 6693	6 5505	
9 6647	13 2888	6 6411	10 5274	7 3531	5 0921	2 3775	
3 8670	0 8648	0 0000	0 0000				
Interface shear equality constraints							
-0 1788E-05	0 1654E-05	-0 8344E-06	0 5115E-06	-0 5960E-06			
0 4196E-06	-0 5396E-05	-0 1192E-06	-0 3963E-05	0 4604E-05			
Boundary shear equality constraints							
0 1072E-05	-0 2031E-06	0 4768E-06	0 2473E-05	-0 5320E-06			
-0 4172E-06							
Yield constraints(inequality)							
-0 3668E-01	-0 7679E+02	-0 3495E-01	-0 5798E-03	-0 8499E+01			
-0 2736E+01	-0 3747E+02	-0 1392E+03	-0 2794E+02	-0 9682E-01			
-0 4162E+01	-0 1287E+02	-0 1210E+00	-0 6299E-01	-0 5987E+01			
-0 3862E-03	-0 2670E-03	-0 3984E-02					
No-tension constraints(inequality)							
-0 1146E+02	-0 9045E+01	-0 1840E+02	-0 4650E+01	-0 1118E+01			
-0 8659E 00	-0 2281E+02	-0 1752E+02	-0 1178E+02	-0 3553E+01			
-0 7002E+01	-0 2006E+01	-0 3864E+01	-0 8659E 00	-0 9469E+01			
-0 6054E+01	-0 1608E+02	-0 6423E+01	-0 7028E+01	-0 1066E+02			
-0 6550E+01	-0 9664E+01	-0 1328E+02	-0 6641E+01	-0 1052E+02			
-0 7353E+01	-0 5092E+01	-0 2377E+01	-0 3867E+01	-0 8648E 00			
Optimal function value							
40 3429							

*All values are normalized with 1000psf (47 9kN/m²)

with $G=1.0$ and $\phi=30^\circ$. Most of the inequality constraints are strictly satisfied being negative values while some of the equality constraints are of such a small order of magnitude that for all practical purposes these may be considered to be satisfied. The remaining constraints which have been underlined are the violated constraints. Using the technique as mentioned the final design vector, constraints and the objective function at the optimum as obtained are presented in Table 4.4. On comparing Table 4.3 and Table 4.4 it is noticed that the violated constraints have become negative and hence getting strictly satisfied. This indicates the efficiency of the present technique in its own category in solving multivariable-multiconstrained nonlinear optimization problem starting from any arbitrary design vector which may even be infeasible. It may further be noted that the term efficiency has been used here to signify the capacity of the method in isolating the optimal solution and not in terms of the economy of computation.

In Figs 4.2(a) and 4.2(b) variation of the objective function with penalty parameter and number of function evaluations is shown for the rough surface footing with $G=1.0$ and $\phi = 30^\circ$ respectively.

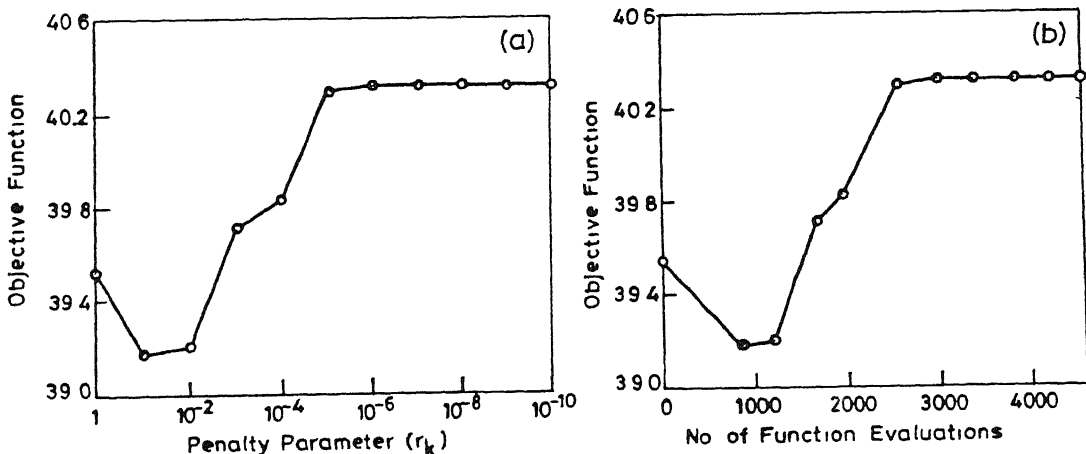


Fig. 4.2 Variation of objective function with (a) Penalty parameter and (b) number of function evaluations

TABLE 4 5*
 Stress field and the stress-strength ratios at the nodal points
 for rough surface footing, ($G=1$ 0 and $\phi=30^\circ$)

Element no	Nodal point no	σ_x	σ_z	τ_{zx}	Stress-strength ratio
1	1	7 0289	22 8167	0 0000	0 9998
1	2	10 6693	29 9426	0 0000	0 8286
1	8	7 0281	17 5263	3 9537	0 9997
2	2	8 5177	24 4345	3 4426	0 9999
2	4	0 1102	10 8068	5 7067	0 9387
2	8	3 2571	7 8704	2 0811	0 9338
3	2	0 6550	18 4099	0 0000	0 7895
3	3	9 6647	13 2888	0 0000	0 0862
3	4	9 6647	6 6411	3 3263	0 6564
4	8	3 2428	4 6501	2 2958	0 9958
4	4	11 0237	10 5274	5 7253	0 9692
4	5	9 7544	7 3531	4 1860	0 8549
5	8	2 8504	1 1186	1 1186	0 9850
5	5	9 5032	5 0921	3 4323	0 9990
5	6	7 1094	2 3775	0 8785	0 8097
6	8	1 7318	0 0000	0 0000	0 9998
6	6	6 2320	1 5000	0 0010	0 9999
6	7	1 7297	0 0000	0 0000	0 9986

*Stress values are normalized with 1000psf(47 9kN/m²)

Lysmer (1970) has stated that satisfying the nonlinear no-yield constraints only at the corners of each triangular element is the necessary and sufficient condition for the obtained solution to be a lower bound. However, he did not prove it and as such, doubts may be expressed whether the bound obtained by using Lysmer's method is a true lower bound or not. To demonstrate this a study was conducted by calculating the stress-strength ratios for a large number of points within and along the edges of the elements and drawing the contours of the stress-strength ratios. Fig 4 3 shows these contours for a typical element (Element no 1), for this purpose 457 points were considered. The figure clearly shows that nowhere within the element stress-strength ratios exceeds unity. This indicates the obtained bound is a true lower

bound. The study being a general one its findings are valid for all the problems studied in this thesis. As such, to avoid the repetition it will not be reported elsewhere.

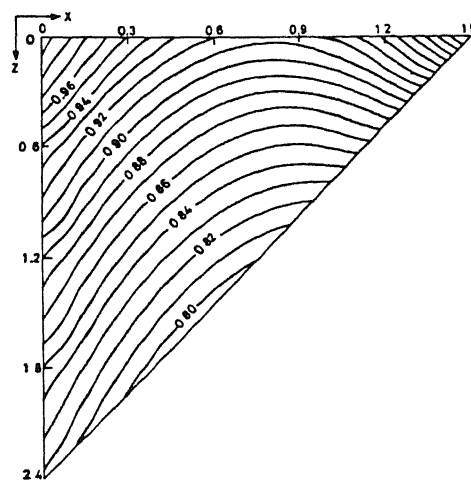


Fig 4.3 Contours of stress-strength ratio

4.3 Embedded footings

In studying the bearing capacity of surface footings, Lysmer (1970) has highlighted the importance of mesh pattern on the obtained solution and suggested that as many elements as possible should have the singularity point as their common vertex. As such it is necessary to study the effect of mesh pattern on the lower bound solutions for an embedded footing.

4.3.1 Statement of the problem

Fig 4.4 shows different mesh patterns for a smooth strip footing embedded at 3.70m depth in a purely cohesive soil with undrained cohesive strength equal to 0.295 MN/m^2 and total unit weight equal to 0.018 MN/m^3 . The objective is to find a generalized mesh pattern which gives the best solution and use it subsequently for obtaining the bearing capacity solutions for different values

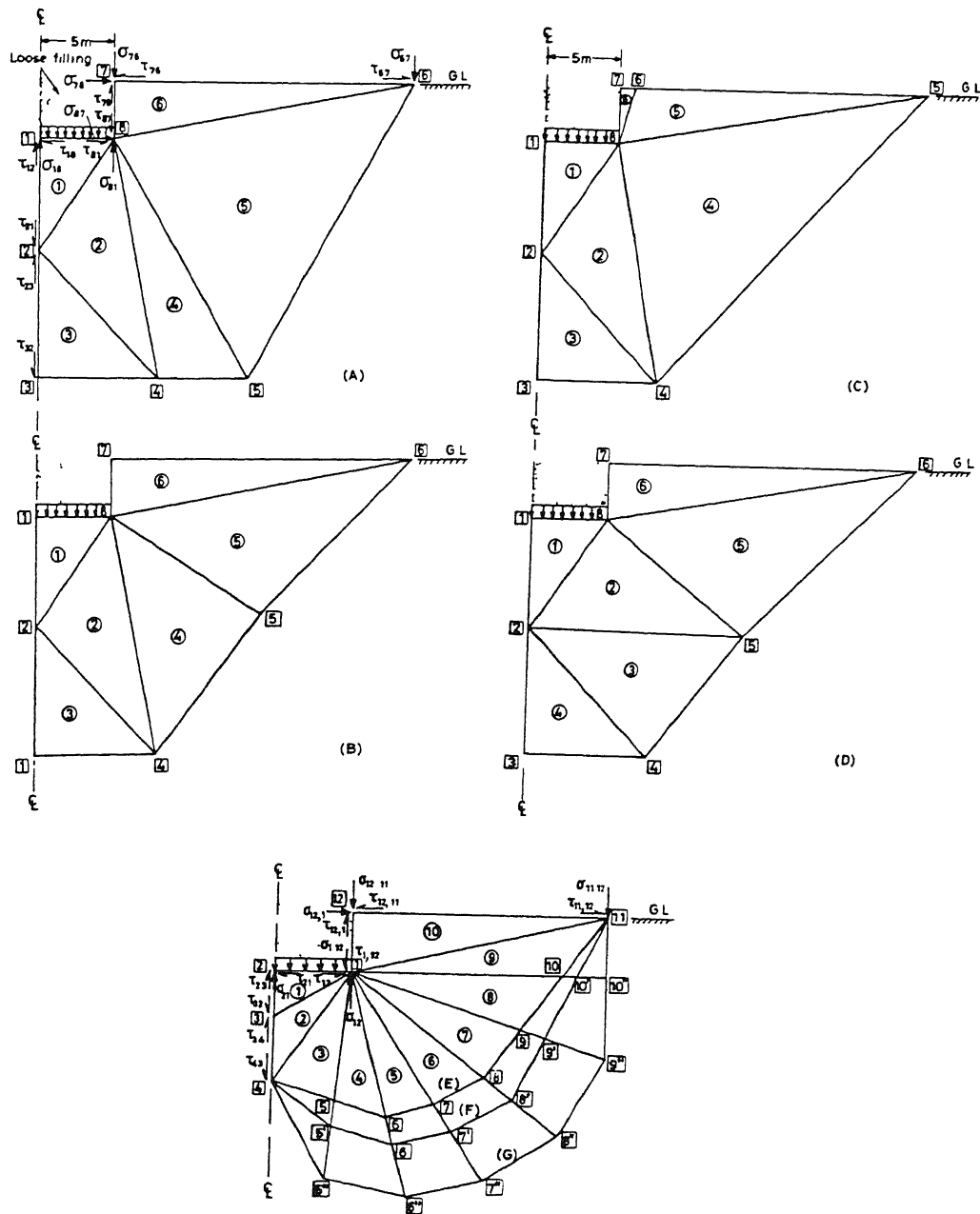


Fig 4.4 Mesh patterns for the embedded strip footing

of angle of internal friction (ϕ), embedment ratios (D/B), and dimensionless parameter G ($=\gamma B/2C$) For rough footings the angle of base friction (δ) has been taken equal to the ϕ value

4 3 2 Boundary conditions and the Objective function

Boundary conditions

With reference to the Fig 4 4 the boundary conditions specified are as follows

Case 1 (Mesh patterns A-D)

$$\begin{aligned}\sigma_{76} &= \sigma_{67} = \sigma_{78} = \sigma_{87} = 0 \quad \text{and,} \\ \tau_{18} &= \tau_{81} = \tau_{12} = \tau_{21} = \tau_{23} = \tau_{32} = \tau_{78} = \tau_{87} = \tau_{76} = \tau_{67} = 0\end{aligned}$$

Case 2 (Mesh patterns E)

$$\begin{aligned}\sigma_{11,12} &= \sigma_{12,11} = \sigma_{1,12} = \sigma_{12,1} = 0 \quad \text{and,} \\ \tau_{11,12} &= \tau_{12,11} = \tau_{1,12} = \tau_{12,1} = \tau_{32} = \tau_{23} = \tau_{34} = \tau_{43} = \tau_{12} = \tau_{21} = 0\end{aligned}$$

(for smooth footing)

and

$$\left. \begin{aligned}1) \tau_{11,12} &= \tau_{12,11} = \tau_{1,12} = \tau_{12,1} = \tau_{32} = \tau_{23} = \tau_{34} = \tau_{43} = 0 \\ 2) \tau_{12} &= C + \sigma_{12} \tan \delta, \quad 3) \tau_{21} &= C + \sigma_{21} \tan \delta\end{aligned} \right\} \text{(rough footings)}$$

Objective function

$$\text{Case 1} \quad -(\sigma_{18} + \sigma_{81}) \quad \text{and} \quad \text{Case 2} \quad -(\sigma_{12} + \sigma_{21})$$

Bearing capacity is equal to half of the objective function

4 3 3 Results and Discussions

In Fig 4 4 nodal points 2 and 8 are the singularity points for mesh patterns A to D and for the mesh pattern E the same is nodal point 1. The predicted results and their percent differences (values in parentheses) from the computed limiting equilibrium bearing capacity solution (15829 MN/m^2) using the approach of Meyerhof (1951) are presented in Table 4 6

51

TABLE 4 6
Effect of mesh pattern on the bearing capacity

Mesh pattern	Objective function (MN/m ²)	Bearing Capacity (MN/m ²)
A	1 1266	0 5633(64 41)
B	1 9757	0 9878(37 59)
C	1 4318	0 7159(54 77)
D	2 2534	1 1267(28 82)
E	3 1256	1 5628(1 27)

It is pertinent to note that although all these mesh patterns predict feasible solutions, tension occurs in the x-direction in element number 5 at nodal point number 8 in case of mesh pattern A, the value being -0.0183 MN/m^2 (as shown in Table 4 7) and at nodal points 8 and 5 in case of mesh pattern C, the value being -0.0028 and -0.0135 MN/m^2 (as shown in Table 4 8). However, these values of tension are much smaller than either $C/9$ ($=0.032 \text{ MN/m}^2$) or $C/10$ ($=0.0295 \text{ MN/m}^2$) which may be allowed as the permissible tension in cohesive soils as suggested by Chen (1975).

It can be seen from Table 4 6 that the mesh pattern E gives a solution which is only 1 27% on the safer side from that of limit equilibrium solution. As such, for embedded footings mesh pattern E has been suggested for evaluating the bearing capacity. This pattern differs from the one suggested by Lysmer (1970) for surface footings, but the suggestion made by him regarding the choice of singularity point as the common point to as many elements as possible has been found to be quite relevant and valid for embedded footing also.

Since the mesh pattern E predicts the best results, extensibility of the stress field has been studied and is reported as follows. The mesh pattern is extended (meshes F and G) as shown in Fig 4 4. It is noticed that the patterns E, F and G predict the

TABLE 4 7

Stress field and the stress-strength ratios at the nodal points
for mesh pattern (A) (stress values are in MN/m²)

Element No	Nodal point No	σ_x	σ_z	τ_{zx}	stress-strength ratio
1	2	0 1676	0 4540	0 0000	0 2357
1	8	0 2088	0 7985	0 0000	0 9990
1	1	0 2088	0 3280	0 0000	0 0408
2	2	0 0574	0 6467	0 0083	0 9986
2	4	0 2025	0 7314	0 0776	0 8730
2	8	0 1243	0 5486	0 1484	0 7705
3	2	0 0491	0 6385	0 0000	0 9978
3	3	0 7342	0 7885	0 0000	0 8484
3	4	0 7342	0 3427	0 0061	0 4406
4	8	0 1648	0 3077	0 2255	0 6433
4	4	0 3238	0 7083	0 2235	0 9986
4	5	0 3169	0 7758	0 1847	0 9972
5	6	0 0006	0 0000	0 0001	-
5	8	-0 0182	0 0669	0 0008	0 0208
5	5	0 1874	0 3472	0 0518	0 1043
6	6	0 0000	0 0000	0 0000	-
6	7	0 0000	0 0000	0 0000	-
6	8	0 0000	0 0676	0 0000	0 0103

TABLE 4 8

Stress field and the stress-strength ratios at the nodal points
for mesh pattern (C) (stress values are in MN/m²)

Element No	Nodal point No	σ_x	σ_z	τ_{zx}	stress-strength ratio
1	2	0 6037	0 5124	0 0000	0 0234
1	8	0 4845	1 0454	0 0000	0 9038
1	1	0 4845	0 3864	0 0000	0 0276
2	2	0 3899	0 9789	0 0169	0 9998
2	4	0 3206	0 8965	0 0586	0 9923
2	8	0 4857	0 8597	0 0654	0 4510
3	2	0 4068	0 9958	0 0000	0 9966
3	3	0 5798	1 1687	0 0000	0 9960
3	4	0 5758	0 4623	0 0288	0 0492
4	8	0 3867	0 1013	0 2580	0 9992
4	4	0 2519	0 1441	0 1882	0 4406
4	5	0 3855	0 0720	0 0351	0 2965
5	6	0 0000	0 0004	0 0001	-
5	8	-0 0028	0 0146	0 0121	0 0026
5	5	-0 0135	0 0036	0 2681	0 8267
6	6	0 0000	0 0000	0 0000	-
6	7	0 0000	0 0000	0 0000	-
6	8	0 0000	0 0666	0 0000	0 0101

bearing capacity values 3 1256, 3 0239 and 3 1673 MN/m² respectively, the difference for all practical purposes may be considered to be negligible. This indicates that the stress field obtained by using mesh pattern E is correct.

The complete stress field along with the stress-strength ratio is shown in Table 4.9. A ratio close to unity signifies the limiting state.

It is impossible to guess a feasible starting point design vector in such analytical problems. The optimal feasible solutions were obtained starting from any arbitrarily chosen design vector. The efficiency of the present technique in its own category in solving multivariable - multiconstrained nonlinear optimization problem starting from any arbitrary design vector has been found to be very good. However, for reasons of space and brevity the details are not presented as it involves 22 design variables and 106 constraints for the mesh pattern E with 10 elements.

Using the general mesh pattern of the Fig 4.4(E) a parametric study has been conducted to compare the obtained solutions by using the Lysmer-Basudhar approach for the reported studies on the rough embedded strip footings over a wide range of parameters. The comparison of the results is presented in Table 4.10.

It is observed from the table that keeping ϕ and G constant as D/B ratio increases from 0.5 to 1.0 the percentage differences also increase. The present study predicts the solutions which are 22.21-24.55% lower than the limit analysis solutions (Chen, 1973). For this case the differences from the Terzaghi (1943) and Hansen (1961) solutions is 3.46-4.34% and 17.75-20.68% respectively. When

TABLE 4 9
 Stress field and the stress-strength ratios at the nodal points
 for mesh pattern (E) (stress values are in MN/m²)

Element No	Nodal point No	σ_x	σ_z	τ_{zx}	stress-strength ratio
1	1	1 1209	1 7034	0 0000	0 9746
1	2	1 1209	1 4222	0 0000	0 2608
1	3	1 0713	1 4762	0 0000	0 4712
2	1	1 1421	1 7110	0 0127	0 9316
2	3	1 0713	1 4762	0 0000	0 4712
2	4	0 9767	1 5584	0 0000	0 9719
3	1	0 9859	1 4049	0 2059	0 9915
3	4	0 9488	1 5036	0 0392	0 9018
3	5	0 8969	1 2222	0 2422	0 9784
4	1	0 9801	0 7820	0 2659	0 9255
4	5	0 8940	0 9108	0 2723	0 8526
4	6	0 8795	0 8536	0 2887	0 9598
5	1	0 9606	0 5315	0 1959	0 9698
5	6	0 8664	0 6862	0 2419	0 7658
5	7	0 8476	0 5036	0 1953	0 7784
6	1	0 9637	0 5379	0 2004	0 9823
6	7	0 8681	0 5455	0 2246	0 8788
6	8	0 7487	0 1821	0 0408	0 9417
7	1	0 5963	0 3344	0 0731	0 2585
7	8	0 5593	0 0771	0 1002	0 7835
7	9	0 8672	1 0454	0 2744	0 9562
8	1	0 5811	0 0956	0 1334	0 8815
8	9	0 8404	0 6252	0 1681	0 4576
8	10	0 5031	0 0719	0 0578	0 5725
9	1	0 6131	0 0956	0 1334	0 9739
9	10	0 4186	0 0719	0 0578	0 3836
9	11	0 4277	0 0203	0 0931	0 5765
10	1	0 0000	0 0666	0 0000	0 0127
10	11	0 0000	0 0000	0 0000	-
10	12	0 0000	0 0000	0 0000	-

TABLE 4 10
 Bearing capacity factors for rough embedded footings

G	ϕ^0	D/B	Chen (1973)	Hansen (1961)	Terzaghi (1943)	Meyerhof (1951)	Present study
0 15	10	0 5	10 40 (22 21)	10 20 (20 68)	8 38 (3 46)	-	8 09
0 15	10	1 0	12 10 (24 55)	11 10 (17 75)	8 75 (4 34)	-	9 13
1 0	30	0 5	83 60 (18 38)	74 80 (8 78)	64 00 (6 61)	82 00 (16 79)	68 23

D/B is constant, the cumulative effect of the increase in G and ϕ values manifests in the increase of bearing capacity factor and the result differs by about 18 38-22 21% on the safer side from Chen's solution. The difference between the present solution and those of Hansen, Terzaghi and Meyerhof for $G=1.0$, $\phi=30^0$ and $D/B=0.5$, are 8 78, 6 61 and 16 79% respectively. The study reveals that the values obtained by the present study agree excellently with the Terzaghi's results and are in close agreement with the other reported results.

As no slip line solution is available for the rough surface and embedded footings bearing on a cohesive soil, the obtained solutions using the present analysis in predicting the bearing capacity could not be compared with any lower bound solution.

The study reveals that when ϕ is increased keeping all other parameters constant the difference in the predicted values from the reported values decreases for embedded footing. Chen and Davidson (1973) have observed that in case of upper bound solutions the difference between the limit analysis and slip line solutions may be of the order of 40%. In the present case it ranges from 18 38 to 24 55% for embedded footing.

In Figs 4 5(a) and 4 5(b) variation of the objective function with penalty parameter and number of function evaluations is shown for the mesh pattern E. It is observed that the minimum is achieved corresponding to the penalty parameter equal to 1E-05 and 3200 function evaluations.

The CPU time required for the various cases studied is from 0.65 to 3.54 seconds.

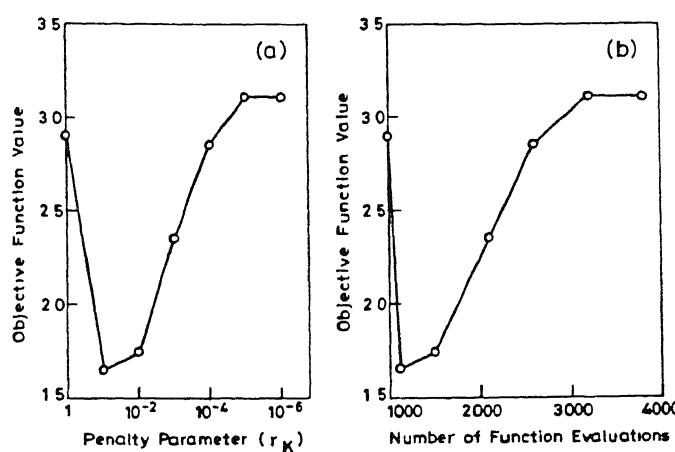


Fig 4.5 Variation of objective function with (a) Penalty parameter and (b) number of function evaluations for mesh pattern E

4.4 Conclusions

On the basis of the presented results and discussions the following generalized conclusions can be drawn

- 1) The Lysmer-Basudhar method using discrete element and nonlinear programming is quite reliable in predicting the lower bound bearing capacity of surface and embedded strip footings
- 2) The obtained results are in good agreement with the results presented in the literature for cohesive soils and thus reduce the bounds for the collapse load. However, for C- ϕ materials as ϕ and embedment ratio increases the differences in the predicted values using the present approach and other analyses also increase
- 3) For surface footing the mesh pattern as suggested by Lysmer (1970) gives excellent results. For embedded footings a new generalized mesh pattern has been suggested and may be adopted to obtain a good lower bound bearing capacity solution
- 4) The sequential unconstrained minimization using the concept of extended penalty function in conjunction with Powell's technique for multivariable search and quadratic interpolation for unidirectional search is found to be efficient in isolating the optimal solution

CHAPTER 5

BEARING CAPACITY OF SURFACE AND EMBEDDED FOOTINGS LOCATED ABOVE CONTINUOUS Voids

5 1 General

The bearing capacity of foundations on a homogeneous soil bed, without a continuous void, under the condition of plain strain has been studied by various investigators as discussed in Chapter 4. Only a few studies are available for the stability of foundations above voids. The earliest studies are by Terzaghi (1936, 1943) on soil arching. Baus and Wang (1983) and Azam et al (1991) have investigated the bearing capacity of strip footings located above a continuous void based on finite element technique assuming a perfectly elasto-plastic soil. These studies show that the classical bearing capacity theory, if applied to evaluate the effect of void on the bearing capacity of foundation, may lead to erroneous results. Based on Hsieh's analysis by using the upper bound theorem of limit analysis, Wang and Hsieh (1987) have presented equations for estimating the bearing capacity of strip footings for different void conditions (Azam et al ,1991). But no lower bound solutions are available for such cases. As such, a study to find out the lower bound bearing capacity of such problems is reported in the subsequent sections.

5 2 Statement of the Problem

Fig 5 1 shows a smooth strip footing situated above a continuous void. As shown in the figure, B, D_f, D, W, H, d, and T, designate the footing width, depth of foundation, depth to void, width of the void, height of the void, vertical distance between

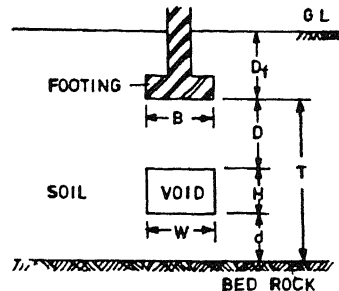


Fig 5 1 Details of a strip footing and a continuous void

bottom of void and bed rock surface and thickness of soil stratum measured from footing base, respectively. The objective is to find the bearing capacity of the footing for different conditions of void location, depth to bed rock, and soil layer characteristics and compare it with the available experimental and finite element results. The material properties of the foundation soil have been adopted from the literature (Baus and Wang, 1983, Azam et al ,1991) and are presented in Table 5 1

TABLE 5 1
Material properties of foundation soils

Case	C (kN/m^2)	ϕ^0	γ (kN/m^3)	Tensile strength (kN/m^2)
A-C	158 50	8 00	13 60	48 2
D	65 60	13 50	15 78	14 0

The following void conditions have been considered

Embedded footing with $B=D_f=51\text{mm}$ and $W=102\text{mm}$ (Azam et al ,1991)

Case A No void condition

Case B A void in the bed rock with its top flushing with bed rock surface ($H=d=0$)

Case C A 102mm square void with its base 76mm above the bed rock surface ($H=102\text{mm}$, $d=76\text{mm}$)

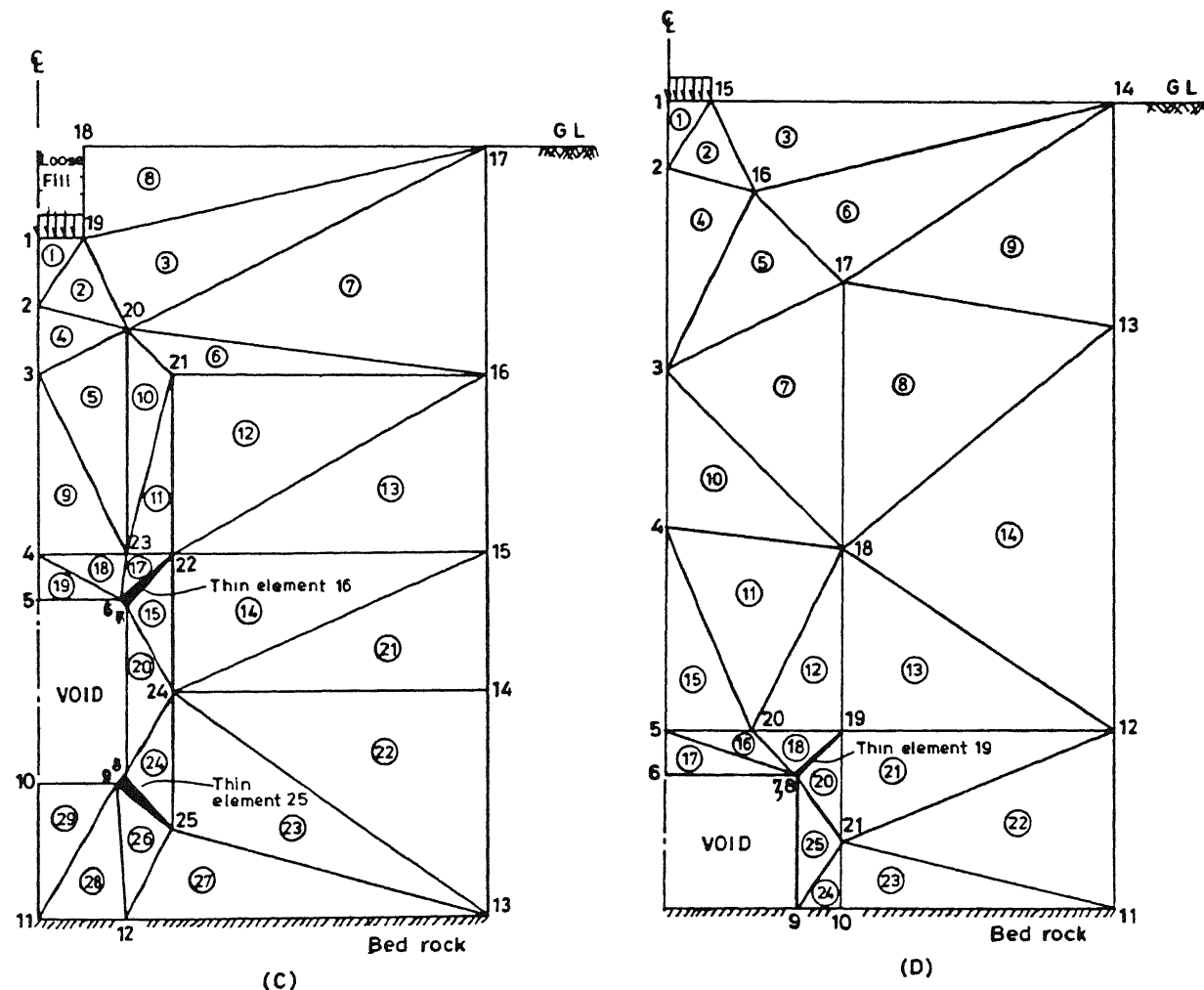
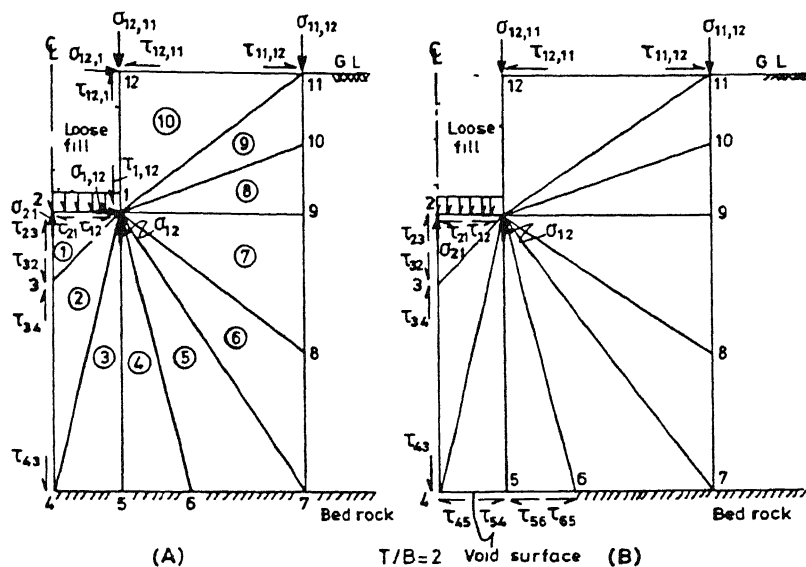


Fig 5.2 Mesh patterns for the strip footing corresponding to the various locations of the void

Surface footing with B=51mm and D=380mm (Baus and Wang, 1983)

Case D A 152mm wide void with height 76mm (W=152mm, H=76mm)

For embedded and surface footings the mesh patterns as shown in Fig 5 2 are adopted corresponding to the different conditions of void (Cases A to D) as described earlier. These are the best possible mesh patterns which have been arrived at after several trials. The mesh patterns for the cases A and B are similar differing only in terms of shear boundary conditions due to the presence of the void, the same for the cases C and D are again almost similar but differ from that of A and B and the choice is necessitated by the void location and its size to take care of the arching of the soil. To isolate the corner points of the voids where stress concentration is likely to occur, very thin elements have been considered. This isolation has been done at both the corner points for case C while for case D it is not necessary for the bottom corner point as the base of the void flushes with the bed rock surface.

5 3 Boundary conditions and the Objective functions

With reference to the Fig 5 2 the specified boundary conditions and the corresponding objective functions are as follows

5 3 1 Embedded footings: 1) Cases A and B

Boundary conditions

$$\sigma_{12,11} = \sigma_{11,12} = \sigma_{12,1} = \sigma_{1,12} = 0$$

$$\tau_{12,11} = \tau_{11,12} = \tau_{12,1} = \tau_{1,12} = \tau_{12} = \tau_{21} = \tau_{23} = \tau_{32} = \tau_{34} = \tau_{43} = 0,$$

along with 4 more shear boundary conditions for Case B as follows

$$\tau_{45} = \tau_{54} = \tau_{56} = \tau_{65} = 0$$

$$\text{Objective function } -(\sigma_{12} + \sigma_{21})$$

2) Case C

Boundary conditions

$$\sigma_{17,18} = \sigma_{18,17} = \sigma_{19,18} = \sigma_{18,19} = \sigma_{56} = \sigma_{65} = \sigma_{67} = \sigma_{76} = 0$$

$$\sigma_{78} = \sigma_{87} = \sigma_{89} = \sigma_{98} = \sigma_{9,10} = \sigma_{10,9} = 0$$

$$\tau_{17,18} = \tau_{18,17} = \tau_{18,19} = \tau_{19,18} = \tau_{1,19} = \tau_{19,1} = \tau_{12} = \tau_{21} = 0$$

$$\tau_{23} = \tau_{32} = \tau_{34} = \tau_{43} = \tau_{45} = \tau_{54} = \tau_{56} = \tau_{65} = 0$$

$$\tau_{67} = \tau_{76} = \tau_{78} = \tau_{87} = \tau_{89} = \tau_{98} = \tau_{9,10} = \tau_{10,9} = 0$$

$$\tau_{10,11} = \tau_{11,10} = 0$$

$$\text{Objective function } -(\sigma_{1,19} + \sigma_{19,1})$$

5.3.2 Surface footing. Case D

Boundary conditions

$$\sigma_{14,15} = \sigma_{15,14} = \sigma_{67} = \sigma_{76} = \sigma_{78} = \sigma_{87} = \sigma_{89} = \sigma_{98} = 0,$$

$$\tau_{14,15} = \tau_{15,14} = \tau_{67} = \tau_{76} = \tau_{78} = \tau_{87} = \tau_{89} = \tau_{98} = \tau_{1,15} = \tau_{15,1} = 0$$

$$\text{and, } \tau_{12} = \tau_{21} = \tau_{23} = \tau_{32} = \tau_{34} = \tau_{43} = \tau_{45} = \tau_{54} = \tau_{56} = \tau_{65} = 0$$

$$\text{Objective function } -(\sigma_{1,15} + \sigma_{15,1})$$

Bearing capacity is estimated by averaging the stress terms involved in the objective function

5.4 Results and Discussions

Typical lower bound bearing capacity solutions as obtained on CONVEX C220 computer system are presented and compared with available solutions in Table 5.2. It is seen from the table that for no void condition (case A) the obtained results are very close to finite element solutions and the absolute percentage differ-

nces range only from -1 69 to 2 38% But, when the top of the void is flushing with the bed rock surface (case B) the same ranges from 14 05 to 20 83% The higher side predictions are contrary to the expectation that the present solution being a lower bound should be lower than the solution given by displacement type of finite element solution which gives the upper bound of the critical load Since the displacement boundary conditions adopted by Azam et al (1991) are not reported it is difficult to comment on the nature of the obtained finite element solutions Furthermore, they did not validate their results as such the correctness of the solutions needs to be verified by conducting model tests

The obtained solutions for Cases C and D are also presented in Table 5 2 It is observed that the present method predicts the results which are -32 80 to -33 46% of the finite element solutions but for Case D where the model test results are available the difference is -36 63% A comparative study of the

TABLE 5 2
Comparison of the bearing capacity solutions

Case	T/B	FEM solution (kN/m ²)	Present study (kN/m ²)	% differences
A	2	1470 0	1445 15	-1 69
	3	1330 0	1361 64	2 38
B	2	1120 0	1353 31	20 83
	3	1190 0	1357 23	14 05
C	7 5	1071 0	705 46	-32 80
D	9 0	700 0	465 78	-33 46
		735 0 *		-36 63

► As read from the graph(Baus and Wang,1983)

* Model footing test(Baus and Wang,1983)

● As read from the graphs(Azam et al ,1991)

results shows that displacement type finite element method using elasto-plastic constitutive relationship predicts the critical load which is very close to the experimental value. The present method predicts the value which is too conservative. However, for C- ϕ materials difference between the lower bound (slip line) and upper bound solutions may be of the order of 40% as observed by Chen and Davidson (1973).

The complete stress field along with the stress-strength ratio is shown in Table 5.3. The ratio close to unity signifies the limiting equilibrium state. From this consideration it may be observed that for the chosen mesh pattern many nodal points are very near to the limiting state.

TABLE 5.3
Stress field and the Stress-strength ratios at the nodal points
for Case A (T/B=2)

Element no	Nodal point no	$\frac{\sigma_x}{C}$	$\frac{\sigma_z}{C}$	$\frac{\tau_{zx}}{C}$	Stress-strength ratio
1	1	5 4897	9 1937	0 0000	0 8472
1	2	5 4897	8 7759	0 0000	0 6865
1	3	4 8977	8 7780	0 0000	0 9982
2	1	4 9364	8 6404	0 5533	0 9978
2	3	4 8977	8 7780	0 0000	0 9982
2	4	4 7816	7 1247	0 0000	0 4148
3	1	4 6714	4 4010	1 6131	0 9965
3	4	4 5059	2 7131	1 1029	0 9066
3	5	4 5780	3 5221	1 3247	0 8422
4	1	4 6714	5 2300	1 6131	0 9504
4	5	4 5780	4 2303	1 3247	0 6945
4	6	4 6501	4 2869	1 5769	0 9694
5	1	4 4764	2 1105	0 8332	0 9977
5	6	4 5645	2 9182	1 2347	0 9645
5	7	4 1988	1 8755	0 5745	0 8412
6	1	4 1693	1 5644	0 4237	0 9719
6	7	4 1418	1 7741	0 4985	0 8394
6	8	3 8305	1 2419	0 0652	0 9308
7	1	2 1470	0 6656	0 9244	0 9976
7	8	2 6864	0 7334	0 6974	0 9545
7	9	1 6985	0 6811	0 9965	0 9369
8	1	1 1840	0 6656	0 9244	0 7361
8	9	1 2202	0 6811	0 9965	0 8456
8	10	1 4655	0 6549	0 9844	0 8754
9	1	1 5893	0 7107	1 0595	0 9942
9	10	1 5420	0 6634	1 0099	0 9272
9	11	1 5350	0 6822	1 0233	0 9382
10	1	0 0000	0 0043	0 0000	0 4816
10	11	0 0000	0 0000	0 0000	0 2764
10	12	0 0000	0 0000	0 0000	0 4418

Table 5 4 presents the number of design variables, total number of constraints, number of function evaluations and the CPU time required to achieve the optimum solution for the various cases studied. It is observed from the table that CPU time required ranges from 0.21 to 1.38 seconds and the number of function evaluations required to reach the optimum lie in the range of 7292 to 28700.

TABLE 5 4
Optimization details for the various cases studied

Case	No of design variables	No of Constraints		No of function evaluations	CPU (Secs)
		Equality	Inequality		
A	22	28	138	9414	0.21
				10013	0.24
B	19	32	138	11592	0.37
				10430	0.33
C	30	94	382	28700	1.38
D	31	80	332	7292	0.49

In Figs 5 3(a) and 5 3(b) variation of the objective function with penalty parameter and number of function evaluations is shown for Case A respectively. It is observed that the minimum value of the objective function (17.9717) is achieved corresponding to the penalty parameter equal to 1E-04 and 7160 function evaluations.

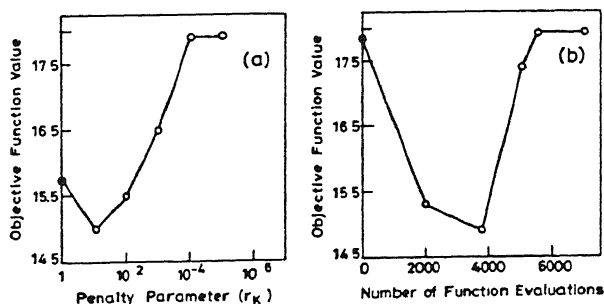


Fig 5 3 Variation of objective function with (a) Penalty parameter and (b) number of function evaluations

5.5 Conclusions

On the basis of the presented results and discussions the following generalized conclusions can be drawn

- 1) The Lysmer-Basudhar approach using discrete elements and nonlinear programming can be used for predicting the lower bound bearing capacity of surface and embedded strip footings above a void with a fair degree of confidence
- 2) For surface and embedded footings the mesh patterns as suggested may be adopted to obtain lower bound bearing capacity solutions
- 3) The sequential unconstrained minimization using extended penalty function in conjunction with Powell's technique for multivariable search and quadratic interpolation for unidirectional search is found to be efficient in isolating the optimal solutions
- 4) Although the differences of the obtained solutions from that of finite element solutions are within the acceptable range, detailed experimental investigations are necessary to judge their accuracy with respect to the true critical loads

CHAPTER 6

PULL OUT CAPACITY OF STRIP ANCHORS IN SAND

6 1 General

Over the years with increased use of the anchorage system to withstand tensile forces acting on foundations of onshore and offshore structures the necessity of adopting refined methods of analysis to predict its behavior has been felt by the researchers and engineers interested in this area. Several investigators developed limiting equilibrium methods to predict the pull out capacity of strip anchors embedded in sand. The procedures commonly used are empirical analysis based on earth cone method, semi empirical method based on anchor tests, limit equilibrium approach, limit analysis and finite element method. An excellent review of the various approaches to predict the anchor behavior has been presented by Das(1990) and, as such, not presented here. Lack of experimental as well as theoretical published data makes it difficult to estimate the anchor capacity within a small range of uncertainty. Limit theorems of plasticity can be used for predicting the pull out resistance enabling one to bracket the collapse load even if it can not be determined exactly. However, solution based on lower bound limit analysis is more relevant as it results in a safe engineering design. But for anchors such solutions are not available. As such, in this chapter suitability of Lysmer-Basudhar approach has been studied for estimating the pull out capacity and the breakout factors of vertical, horizontal and inclined anchors.

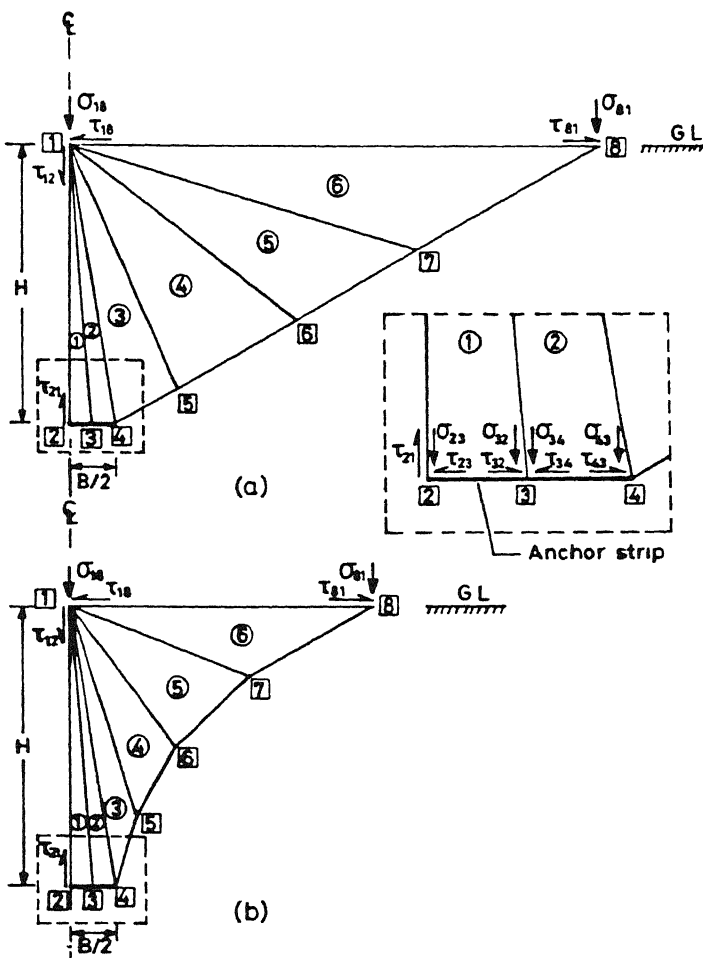


Fig 6.1 (a) Mesh pattern for shallow horizontal anchors
 (b) Mesh pattern for deep horizontal anchors

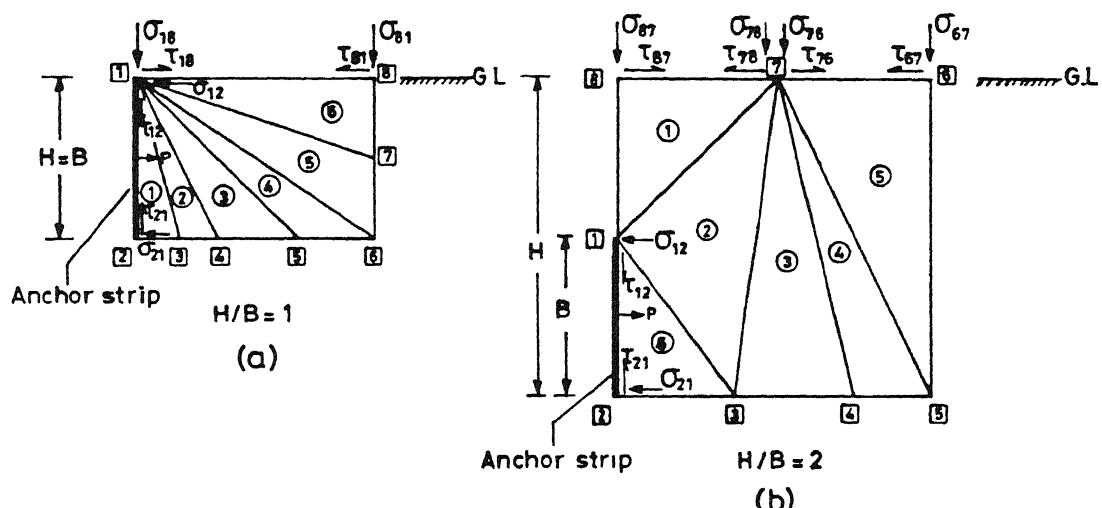


Fig 6.2 (a) Mesh pattern for shallow vertical anchors
 (b) Mesh pattern for deep vertical anchors

6 2 Statement of the Problem

Figs 6 1 and 6 2 show a horizontal and a vertical strip anchor respectively embedded in homogeneous and purely frictional soil ($\phi=32^0, 35^0$ and 38^0) deposit having a unit weight of 15 OkN/m^3

Fig 6 3 shows a strip anchor in sand inclined at an angle α to the horizontal. Inclination angles of $30^0, 45^0$ and 60^0 have been considered for analysis. The angle of internal friction and the unit weight of the sand are 35^0 and 17 OkN/m^3 respectively.

The objective is to find the pull out capacity of these anchors. The breakout factors are then subsequently computed. Both smooth and rough ($\delta=30^0$) strips have been considered.

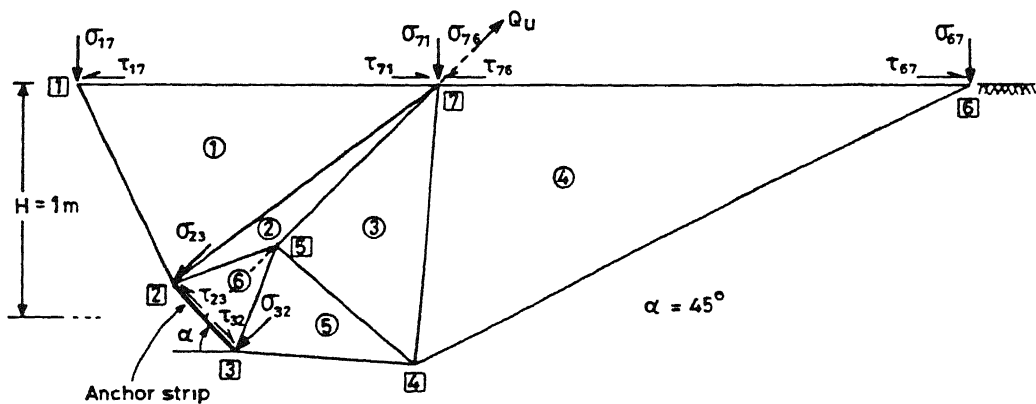


Fig 6 3 Mesh pattern for an anchor inclined at 45^0

6 3 Boundary conditions and the Objective functions

The boundary conditions and the respective objective functions are presented as follows

6 3 1 Horizontal anchors (Fig 6 1)

$$\sigma_{18} = \sigma_{81} = \tau_{18} = \tau_{81} = \tau_{12} = \tau_{21} = 0$$

$$\tau_{23} = \tau_{32} = \tau_{34} = \tau_{43} = 0 \quad (\text{for a smooth strip})$$

$$\left. \begin{array}{l} (\tau_{23} - \sigma_{23} \tan\delta) \leq 0, (\tau_{32} - \sigma_{32} \tan\delta) \leq 0 \\ (\tau_{34} - \sigma_{34} \tan\delta) \leq 0, (\tau_{43} - \sigma_{43} \tan\delta) \leq 0 \end{array} \right\} \text{(for a rough strip)}$$

Objective function $-(\sigma_{23} + \sigma_{32} + \sigma_{34} + \sigma_{43})$

6.3.2 Vertical anchors (Fig 6.2)

for $H/B = 1.0$, $\sigma_{18} = \sigma_{81} = \tau_{18} = \tau_{81} = 0$

and for $H/B > 1.0$, $\sigma_{87} = \sigma_{78} = \sigma_{76} = \sigma_{67} = \tau_{87} = \tau_{78} = \tau_{76} = \tau_{67} = 0$

$$\tau_{12} = \tau_{21} = 0 \quad \text{(for a smooth strip)}$$

$$(\tau_{12} - \sigma_{12} \tan\delta) \leq 0 \quad \left. \right\} \text{(for a rough strip)}$$

and $(\tau_{21} - \sigma_{21} \tan\delta) \leq 0 \quad \left. \right\} \text{(for a rough strip)}$

Objective function $-(\sigma_{12} + \sigma_{21})$ for both the cases

6.3.3 Inclined anchors (Fig 6.3)

$$\sigma_{67} = \sigma_{76} = \sigma_{71} = \sigma_{17} = 0$$

$$\tau_{76} = \tau_{67} = \tau_{17} = \tau_{71} = 0$$

$$\tau_{23} = \tau_{32} = 0 \quad \text{(for a smooth strip)}$$

$$(\tau_{23} - \sigma_{23} \tan\delta) \leq 0 \quad \left. \right\} \text{(for a rough strip)}$$

and $(\tau_{32} - \sigma_{32} \tan\delta) \leq 0 \quad \left. \right\} \text{(for a rough strip)}$

Objective function is $-(\sigma_{23} + \sigma_{32})$

The pullout capacity is obtained by averaging the terms involved in the objective functions

6.4 Results and Discussions

To validate and show the effectiveness of the proposed method in solving both smooth and rough ($\delta=30^\circ$) horizontal, vertical and inclined strip anchors results were obtained, using HP-9000/850s computer system. Different values of the ratio of the length to the width of the anchor (L/B) and the ratio of the depth of

embedment of the anchor to its width defined as the embedment ratio (H/B) for the horizontal and vertical anchors have been considered. In general the choice of mesh patterns is governed by previous experimental and theoretical studies available in the literature (Das, 1990). The parameters have been so chosen to facilitate the comparison of the obtained results with the reported solutions. The obtained results are presented and discussed as follows.

6.4.1 Horizontal anchors

Using the mesh patterns of Fig 6.1 the obtained results and their percentage differences from the limit equilibrium (Vermeer and Sutjiadi, 1985) and experimental results (Rowe and Davis, 1982b) are presented in Table 6.1. It is observed that the mesh pattern as shown in Fig 6.1(a) remains valid up to an embedment ratio equal to 4 and 3 corresponding to L/B ratios equal to 5 and 8.75 respectively. Beyond these values of embedment ratios no solution could be obtained using this mesh pattern. The predicted breakout factors compare very well up to H/B ratio equal to 3 (difference from the limit equilibrium solution being $\leq 5\%$) as compared to the predictions made with the mesh pattern depicted in Fig 6.1(b) (differences from limit equilibrium solution being as high as 17.0%). With mesh pattern shown in Fig 6.1(a) the obtained solution is only within 7.5% from that of experimental values for L/B ratios equal to 5 and 8.75 whereas for the mesh pattern shown in Fig 6.1(b) it is within 13.79%. These differences are well within the permissible limits. This phenomenon supports the argument for the classification of Horizontal plate anchors into

TABLE 6 1
Present solution and its percentage differences from the results
reported in the literature (for smooth horizontal anchors)

H/B L/B \	1	2	3	4	5	6	7	8
5 0	1 60 [•] 3 00 ⁺	2 25 [•] 2 00 ⁺	2 85 [•] 5 00 [*]	3 45 [•] 6 30 ⁺	-	-	-	-
			3 64 [*]					
8 75	1 95 [•] 17 00 ⁺	2 05 [•] 13 50 ⁺	3 45 [•] 6 30 ⁺	4 15 [•] 4 40 [*]	4 85 [•] 3 00 [*]	5 25 [•] 7 00 ⁺	6 10 [•] 3 20 [*]	2 40 [*]
		7 27 [*]		10 67 [*]	6 73 [*]			

► Fig 6 1(a) + % difference from Vermeer and Sutjiadi(1985)

► Fig 6 1(b) * % difference from Rowe and Davis(1982b)

● Present study

shallow and deep, based on the critical embedment ratio. The value of critical embedment ratio of 3 agrees well with that as suggested by Rowe and Davis (1982b). Incidentally Clemence and Veesaert (1977) have suggested the critical embedment ratio to be less or equal to 5.

The complete stress field for a smooth anchor, along with the stress-strength ratio is shown in Table 6 2, for H/b=5 and L/B=5. It is observed that the nodal point number 4 in element number 2 is very close to the limiting state. Similar stress fields are obtained for other embedment ratios too. However, for the sake of brevity these are not presented herein.

TABLE 6 2 *
Stress field for smooth horizontal anchor (H/B=5, L/B=5)

Element No	Nodal Point	σ_x	σ_z	τ_{zx}	Stress-strength ratio
1	1	0 0000	0 0000	0 0000	-
1	2	1 0133	1 0000	0 0000	0 0001
1	3	1 0133	2 0561	0 0000	0 4109
2	1	0 0000	0 0000	0 0000	-
2	3	1 0133	2 0561	0 0000	0 4110
2	4	1 0133	3 1122	0 0000	0 9217
3	1	0 0000	0 0000	0 0000	-
3	4	0 9872	0 4950	0 2617	0 8368
3	5	0 7698	0 3489	0 1505	0 7617
4	1	0 0000	0 0000	0 0000	-
4	5	0 7769	0 4877	0 1191	0 3125
4	6	0 5838	0 6492	0 0663	0 0512
5	1	0 0000	0 0000	0 0000	-
5	6	0 5091	0 4668	0 0504	0 0446
5	7	0 3249	0 2584	0 0186	0 0609
6	1	0 0000	0 0000	0 0000	-
6	7	0 2799	0 2500	0 0007	0 0114
6	8	0 0032	0 0000	0 0000	-

* Stress values are normalized with 15 0 kPa

Figs 6 4(a) and 6 4(b), show the variation of the objective function with the penalty parameter (r_k) and the number of function evaluations respectively. It can be seen from Fig 6 4(a) that as r_k reaches the value of 1E-04 the objective function attains a steady value (8 2243) The corresponding number of function evaluations is 460 as shown in Fig 6 4(b) This steady nature of the objective function indicates convergent solution

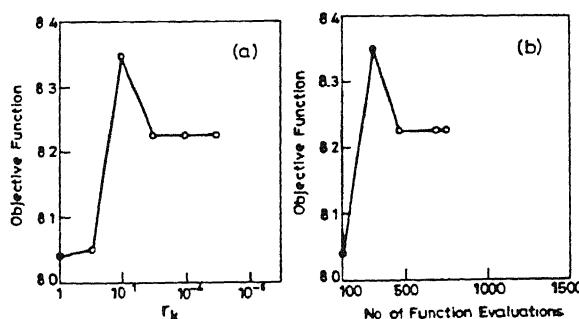


Fig 6 4 Variation of objective function with (a) Penalty parameter and (b) number of function evaluations for horizontal anchors

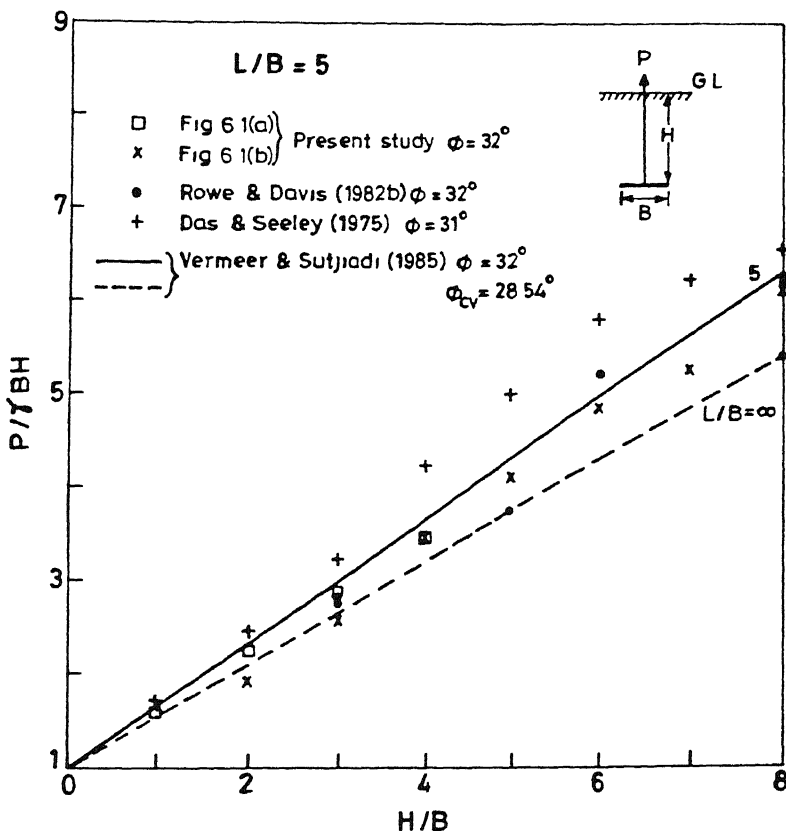


Fig 6 5 Breakout factor vs embedment ratio relationship for horizontal anchors

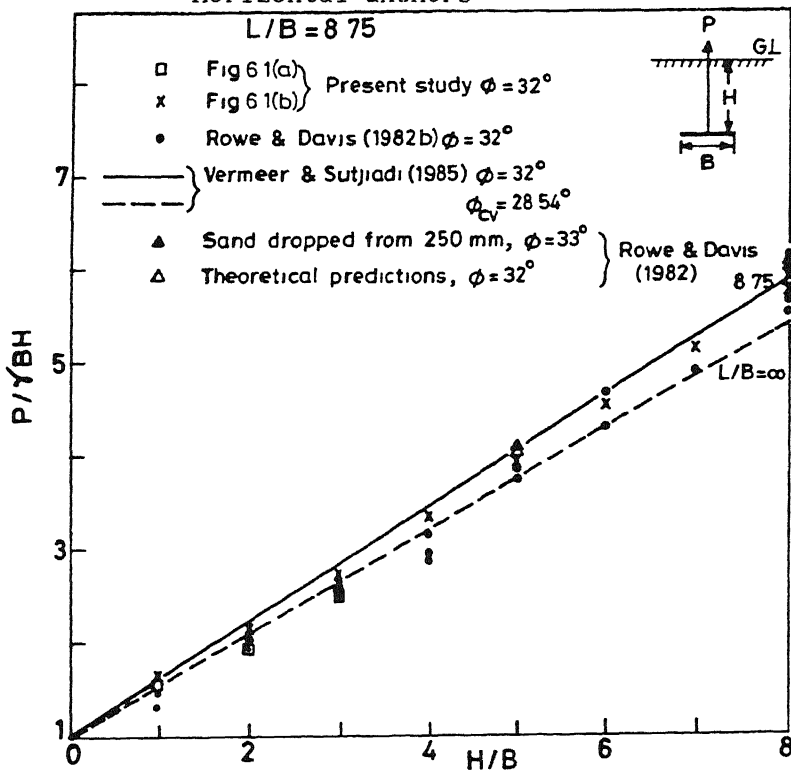


Fig 6 6 Breakout factor vs embedment ratio relationship for horizontal anchors

In Figs 6 5 and 6 6 computed values of the breakout factor ($P/\gamma HB$) corresponding to different embedment ratios (H/B) and L/B ratios of 5 and 8 75 respectively are shown and compared with the limit equilibrium solutions (Vermeer and Sutjiadi, 1985) and experimental results (Rowe and Davis, 1982, Das and Seeley, 1975) It can be observed from these figures that the obtained solutions are in good agreement with the results reported in the literature

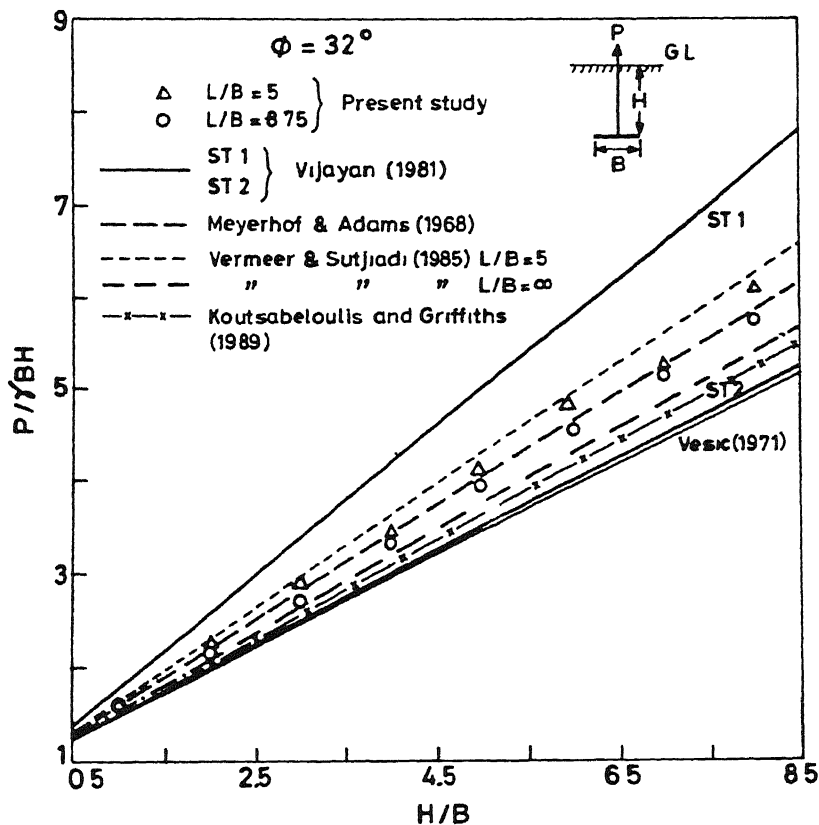


Fig 6 7 Comparison of the obtained results with the results reported in the literature for horizontal anchors

Fig 6 7 presents the comparison of breakout factors obtained using different theories The results obtained are very close to the values given by Meyerhof and Adams (1968) for the entire range of embedment ratios However, for some specific values of

embedment ratios the predictions are closer to those of Vermeer and Sutjiadi (1985) It can also be seen that the obtained solutions lie within the range defined by the envelopes ST-1 and ST-2 proposed by Vijayan (1981) and are closer to those predicted by ST-2, Vesic (1971) and Koutsabeloulis and Griffiths (1989)

In Table 6 3 breakout factors for rough ($\delta=30^0$) anchors embedded in sand ($\phi=32^0$) for L/B ratio equal to 5 and 8 75 for different embedment ratios have been presented and compared with the values obtained for smooth anchors to bring out the effect of anchor roughness on the breakout factors The general trend shows that breakout factors increase substantially for rough anchors in comparison to the corresponding values for smooth anchors It is observed that the increase ranges from 23 08-54 38% The present solutions could not be compared with other solutions due to the lack of reported data

TABLE 6 3
Effect of roughness on the breakout factors for horizontal anchors.

L/B	H/B	1	2	3	4	5	6	7	8
5 0	smooth	1 60	2 25	2 85	3 45	4 15	4 85	5 25	6 10
	rough	2 38	3 05	4 40	5 15	5 50	6 20	7 20	8 25
	%increase	48 75	35 55	54 38	49 27	32 53	27 84	37 14	35 25
8 75	smooth	1 55	2 15	2 75	3 35	3 90	4 55	5 15	5 75
	rough	2 25	2 84	4 15	4 6	5 05	5 60	6 50	7 74
	%increase	45 16	32 09	50 91	37 6	29 48	23 08	26 21	34 61

Table 6 4 presents the final design variables along with the various constraints and objective function value at the optimum Most of the constraints are strictly satisfied being negative values while, others are so small in magnitude that for all

practical purposes these may be considered to be satisfied. The objective function value obtained at the optimum gives the lower bound pull out capacity of the horizontal anchor

TABLE 6 4*

Final design vector, constraints and optimal function value for a smooth horizontal anchor (H/B=5, L/B=5)

(D)vector							
0 8154	0 6610	0 5953	0 5696	0 4368	0 3089		
0 2557	3 1121						
(σ) vector							
0 0000	0 0000	0 0000	0 0000	0 0000	0 0000	0 0000	
1 0133	0 0000	1 0159	0 0000	1 0341	0 0000	0 8142	
0 0000	0 5426	0 0000	0 2552	0 0000	0 0000	1 0000	
2 0561	2 0561	3 1121	0 8155	0 6610	0 5953	0 6596	
0 4368	0 3089	0 2557	0 0007				
Interface shear stress equality constraints							
-0 1421E-13	-0 9462E-06	0 1767E-13	0 3725E-07	-0 1576E-13			
-0 41723E-06	0 4441E-14	-0 8941E-07	-0 4441E-14	-0 2980E-07			
Boundary shear stress equality constraints							
0 4172E-06	0 4191E-06	-0 2123E-06	-0 1993E-06	-0 8994E-08			
0 0000	0 1421E-13	-0 4172E-06					
Yield constraints(inequality)							
0 2258E-15	-0 1138E+01	-0 1559E+01	0 2258E-15	-0 1558E+01			
-0 3742E+01	0 1681E-13	-0 1007E+00	-0 8374E-01	0 1435E-14			
-0 3088E+00	-0 4050E+00	0 1655E-14	-0 2555E+00	-0 8972E-01			
0 1181E-14	-0 7796E-01	0 7543E-05					
No-tension constraints(inequality)							
0 1772E-07	-0 1013E+01	0 1767E-07	-0 1016E+01	0 1754E-07			
-0 10434E+01	0 1498E-07	-0 8141E+00	0 1432E-07	-0 5426E+00			
0 1195E-07	-0 2552E+00	-0 1000E+01	-0 2056E+01	-0 2056E+01			
-0 3112E+01	-0 8155E+00	-0 6610E+00	-0 5953E+00	-0 6596E+00			
-0 4367E+00	-0 3089E+00	-0 2557E+00	-0 6910E-03				

Optimal function value = 8 2243

* values are normalized with 15 0 kPa

Similar to the smooth anchors complete stress field along with stress-strength ratios, studies for variation of the objective function with penalty parameter and the number of function evaluations were conducted for rough anchors also, however, these are not presented herein to avoid repetition

6 4.2 Vertical anchors

The breakout factors obtained for the vertical anchors for $L/B=5$, are shown in Fig 6.8. The obtained results are superimposed on the reported theoretical and experimental values (Rowe and Davis, 1982b) and compared. The percentage differences between the predicted values from the reported theoretical solutions and experimental values are given in Table 6.5. For smooth anchors the range of these differences from theoretical values is 10.0-22.0% but for the rough anchors the same is between 8.88-24.30%. However, it can be seen that the present solution deviates from experimental values by 34.0-68.13% (values within parentheses).

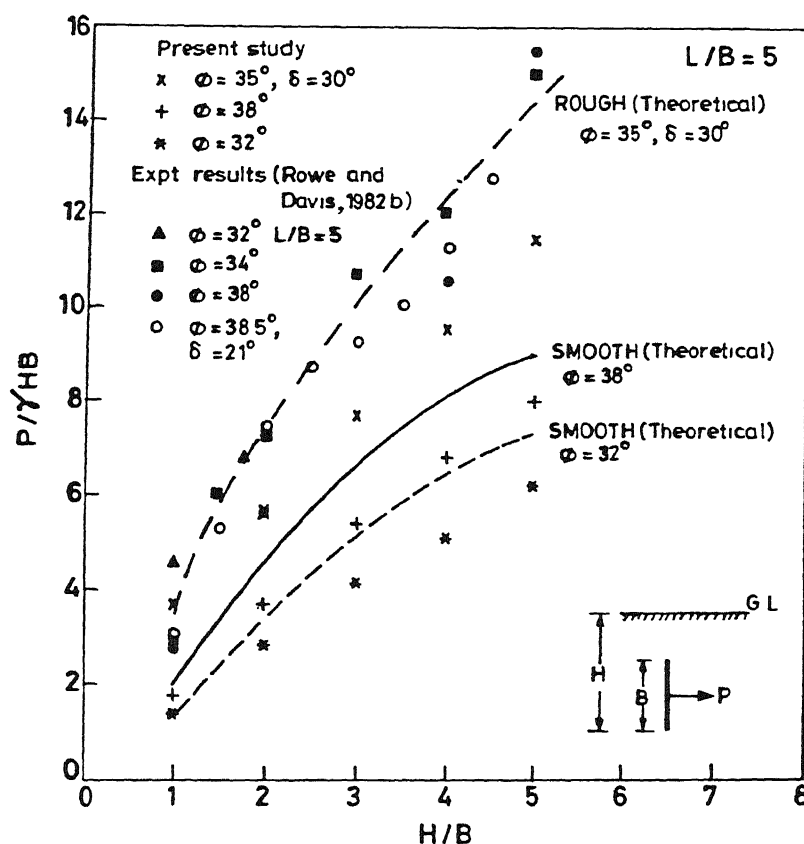


Fig 6.8 Breakout factor vs embedment ratio relationship for vertical anchors

TABLE 6.5

Percentage differences of the present solutions from experimental and theoretical results for vertical anchors (L/B=5)

H/B	1	2	3	4	5
Rough	$\phi = 35^0$				
	8 88	24 3	23 0	22 5	20 0
Smooth	$\phi = 38^0$	10 0 (34 55)	17 7 (33 93)	18 2	15 0 (35 24)
	$\phi = 32^0$	0 0 (68 13)	15 0	18 0	22 0
					10 1 (48 38)

The complete stress field along with the stress-strength ratio is depicted in Table 6.6 for H/B=2 and $\phi=32^0$ for a smooth vertical anchor. It is observed that nodal points 2, 3 and 4 in elements 2, 4 and 6 respectively are very close to the limiting state. Similar results were obtained for other embedment ratios also.

TABLE 6.6*

Stress field for smooth vertical anchor (H/B=2, L/B=5, $\phi=32^0$)

Element No	Nodal Point	σ_x	σ_z	τ_{zx}	Stress-strength ratio
1	7	0 0000	0 0000	0 0000	-
1	8	0 0005	0 0000	0 0000	-
1	1	0 6485	0 3000	0 0005	0 4808
2	7	0 0000	0 0000	0 0000	-
2	1	0 6105	0 7593	0 2102	0 3774
2	3	1 6082	0 7342	0 4397	0 9977
3	7	0 0000	0 0000	0 0000	-
3	3	1 3428	2 2508	0 5268	0 5335
3	4	1 2218	2 1975	0 0856	0 2988
4	7	0 0000	0 0000	0 0000	-
4	4	1 6162	0 8830	0 5388	0 9685
4	5	1 1451	0 6603	0 2708	0 5773
5	7	0 0000	0 0000	0 0000	-
5	5	0 6635	0 6000	0 0001	0 0090
5	6	0 0001	0 0000	0 0000	-
6	1	0 9617	0 6954	0 0000	0 0919
6	2	2 3939	0 7917	0 0000	0 9008
6	3	2 3939	0 9174	0 1527	0 7383

* stress values are normalized with 10 0 kPa

The variations of objective function with penalty term (r_k) and number of function evaluations are shown in Figs 6 9(a) and 6 9(b) respectively. The value of objective function becomes steady (3.3556) as r_k reaches $1E-04$ and the required number of function evaluations to reach the steady state signifying convergence of the solution is 1200

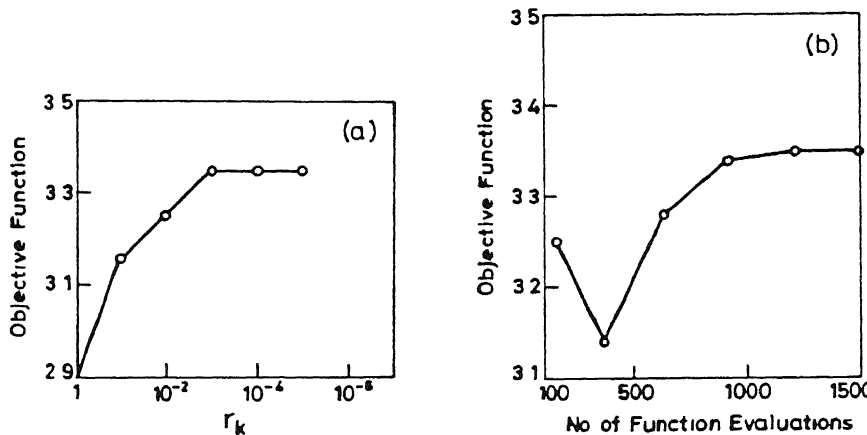


Fig 6.9 Variation of objective function with (a) Penalty parameter and (b) number of function evaluations for vertical anchors

Table 6.7 presents the final design variables along with the various constraints and objective function value at the optimum. Most of the constraints are strictly satisfied being negative values while, others are so small in magnitude that for all practical purposes these may be considered to be satisfied. The objective function value obtained at the optimum gives the lower bound pull out capacity of the vertical anchor.

In Table 6.8 breakout factors for both smooth and rough ($\delta = 30^\circ$) anchors embedded in sand ($\phi = 32^\circ$) with L/B ratio equal to 8 for different embedment ratios have been presented and compared with the available field test values reported by Rowe and Davis (1982) wherein no information has been provided about the anchor surface roughness. The comparison of the results reveals that the

TABLE 6 7*

Final design vector, constraints and optimal function value
for vertical anchor (H/B=2, L/B=5, $\phi=32^\circ$)

(D) vector

2 2508	0 8830	2 3939	2 1975	0 6954	0 6635
0 6485	0 7917	0 0005			

(r) vector

0 0000	0 0000	0 0000	0 0000	0 0000	0 6954	0 9617
2 3939	0 7917	0 9174	2 2508	2 1975	0 8830	0 6603
0 6635	0 0000	0 0000	0 0000	0 0000	0 0000	0 6485
0 0005	0 4747	0 0000	1 4865	0 0000	1 3195	0 0000
0 6318	0 0000	0 8658	1 7157			

Interface shear stress equality constraints

-0 4407E-07	0 6217E-14	-0 8882E-14	0 8941E-07	0 1243E-13
-0 1192E-06	0 1039E-07	0 1490E-06	-0 1192E-06	0 1788E-06

Boundary shear stress equality constraints

0 8882E-15	0 7451E-08	-0 7451E-07	0 2222E-07	-0 5960E-07
0 5960E-07				

Yield constraints (inequality)

0 5239E-21	0 1475E-06	-0 1312E 00	-0 6663E-15	-0 3280E 00
-0 3473E-02	0 3113E-13	-0 1691E+01	-0 2302E+01	0 2143E-15
-0 5527E-01	-0 3869E 00	0 1975E-14	-0 4443E 00	0 5398E-08
-0 7002E	-0 2827E 00	-0 8058E 00		

No-tension constraints (inequality)

-0 6954E 00	-0 9617E 00	-0 2394E+01	-0 7917E 00	-0 9174E 00
-0 2251E+01	-0 2197E+01	-0 8830E 00	-0 6603E 00	-0 6635E 00
-0 8664E-04	-0 6485E 00	-0 4528E-03	-0 4747E 00	0 1935E-07
-0 1486E+01	0 2197E-08	-0 1319E+01	-0 3484E-07	-0 6318E 00
-0 3211E-07	-0 8658E 00	-0 1716E+01		

Optimal function value = 3 3556

*values are normalized with 10 0 kPa

TABLE 6 8

Comparative study of breakout factors and effect of roughness for
vertical anchors (L/B=8, $\phi=32^\circ$)

H/B	1	1 65	2	2 3	3	4	5
Field Tests	3 20	5 50	-	7 50	-	-	-
<u>Present solutions</u>							
Smooth	1 70 (46 87)*	2 15 (60 91)*	-	3 80 (49 33)*	4 42	5 50	7 70
rough ($\delta =30^\circ$)	2 80 (12 50)*	3 50 (36 36)*	-	6 10 (18 67)*	7 25	10 40	11 40
% increase due to roughness	64 71	62 79	-	60 53	64 03	89 09	48 05

* percentage differences from the field tests values

obtained solutions for the rough anchors are closer to the field test values as compared to the smooth anchors. It is observed that when the anchor is rough there is a substantial increase (48% to 89%) in the breakout factors over the smooth ones. The percentage differences of the present solutions from field test values are given in the parentheses. It is observed that for smooth anchors the differences are large and lie in 46-61% range whereas, for rough anchors the same is less being 12.5-36.36%.

The complete stress field, stress-strength ratios and studies for variation of the objective function with penalty parameter and the number of function evaluations were also conducted with $L/B=8$, however, these are not presented herein to avoid the repetition.

6.4.3 Inclined anchors

The mesh pattern as shown in Fig 6.3 is for anchor inclination angle of 45° . For other angles of inclination, except for the coordinates of the nodal point numbers 2 and 3, every thing else remains unchanged. The obtained pull out capacity is compared with other solutions as reported by Das (1990) and their percent differences (from the present study) are presented in Table 6.9. It is observed from the table that the value of pull out capacity for smooth strip as predicted by the present study is in very close agreement with that of Meyerhof (1973) while the same as given by Maia et al (1986) and Hanna et al (1988) are 14.37% and 40.46% higher than the arrived at in the present study. The present analysis predicts a lower bound solution whereas Meyerhof's method is not known to give a lower bound solution. As such, it can be inferred that the exact pull out value (Q_u) will be within the

TABLE 6 9

Comparison of the present solutions with the reported values

Method of analysis	Qu (kN/m)		
	$\alpha = 30^\circ$	45°	60°
Meyerhof(1973)*	21 00 (1 70)	23 81 (3 40)	28 90 (-0 1)
Maia et al (1986)*	22 00 (6 20)	26 86 (14 33)	34 00 (14 9)
Hanna et al (1988)*	29 12 (29 20)	38 63 (40 46)	87 63 (66 98)
present solutions	Smooth strip	20 63	23 00
	Rough strip	23 27	26 46
% increase due to roughness		12 79	15 04
			9 40

*Das(1990)

Note Values in parentheses are the percentage differences from the present study

range of Present solution $\leq Qu \leq$ Meyerhof(1973) solution for the smooth strip anchors. It is further observed from the Table 6 9 that when the anchor is rough ($\delta=30^\circ$) there is a substantial increase (9 40-15 0%) in the obtained pull out capacity values over the smooth ones

The complete stress field along with the stress-strength ratios is presented in Table 6 10. A ratio close to unity indicates the limiting condition

Table 6 11 presents the final design variables along with the various constraints and objective function value at the optimum. Most of the constraints are strictly satisfied being negative values while, others are so small in magnitude that for all

Stress field and stress-strength ratios at the nodal points for a smooth anchor inclined at 45°

Element No	Nodal point No	σ_x	σ_z	τ_{zx}	Stress-strength ratio
1	1	0 0000	0 0000	0 0000	-
1	2	2 1886	0 8600	0 0000	0 5773
1	7	0 0000	0 0000	0 0000	-
2	7	0 0000	0 0000	0 0000	-
2	2	2 1302	1 2454	0 2334	0 2669
2	5	1 1507	0 5696	0 2966	0 7082
3	7	0 0000	0 0000	0 0000	-
3	5	0 8442	1 0342	0 2175	0 1942
3	4	1 0166	1 1590	0 4617	0 5606
4	7	0 0000	0 0000	0 0000	-
4	4	1 0933	1 2000	0 0000	0 0065
4	6	0 0001	0 0000	0 0000	-
5	5	1 5731	0 6049	0 2637	0 7789
5	3	1 1957	0 4758	0 1000	0 6072
5	4	1 2005	1 4658	0 7224	0 9226
6	5	1 8149	0 7693	0 0987	0 5154
6	2	1 2296	1 2296	0 0479	0 0046
6	3	1 5389	1 5389	0 5652	0 4100

*stress values are normalized with (γH)

TABLE 6 11*

Final design vector, constraints and optimal objective function value for a smooth anchor inclined at 45°

(D)vector

1 2775 1 9130 2 1041 0 6465 1 6294

(σ)vector

0 0000	0 0000	0 0000	0 0000	0 5695	1 3908	0 0000
1 9130	1 2775	2 1041	0 4646	1 3508	0 6465	0 7424
1 1988	0 8279	1 1799	0 0000	1 0939	0 0000	1 1567
0 0000	0 0000	0 0000	0 0000	0 0000	1 3418	0 0000
1 1758	1 6294					

Interface shear equality constraints

0 5960E-07	-0 1937E-06	0 1028E-05	0 1192E-06	-0 2384E-06
0 8392E-09	-0 5960E-06	0 5954E-08	0 5960E-07	-0 2980E-06
0 2384E-06	-0 1487E-06			

Boundary shear equality constraints

-0 1192E-06	-0 6163E-06	0 3608E-15	0 2980E-06	-0 2608E-07
0 0000				

Yield constraints(inequality)

0 1991E-19	-0 1292E+01	0 4971E-11	0 1453E-10	-0 2748E+01
-0 2841E 00	0 3776E-10	-0 9354E 00	-0 6842E 00	0 5939E-11
-0 1718E+01	0 2374E-07	-0 3451E 00	-0 3610E 00	-0 1810E 00
-0 1064E+01	-0 1980E+01	-0 1838E+01		

No-tension constraints(inequality)

-0 5696E 00	-0 1391E+01	-0 1076E-08	-0 1913E+01	-0 1277E+01
-0 2104E+01	-0 4646E 00	-0 1351E+01	-0 6465E 00	-0 7424E 00
-0 1199E+01	-0 8279E 00	-0 1180E+01	-0 3539E-04	-0 1094E+01
0 2416E-05	-0 1157E+01	-0 1202E-05	-0 1342E+01	-0 6795E-06
-0 1176E+01	-0 1629E+01			

Optimal function value 3 3816

3 3816

practical purposes these may be considered to be satisfied. The objective function value obtained at the optimum gives the lower bound pull out capacity of the anchor.

It is shown in Fig 6.10 that for a penalty parameter less than $1E-05$ and the corresponding number of function evaluations beyond 725 there is practically no change in the objective function value indicating convergence of the solution.

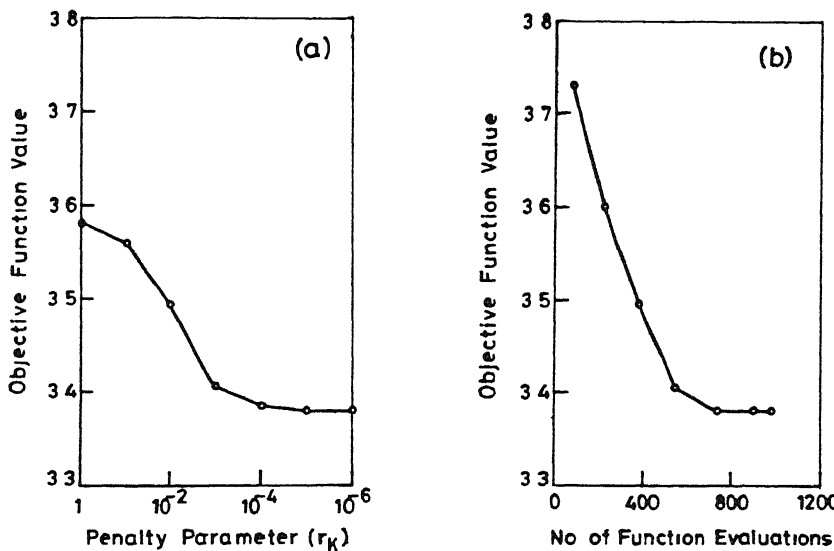


Fig 6.10 Variation of objective function with (a)Penalty parameter and (b)number of function evaluations, for inclined anchor ($\alpha=45^\circ$)

The CPU time required for different cases studied is 0.66 to 1.37 seconds

6.5 Conclusions

Based on the results and discussions presented in the previous section the following conclusions can be drawn

- 1) The Lysmer-Basudhar approach to predict the lower bound for the breakout factor of horizontal, vertical and inclined anchors using finite elements and sequential unconstrained minimization technique to isolate the optimal stress field is reliable
- 2) Choice of mesh pattern depending on the embedment ratio is very

important for correct estimation of the breakout factor and the suggested mesh patterns can be adopted in general

3)For smooth horizontal anchors the deviation of the present solutions from the reported theoretical and experimental values do not exceed 13.5% and 13.79% respectively but consideration of anchor strip roughness increases the lower bound breakout factors by 23.08-54.38%

4)For smooth vertical anchors the range of deviation of the present solution from the reported theoretical and experimental values are 0-22% and 33.93-68.13% respectively while for rough vertical anchors the deviation from the theoretical values ranges from 8.88-24.30% It is observed that due to the anchor roughness increase in the lower bound values ranges from 48-89% over the values for smooth anchors

5)The obtained lower bound pull out solutions for smooth inclined strip anchors compare excellently with the solution reported by Meyerhof (1973) It is observed that due to the anchor roughness increase in the lower bound values ranges from 9.4-15.04% over the values for smooth anchors

6)The sequential unconstrained minimization using the concept of extended penalty function in conjunction with Powell's technique for multivariable search and quadratic interpolation for unidirectional search is found to be very efficient in isolating the optimal solution

CHAPTER 7

BEARING CAPACITY OF REINFORCED SOIL STRUCTURES

7 1 General

Prediction of the bearing capacity of reinforced soils is one of the most interesting topics in geotechnical engineering. Most of the methods that were originally developed for predicting the bearing capacity of soils with no reinforcement are being extended to soils reinforced with geotextiles, geogrids or other reinforcing material, for such predictions. Majority of these models are based on limit equilibrium approach (Schmertmann et al ,1987) and finite elements with displacement formulation (Brown and Poulos, 1981). Strictly speaking the assumptions like the use of circular failure surfaces, incorrectly oriented slip lines and unsatisfied equilibrium conditions invalidate the limit equilibrium methods from the stand point of engineering mechanics. However, these semi empirical methods have acquitted themselves well in engineering mechanics. All the same, it is preferable to evolve methods for design and analysis using rational theories like plasticity theory as they estimate the possible errors due to simplifying assumptions of the semi empirical solutions. With the work of Drucker et al (1952) proving the validity of limit theorems to soils, the theory of plasticity has been applied to many problems of stability of soil masses. For the materials with associated flow rule, with the help of limit theorems, it is possible to find the lower and upper bound solutions for the critical load even if it can not be determined exactly. Methods based on these limit theorems have been evolved and adopted to

solve problems for the unreinforced soils, in this regard the works published by Sokolovskii (1965), Lysmer (1970), Chen (1975), Heyman (1973), Basudhar (1976) and Sloan (1988,1989) need a specific mention. It is only very recently that techniques based on these limit theorems have been extended to reinforced soils by Sawicki (1988), Sawicki and Lesniewska (1987,1988) and de Buhan et al (1989). Thamm et al (1990) reported a full scale test of a geotextile reinforced soil wall and compared the results with those predicted by different approaches like wedge analysis, slip circle analysis and analysis by the method of characteristics. All these methods have been found to be very handy and useful in dealing with such problems. However, intuitively it can be said that the method of characteristics to predict the lower bound limit load is likely to be highly complicated and involved analytically if heterogeneity of the soil medium and boundary irregularities are to be considered and incorporated in the analysis. As such, there is a great need to demonstrate the suitability of more general methods to accommodate such cases. In the following sections the generalized Lysmer-Basudhar approach has been extended to study the stability of reinforced soil structures viz retaining walls and cohesive soil slopes.

7.2 Statement of the Problem

A retaining wall uniformly reinforced in X direction is shown in Fig 7.1. The mechanical properties of the constituents of the reinforced soil are, the internal friction angle (ϕ) of the soil and the ultimate tensile strength (σ_0) of the reinforced strips. The average value of ϕ is 34° and the unit weight of the backfill

soil is 16 OkN/m^3 . The values of ultimate tensile strengths for Aluminium bands, Textile strips and Novita geotextiles are taken to be the same as adopted by Sawicki and Lesniewska (1987) and the respective values are 2.02 , 3.70 and 10 ON/cm^2

A reinforced soil slope of height 5m is shown in Fig 7.2. The effective angle of shearing resistance (ϕ') and the effective cohesion (C') of the reinforced soil are 25° and 50kN/m^2 respectively. The ultimate tensile strength (σ_0) of the reinforcement is 100kN/m^2 . The reinforced soil is treated as macroscopically homogeneous anisotropic material with a unit weight of 21.57kN/m^3 . Results have been obtained corresponding to slope angles (β) equal to 70° , 80° and 90° . The problem was previously solved by Sawicki and Lesniewska (1988) using the method of characteristics.

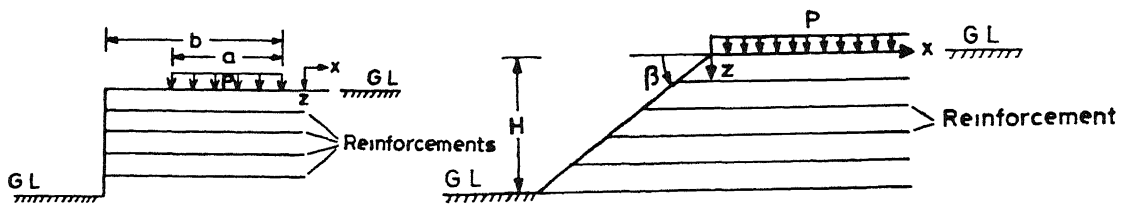


Fig 7.1
Reinforced soil retaining wall

Fig 7.2
Reinforced soil slope

The objective is to predict the safe load p , uniformly distributed over the length a , which the reinforced wall (Fig 7.1) and the slope (Fig 7.2) can withstand.

7.3 Assumptions

The reinforced soil is treated as macroscopically homogeneous anisotropic perfectly plastic Mohr-Coulomb material. The reinforcement works in tension in one direction only. Both components of the equivalent homogenized anisotropic material are assumed to work together due to perfect bonding between the soil and the

reinforcement and, as such, no slipping phenomenon localized at their interface is considered in this analysis. The assumption of treating the reinforced soil as an uniform continuum with no modeling of individual strips, relies on the fulfillment of the following two conditions (de Buhan et al ,1989)

- 1)The reinforced elements must be placed in to the backfill soil in a regular pattern
- 2)The vertical spacing between two successive reinforcement layers should be small enough as compared to the height of the wall

The reinforced soil wall and slope are built of dry sand and clay reinforced with appropriate strips fixed to smooth facing elements of low stiffness

7.4 Boundary conditions and the Objective functions

The zones of influence as shown in Figs 7 3(a), 7 3(b) and 7 4(a) and 7 4(b) are based on the studies of most likely failure modes as observed by experimental investigations Sawicki and Lesniewska (1987,1988) In most of the cases when a reinforced soil retaining wall or a slope is loaded with a uniformly distributed load up to failure the failure surface would be confined within this zone for both weighty and weightless materials As such, elements beyond this zone may not be needed However, it has been observed that for weighty materials significant influence zone may extend marginally beyond the footing Hence, mesh pattern as shown in Fig 7 3(c) has also been tried The base of strip footing (uniformly distributed load) is considered to be friction less As the wall and slope are considered very flexible and smooth, the normal and shear stresses at their faces are considered to be zero

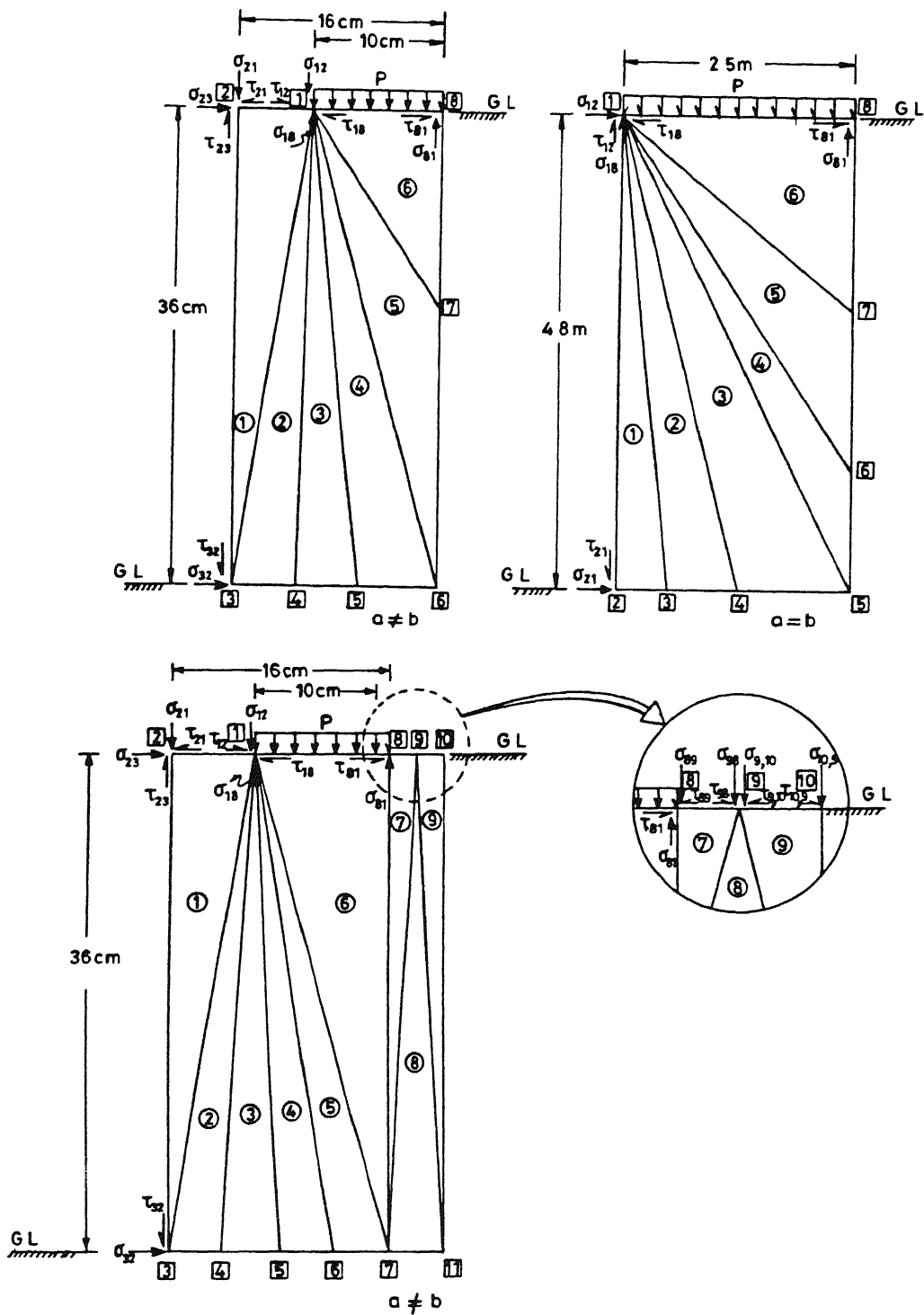


Fig 7.3 Mesh patterns for the reinforced retaining wall with (a) $a \neq b$, (b) $a = b$ and (c) extended beyond the footing for $a \neq b$

The boundary conditions and the respective objective functions are presented as follows

7 4.1 Reinforced cohesionless soil retaining wall

Boundary conditions

Case1 (Fig 7 3(a)) when $a \neq b$

$$\sigma_{12} = \sigma_{21} = \sigma_{23} = \sigma_{32} = \tau_{12} = \tau_{21} = \tau_{23} = \tau_{32} = \tau_{18} = \tau_{81} = 0$$

Case2 (Fig 7 3(b)) when $a=b$

$$\sigma_{12} = \sigma_{21} = \tau_{18} = \tau_{81} = \tau_{12} = \tau_{21} = 0$$

Case3 (Fig 7 3(c)) when $a \neq b$

$$\sigma_{12} = \sigma_{21} = \sigma_{23} = \sigma_{32} = \tau_{12} = \tau_{21} = \tau_{23} = \tau_{32} = \tau_{18} = \tau_{81} = 0$$

$$\sigma_{89} = \sigma_{98} = \sigma_{9,10} = \sigma_{10,9} = \tau_{89} = \tau_{98} = \tau_{9,10} = \tau_{10,9} = 0$$

Objective function $-(\sigma_{18} + \sigma_{81})$

7 4 2 Reinforced cohesive soil slope

Boundary conditions

Case 1 (Fig 7 4(a)) $\beta=90^\circ$

$$\sigma_{12} = \sigma_{21} = \tau_{18} = \tau_{81} = \tau_{21} = \tau_{12} = 0$$

Case 2 (Fig 7 4(b)) $\beta=70^\circ$ and 80°

$$\sigma_{12} = \sigma_{21} = \sigma_{23} = \sigma_{32} = \tau_{12} = \tau_{21} = \tau_{23} = \tau_{32} = \tau_{18} = \tau_{81} = 0$$

Objective function $-(\sigma_{18} + \sigma_{81})$

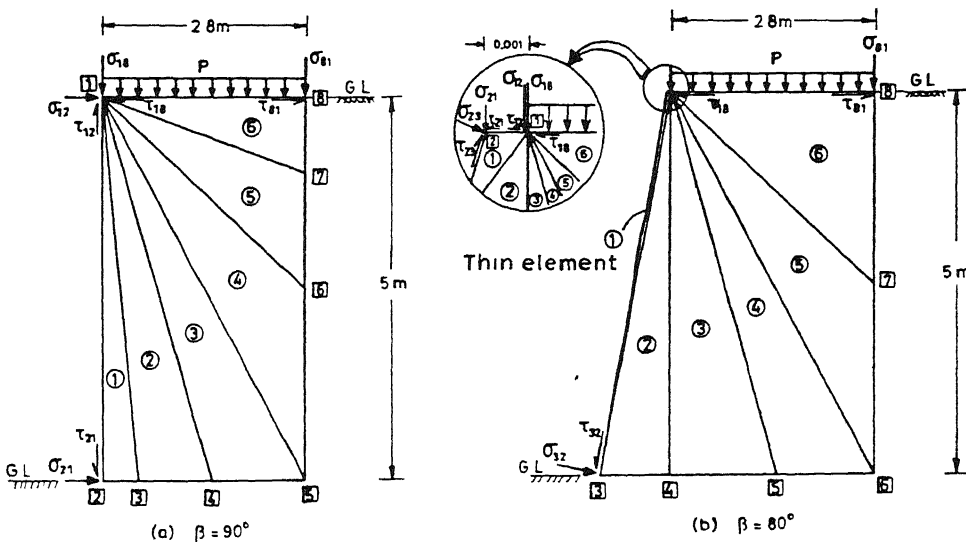


Fig 7 4 Mesh patterns for the reinforced soil slopes with
 (a) $\beta=90^\circ$ and (b) $\beta=80^\circ$

The bearing capacity is obtained by averaging the stress terms involved in the objective functions

7 5 Results and Discussions

The results were obtained on HP 9000/850 series of computer system To validate the effectiveness of the proposed method in predicting the bearing capacity of reinforced soil structures different cases as studied by Sawicki and Lesniewska (1987, 1988) have been considered The obtained results are presented and discussed as follows

7 5 1 Reinforced cohesionless soil retaining wall

Table 7 1 gives the details of the reinforcing materials used, the width (a) and placement distance (b) of the strip load

TABLE 7.1
Various cases considered for the present study

Cases	Geotextile	a(cm)	b(cm)	Height(cm)
A	Aluminium bands	7 0	11 5	36 0
B	Aluminium bands	10 0	13 0	36 0
C	Aluminium bands	10 0	16 0	36 0
D	Textile strips	10 0	10 0	18 8
E	Novita	-	-	480 0

Most of the time it is impossible to guess a feasible starting point design vector in such analytical problems As such, the iteration to obtain the optimal solution were carried out starting from any arbitrarily chosen design vector whose all the elements had been considered to be zero

Table 7 2 presents a comparison of the results obtained by Sawicki and Lesniewska (1987) and the present method for weightless backfill soil which may be a suitable assumption for

small scale tests. It is observed that the lower bound loads obtained by the present study are in general much better than those reported by Sawicki and Lesniewska (1987) and fall within the range of lower and upper bound solutions as predicted by them. But for Case D where textile strips have been used, the present solution is lower than that of Sawicki and Lesniewska (1987) by a very small amount, their values may be considered to be exact, the lower and upper bound solutions being identical. Percent

TABLE 7 2
Comparison of present solutions with other experimental and theoretical results (weightless soil)

Case	Sawicki and Lesniewska (1987)			Present study	% Differences from		
	P_{expt} (N/cm ²)	P_l (N/cm ²)	P_u (N/cm ²)		P_l (N/cm ²)	P_l	P_u
A	7 22	7 145	11 74	8 63	20 78	-26 49	19 53
B	8 39	7 145	9 29	7 98	11 69	-14 09	-4 88
C	11 31	7 145	11 43	9 17	28 34	-19 77	-18 92
D	14 08	13 090	13 09	11 94	-8 80	-8 80	-15 21

difference of the present solutions from the solutions (P_l and P_u) given by Sawicki and Lesniewska (1987) are also presented in the table. The differences between these two lower bound solutions ranges from -8 8 to 28 34% and the same between the lower bound and the upper bound is -8 8 to -26 49%. The percentage differences of the obtained lower bounds with the experimental values lie in a small range of -4 88 to -18 92% except for the Case A where the obtained lower bound is 19 53% higher than the experimental value of Sawicki and Lesniewska (1987). The predicted values using the present method can be considered to be very good matching both experimental and theoretical results (Sawicki and

Lesniewska, 1987)

For the weighty soils, Table 7.3 presents a comparative study of the upper and lower bound solutions estimated from the expressions suggested by Sawicki and Lesniewska (1987) and the lower bound solutions obtained by using the present approach. The table shows that except for Case D the lower bound solutions obtained by using the present analysis are higher than the corresponding values predicted by them. The present solution appears to be better as it reduces the interval between the upper and the lower

TABLE 7.3
Comparison of the present solutions with other theoretical results
(weighty soil)

	Sawicki & Lesniewska (1987)		Present Study	% differences from	
Case	P_1 (N/cm ²)	P_u (N/cm ²)	P_1 (N/cm ²)	P_1	P_u
A	6 57	14 45	8 670 6 670**	31 96 1 52	40 00 53 84
B	6 57	9 00	7 950 6 670**	21 00 1 52	11 67 25 89
C	6 57	11 14	8 990 6 680**	36 83 1 67	19 29 66 77
D	12 78 11 95*	12 94	12 190	-4 62 2 00	5 79
Nov- -ita	27 69	31 53	28 156	1 68	10 70

* Sawicki and Lesniewska (1987) have reported this using their computer program

**from Fig 7.2(c)

bound to bracket the critical load and also uses a more refined analysis. It can also be seen that the present solution is higher by about 21 0-36 83% for the Aluminium band (Cases A, B and C) reinforced earth walls than the computed lower bounds using the expressions given by Sawicki and Lesniewska (1987). But for the

Textile strip (Case D) and Novita this difference is small. The percentage differences of the obtained lower bounds from the computed values of upper bounds lie in the range from 5.0-19.29% except for the case A, where, it differs by a large extent (40%). The lower bound solution obtained for Case C by using mesh as shown in Fig 7.3(c) gives a very low value (6.68 N/cm^2) of lower bound and as such this mesh is not recommended for such studies, however, the resulting lower bound indicates that the Lysmer's stress field can be extended throughout the body around the footing in a statically admissible manner. This also further demonstrates that the present method is not restricted to the use of only six elements.

The complete stress field along with the stress-strength ratio is shown in Table 7.4, for Aluminium bands reinforced wall (Case C, weightless). The stress-strength ratio very close to unity signifies limiting equilibrium state. It can be seen from the table that the obtained stress field is very good as indicated by stress-strength ratios at the different nodes for all the elements being close to unity. Similar stress fields were also obtained for various cases studied. But for the sake of brevity these are not presented herein.

The equality and inequality constraints along with the final optimal objective function values as obtained, starting from the arbitrarily chosen design vector are given in Table 7.5

The order of magnitude of the equality constraints is so small that for all practical purposes these may be considered to be equal to zero and hence satisfied. The inequality constraints with negative sign signify that these are strictly satisfied.

The variation of objective function with Penalty term (r_k) and number of function evaluations is shown in Fig 7.5(a) and 7.5(b). It is observed that the minimum value of the objective function (18.3421) is achieved when the penalty term is 1E-04 and the corresponding number of function evaluations is 1298.

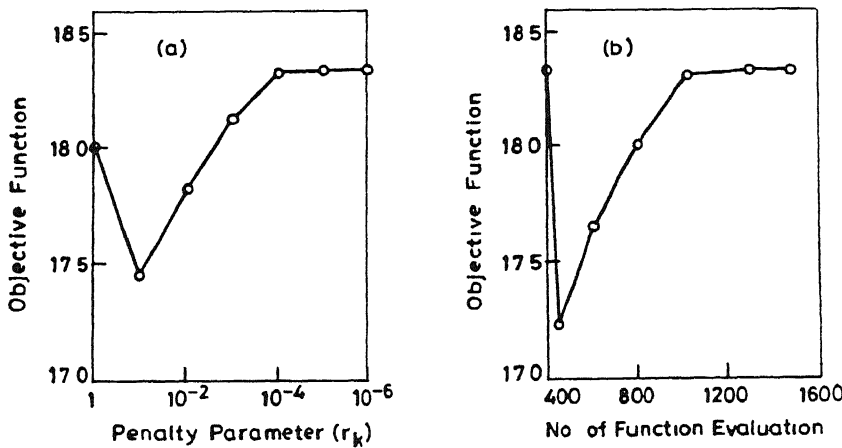


Fig 7.5 Variation of the objective function with (a) penalty parameter and (b) number of function evaluations, for the reinforced soil retaining wall (Case C, weightless soil)

From the presented results and discussion it is evident that the obtained results are fairly accurate in terms of their closeness to the experimental results and being comparable to other reported values (Sawicki and Lesniewska, 1987).

The CPU time required for the problems studied never exceeded

case C, weightless soil (Stress values in N/cm²)

Element No	Nodal point No	σ_z	σ_x	τ_{zx}	Stress-strength ratio
1	2	0 0000	0 0000	0 0000	-
1	3	0 0000	0 0000	0 0000	-
1	1	0 0000	0 0000	0 0000	-
2	1	6 5942	2 2031	1 0990	0 9964
2	3	6 6080	2 2035	1 1013	0 9988
2	4	6 5954	2 2038	1 1011	0 9969
3	1	6 5927	2 2031	1 0990	0 9961
3	4	6 5274	2 2037	1 0992	0 9869
3	5	6 5053	2 2035	1 0895	0 9805
4	1	5 1868	2 1858	1 2552	0 9006
4	5	5 8673	2 1956	1 1604	0 9281
4	6	5 7145	2 1654	1 2908	0 9920
5	1	8 5752	2 4472	0 3139	0 9988
5	6	7 2820	2 2863	0 8554	0 9739
5	7	9 2529	2 6200	0 0078	0 9980
6	1	9 0462	2 6565	0 0000	0 9533
6	7	9 2958	2 6391	0 0365	0 9949
6	8	9 2958	2 6322	0 0000	0 9980

TABLE 7.5

Final design vector, constraints and optimal objective function value for case C; weightless soil (all values in N/cm²)

(D)vector

6 5942 9 0462 9 2958 6 6080 6 5954 6 5274 6 5053
5 8674 5 7145 6 5927 0 6000 0 6191 5 1868

(σ)vector

0 0000 6 5942 6 5927 5 1868 0 4272 0 6365 0 0000
0 0000 0 0000 0 0000 0 1271 0 1276 0 5025 0 4998
1 1728 1 2101 3 2241 3 2551 9 0462 9 2958 0 0000
0 0000 6 6080 6 5954 6 5274 6 5053 5 8673 5 7145
0 2663 0 6000 0 6191 0 6122

Interface shear equality constraints

-0 1069E-06 -0 3278E-06 -0 7993E-08 0 0000 -0 2206E-06
0 1788E-06 0 5066E-06 0 7152E-06 -0 497814E-06 -0 6556E-06

Boundary shear equality constraints

0 0000 0 0000 0 4683E-06 0 2384E-06 0 0000 0 0000

Yield constraints(inequality)

0 0000 0 0000 0 0000 -0 8783E-01 -0 2769E-01 -0 7505E-01
-0 9330E-01 -0 3108E 00 -0 4624E 00 -0 1688E+01 -0 1461E+01
-0 1547E 00 -0 4470E-01 -0 7446E 00 -0 8457E-01 -0 1998E+01
-0 2241E 01 -0 8694E-01

No-tension constraints(inequality)

-0 6594E+01 -0 6592E+01 -0 5186E+01 -0 4272E 00 -0 6365E 00
0 0000 0 0000 -0 1271E 00 -0 1276E 00 -0 5025E 00
-0 4998E 00 -0 1172E+01 -0 1210E+01 -0 3224E+01 -0 3255E+01
-0 9046E+01 -0 9295E+01 -0 6608E+01 -0 6595E+01 -0 6527E+01
-0 6505E+01 -0 5867E+01 -0 5714E+01 -0 2663E 00 -0 6000E 00
-0 6191E 00 -0 6122E 00

Optimal function value 18 3421

1 37seconds for six elements (Figs 7 3(a) and (b)) and 7 43seconds for nine elements (Fig 7 3(c)) mesh pattern respectively

7 5.2 Reinforced cohesive soil slope

The lower bound bearing capacity values have been obtained by using the failure criterion as suggested by Sawicki and Lesniewska (1988) The failure criterion is given as follows

$$f = (\sigma_z - \sigma_x - \sigma_0)^2 + (2 \tau_{zx})^2 - [(\sigma_z + \sigma_x + \sigma_0 + 2H) \sin\phi']^2 = 0$$

where, $H = C' \cot\phi'$

For vertical slope ($\beta=90^0$) the element mesh pattern as shown in Fig 7 4(a) has been found to be quite efficient while for other slope angles a very thin element (element 1) as shown in Fig 7 4(b) had to be introduced to get a feasible solution, the nodal point 2 being a singular point has to be isolated to overcome the numerical difficulty

Table 7 6 presents a comparative study of the present solutions with those reported by Sawicki and Lesniewska (1988) It is observed from the table that there is an improvement over the lower bound solutions as obtained and reported by Sawicki and Lesniewska, the order of magnitude of the percent difference between the solutions is 6 15-7 10% for the slope angles equal to 70^0

TABLE 7 6
Comparison of the present study with the reported values

Slope angle (β^0)	P(KN/m)		% Diff from Sawicki and Lesniewska(1988)
	Sawicki and Lesniewska (1988)	Prsent study	
70	1763 0	1871 43	6 15
80	1355 0	1451 31	7 10
90	997 0	837 94	-15 95

and 80^0 But for vertical slope the obtained values are 15 95% on the lower side of that reported by Sawicki and Lesniewska These differences in the solutions are likely due to the difference in the approach of analyses

The state of stress within the soil mass has been presented in Table 7 7 for 80^0 slope along with the stress-strength ratio at various nodal points This ratio when close to unity signifies the limiting state

The equality and inequality constraints along with the final optimal objective function values as obtained, are given in Table 7 8 It is observed that most of the constraints are strictly satisfied being negative values while others are of such a small order of magnitude that for all practical purposes these may be considered to be satisfied This indicates the efficiency of the present technique in solving multivariable - multiconstrained optimization problem starting from any arbitrary design vector

In Fig 7 6 variation of the objective function with number of function evaluations and penalty term is shown The constant value

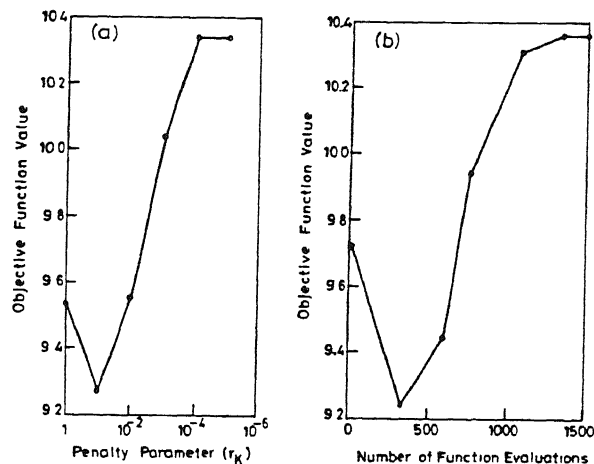


Fig 7 6 Variation of the objective function with (a) penalty parameter and (b) number of function evaluations, for the reinforced soil slope ($\beta=80^0$)

Element No	Nodal point No	σ_x	σ_z	τ_{zx}	Stress-strength ratio
1	3	0 0000	0 0000	0 0000	-
1	1	0 0000	0 0000	0 0000	-
1	2	0 0000	0 0000	0 0000	-
2	3	0 0000	0 0000	0 0000	-
2	4	2 3238	1 0785	0 9892	0 9945
2	1	0 1783	0 0000	0 0000	0 0329
3	1	1 1783	4 4635	0 0009	0 9967
3	4	2 3239	3 5303	0 9897	0 4703
3	5	2 6204	7 5662	0 3870	0 9227
4	1	1 1781	4 4617	0 0014	0 9962
4	5	2 6085	7 4339	0 4267	0 9052
4	6	2 5259	6 9277	1 0708	0 9973
5	1	1 1793	4 4654	0 0006	0 9965
5	6	2 5617	7 0418	1 0069	0 9787
5	7	2 1242	6 4123	0 5537	0 9626
6	1	1 1786	4 4648	0 0000	0 9969
6	7	2 1601	6 4409	0 5216	0 9414
6	8	1 7626	5 9017	0 0000	0 9969

*Stress values normalized with 100kN/m^2

TABLE 7 8*

Final design vector, constraints and optimal objective function value for 80° slope

(D)vector

4 4617 5 9017 4 4635 1 3235 3 5303 7 5662
7 4339 6 9277 1 5617 1 1242 1 1601 0 7626

(σ)vector

0 0000 0 0000 4 4635 4 4617 0 1792 0 1785 0 0000
0 0000 0 0000 0 0000 0 1782 1 3234 0 5321 2 3236
1 2014 3 7276 2 5627 4 6158 4 4648 5 9016 0 0000
0 0000 0 0000 1 6611 3 5302 7 5662 7 4338 6 9277
1 5617 1 1242 1 1601 0 7625

Interface shear equality constraints

0 1937E-06 0 0000 -0 2980E-07 0 3576E-06 -0 4034E-06
0 4768E-06 0 4015E-06 -0 8941E-07 0 1755E-06 0 4768E-06

Boundary shear equality constraints

0 1937E-06 0 3222E-06 0 0000 0 0000 0 0000 0 0000

Yield constraints(inequality)

-0 8214E 00 -0 8214E 00 -0 8214E 00 -0 8214E 00 -0 2996E-01
-0 9318E 00 -0 3529E-01 -0 6053E+01 -0 2098E+01 -0 4069E-01
-0 2514E+01 -0 6413E-01 -0 3753E-01 -0 5240E+00 -0 7623E+00
-0 3312E-01 -0 1209E+01 -0 5175E-01

No-tension constraints(inequality)

-0 4464E+01 -0 4462E+01 -0 1793E 00 -0 1786E 00 0 0000
0 0000 -0 1783E 00 -0 1323E+00 -0 5321E+00 -0 2324E+01
-0 1201E+01 -0 3728E+01 -0 2563E+01 -0 4616E+01 -0 4465E+01
-0 5902E+01 -0 0000 -0 1661E+01 -0 3530E+01 -0 7566E+01
-0 7434E+01 -0 6928E+01 -0 1562E+01 -0 1124E+01 -0 1160E+01
-0 7626E 00

Optimal function value 10 3665

*values normalized with 100KN/m^2

of objective function (10 3665) is obtained when the penalty term is less than 1E-05 and corresponding number of function evaluation being 1500 approximately

7 6 CONCLUSIONS

Based on the results and discussions presented in the previous section the following generalized conclusions can be drawn

- 1)The Lysmer-Basudhar approach using finite element and nonlinear programming is quite reliable and capable in predicting the lower bound bearing capacity of reinforced soil structures viz retaining walls and slopes
- 2)The obtained lower bounds improve upon the results reported in the literature (Sawicki and Lesniewska,1987,1988)
- 3)The choice of mesh pattern is important in predicting the limit load for the strip footing depending upon its location from the face of the wall and for slope angles less than 90^0 introduction of thin element at the sloping face is necessary to obtain a feasible solution
- 4)The sequential unconstrained minimization using the concept of extended penalty function in conjunction with Powell's technique for multivariable search and Quadratic interpolation technique for unidirectional search has been found to be efficient in isolating the optimal limit loads of reinforced soil structures

CHAPTER 8

STABILITY OF VERTICAL CUTS IN HOMOGENEOUS SOILS

8.1 General

Stability of vertical cuts in homogeneous soils has fascinated the geotechnical engineers since long. Through the efforts of various researchers (Drucker and Prager, 1952, Heyman, 1973, Chen, 1975, Pastor, 1978 and De Jong, 1980), it is now possible to bracket the true stability number, when both upper and lower bound values of stability numbers are identical, for a vertical cut in a purely cohesive soil within a small range of 3.64 (Pastor, 1978) to 3.783 (de Jong, 1980) instead of 2 to 4 (Drucker and Prager, 1953). But, Drucker (1953) reported that for purely cohesive soils unable to take tension the upper and lower values are identical and are equal to 2. In the present study, an effort is made to explore the possibility of identifying the range of uncertainty of critical stability number for soils capable of taking tension by obtaining an improved lower bound value than the reported ones using Lysmer-Basudhar approach.

The method has also been used for a general cohesive-frictional ($C-\phi$) soil and the result is then compared with elasto-plastic finite element solution (Snitbhan and Chen, 1978).

8.2 Statement of the Problem

Fig 8.1 depicts a vertical cut of height, H in a soil with cohesion, C and angle of shearing resistance, ϕ . The total unit weight of soil is γ . The objective is to find the maximum value of lower bound stability number, $(\gamma H/C) \cot(45^\circ + \phi/2)$ for the cut. This can be obtained either by changing the height of the cut

keeping the soil parameters constant or by hypothetically varying the total unit weight keeping the other parameters constant. In the present study, first option has been adopted to avoid repeated change of mesh geometry and the resulting computational efforts

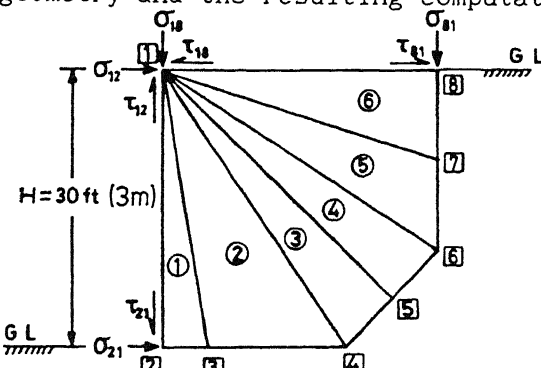


Fig 8.1 (a) Mesh pattern for the vertical cut

For validating the method of analysis the problem solved by Snitbhan and Chen (1978) is considered. As such, the height of the slope (H), the cohesion (C) and the angle of shearing resistance of soil (ϕ) are taken as 30 0ft(9 0m), 810 0psf (38.8kN/m²) and 10^0 respectively. For cuts in purely cohesive soils, results are obtained for $\phi=0^0$ keeping other parameters same.

8.3 Boundary conditions and the Objective function

With reference to the Fig 8.1 the specified boundary conditions are as follows

Boundary conditions

$$\tau_{12} = \tau_{21} = \tau_{18} = \tau_{81} = 0$$

$$\sigma_{12} = \sigma_{21} = \sigma_{18} = \sigma_{81} = 0$$

$$\text{Objective function} \quad \frac{\gamma H \cot(45^0 + \phi/2)}{C}$$

8.4 Results and Discussions

The results were obtained using a CONVEX C220 computer system and are presented and discussed as follows

As lower bound analysis involves the generation of statically admissible stress field, it is of interest to study the state of stress at the limiting state corresponding to the optimal solution in the soil medium. The complete stress field along with the stress-strength ratio is shown in Table 8 1 for a purely cohesive soil ($\phi=0^0$). When close to unity the ratio signifies the limiting equilibrium state. As per this criterion, the nodal point no 4 in element no 2 is very near to the limiting state (the stress-strength ratio equal to 0.9994). It is also noticed from the table

TABLE 8 1
Stress field and the stress-strength ratios at the nodal points.

Element No	Nodal point No	σ_x	σ_z	τ_{zx}	stress-strength ratio
1	1	0 0000	0 0000	0 0000	-
1	2	0 0000	0 4560	0 0000	0.7131
1	3	0 0000	0 3653	0 0760	0.5368
2	1	0 0000	0 0000	0 0000	-
2	3	-0.0035	0 2370	0 0974	0.3286
2	4	0.0306	0 4243	0 1847	0.9994
3	1	0 0000	0 0000	0 0000	-
3	4	0 2833	0 6050	0 1944	0.8734
3	5	0 0854	0 2962	0 0246	0.1607
4	1	0 0000	0 0000	0 0000	-
4	5	0 1916	0 5132	0 0816	0.4462
4	6	0 2656	0 5614	0 1770	0.7299
5	1	0 0000	0 0000	0 0000	-
5	6	0 0001	0 4434	0 0000	0.6738
5	7	0 0000	0 1108	0 0000	0.0421
6	1	0 0000	0 0000	0 0000	-
6	7	0 0000	0 3325	0 0000	0.3792
6	8	0 0000	0 0000	0 0000	-

* All stress values are normalized with 3000 Opsf(143.7 kN/m^2)

that nodal point 3 (element no 2) is under a small tension, the actual tension in the x-direction is 10.68psf(0.51 kN/m^2). This value of the tension is much smaller than either $C/9$ ($=4.31 \text{ kN/m}^2$) or $C/10$ ($=3.88 \text{ kN/m}^2$) which may be allowed as the permissible

tension in cohesive soils as suggested by Chen (1975)

Table 8.2 presents the design vector, sigma vector, equality and inequality constraints along with the objective function value at the optimum. All the inequality constraints being negative values are strictly satisfied. Some of the equality constraints being zero are identically satisfied, the others are of such a small order of magnitude that for all practical purposes may also be considered to be satisfied. It can be seen from the table that the no-tension constraints on the principal unknowns are strictly

TABLE 8.2
Design vector, sigma vector, constraints and objective function value at the optimum.

(D)vector*						
0 4560	0 4243	0 4169	0 0000	0 2123	0 4243	0 3653
0 0000	0 0000	0 0000	99 76035	(optimal value of γ)		
(σ)vector*						
0 0000	0 0000	0 0000	0 0000	0 0000	0 0000	0 0000
0 0000	0 0000	0 0345	0 0000	0 3222	0 0000	0 3816
0 0000	0 4604	0 0000	0 2993	0 0000	0 0000	0 4560
0 3653	0 2370	0 4243	0 4169	0 0000	0 2123	0 4243
0 0001	0 0000	0 0000	0 0000			
Interface shear equality constraints						
0 0000	0 0000	0 0000		-0 1639E-06	0 0000	
0 2570E-06	0 0000	-0 8941E-07		0 0000	-0 5298E-07	
Boundary shear equality constraints						
0 0000	-0 5960E-07	0 0000		0 2235E-07		
Yield constraints (inequality)*						
-0 2916E 00	-0 8366E-01	-0 1350E 00		-0 2916E 00	-0 1958E 00	
-0 1713E-03	-0 2916E 00	-0 3690E-01		-0 2447E 00	-0 2916E 00	
-0 1615E 00	-0 7874E-01	-0 2916E 00		-0 9512E-01	-0 2793E 00	
-0 2916E 00	-0 1810E 00	-0 2916E 00				
No-tension constraints (inequality)						
0 0000	-0 3452E-01	0 0000		-0 3221E 00	0 0000	
-0 3816E 00	0 0000	-0 4604E 00		0 0000	-0 2993E 00	
-0 4560E 00	-0 3653E 00	-0 2370E 00		-0 4243E 00	-0 4169E 00	
0 0000	-0 2123E 00	-0 4243E 00		-0 1297E-03	0 0000	
0 0000	0 0000					
Optimal function value						
			3 69483			

* All values are normalized with 3000 Opsf (143 7kN/m²)

satisfied, however, it should be noted that satisfaction of these constraints could not prevent the development of tension on other planes as evident from Table 8 1 and discussed earlier. It can further be observed that the optimal value of the objective function which in the present study is the stability number of 3.69483 is marginally higher than the value 3.64 (Pastor, 1978) and is closer (even though by a marginal amount) to the upper bound solution of 3.783 (De Jong, 1980). Thus, the present study helps in reducing the range within which the critical height of a vertical cut in homogeneous clays would lie.

In Table 8 3, the stress-strength ratios, obtained for different nodal points within the soil mass using the present method of analysis are compared with the values computed from the stress functions proposed by Heyman (1973) for different zones as shown in Fig 8 2.

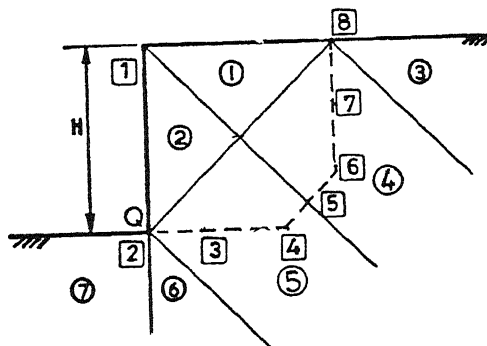


Fig 8 2 Different zones for the vertical cut (Heyman, 1973)

It can be seen from the table that in general the present analysis results in higher values of stress-strength ratios at the nodal points and thus gives a higher value for the stability number. The obtained stress field could not be compared with those of other methods as such data is not available.

TABLE 8.3
Comparison of stress-strength ratios for different nodal points

Nodal points	Heyman (1970)		Present study	
	Zone no	ratio	Element no	ratio
1	1, 2	-	1, 2, 3, 4, 5, 6	-
2	2	0.5000	1	0.7131
3	5	0.5937	1	0.5368
			2	0.3286
4	5	0.5000	2	0.9994
			3	0.8734
5	5	0.6250	3	0.1607
		0.6250	4	0.4462
6	4	0.5555	4	0.7299
			5	0.6738
7	4	0.5138	5	0.0421
			6	0.3792
8	1	0.5000	6	-
	4	0.5000		

The variation of objective function with penalty parameter (r_k) and number of function evaluations is shown in Fig 8.3(a) and 8.3(b) respectively. It is observed that the minimum value of the objective function (3.69483) is achieved when r_k is 1E-03 and the corresponding number of function evaluations is 300. The steady nature of the objective function indicates a convergent solution.

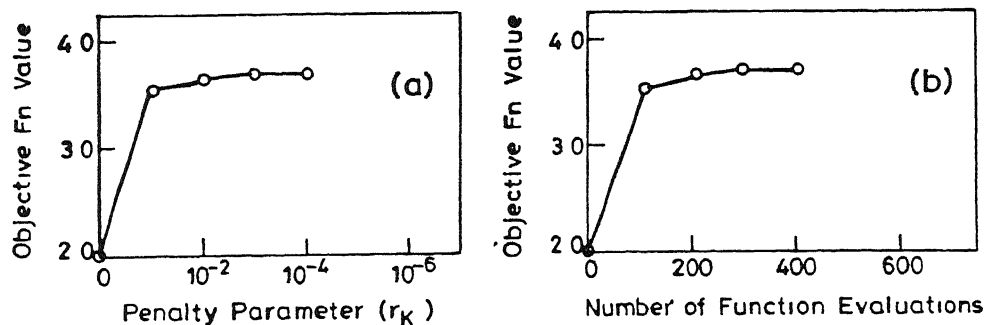


Fig 8.3 Variation of objective function with (a) Penalty parameter and (b) number of function evaluations for a vertical cut ($\phi=0$)

For a general C- ϕ soil, the obtained total unit weight (γ) using the present approach is 118.89pcf (18.67kN/m³) This value is lower than 150pcf (23.55kN/m³) obtained by Snitbhan and Chen (1978) using finite element method and treating the soil to be an elasto-plastic material by 20.74% The CPU time required to achieve the optimal solution is 0.847 seconds

8.5 Conclusions

Based on the presented results and discussions the following conclusions can be drawn

- 1)The Lysmer-Basudhar approach based on discrete elements and nonlinear programming is quite effective in analyzing the stability of vertical cuts in homogeneous soils
- 2)The obtained lower bound stability number (3.69483) for vertical cuts in pure clays is marginally greater than the reported lower bound value 3.64 and is closer to the upper bound solution 3.783
- 3)For a general C- ϕ soil, the calculated value of total unit weight differs from that of finite element elasto-plastic solution by 20.74% on the lower side
- 4)The study enables to reduce marginally the bound within which the critical height would lie

CHAPTER 9

STABILITY OF A TRAPDOOR IN COHESIVE SOILS

9 1 General

Using the limit theorems of plasticity Davis (1968) and Gunn (1980) analyzed Terzaghi's trapdoor problem in cohesive soils. The same has been used as a test problem by Sloan (1989) and Sloan et al (1990) to validate their analyses using finite element technique in conjunction with active set algorithm of linear programming. The study reported herein pertains to the successful application of the Lysmer-Basudhar approach to study the stability of trapdoors in purely cohesive soils. The study also brings out a comparison of the solutions obtained by using nonlinear and linear programming approaches of isolating the optimal stress fields.

9 2 Statement of the Problem

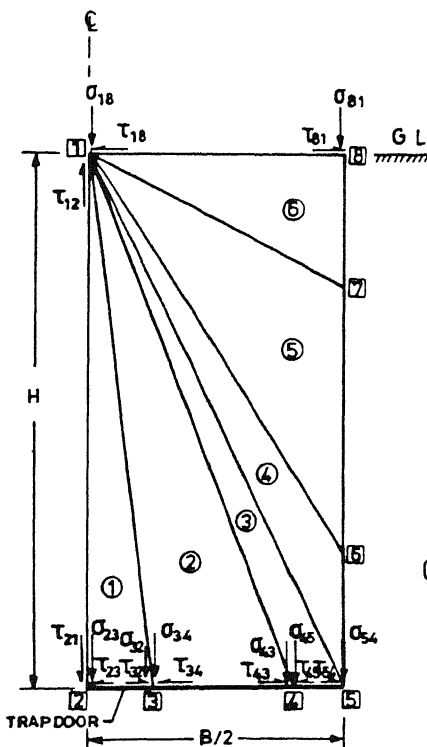
Figs 9 1(a) and 9 1(b) show a smooth trapdoor embedded at a depth, H , in a purely cohesive soil with undrained shear strength, C_u and unit weight, γ along with the discretization of the soil mass under consideration. For different embedment ratios the objective is to find the stability numbers (N) defined as

$$N = \frac{(\gamma H - q)}{C_u}$$

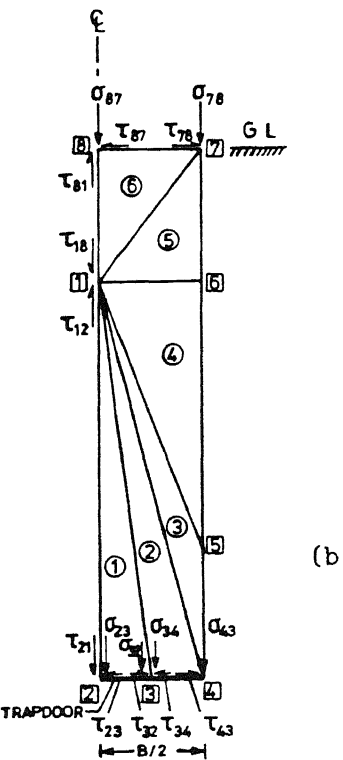
where, q is the average uniformly distributed stress on the trapdoor

9 3 Boundary conditions and the Objective functions

The boundary conditions and the objective functions corresponding to shallow and deep trapdoors are presented as follows



(a)



(b)

Fig 9.1 Mesh patterns for a (a) shallow and (b) deep trapdoor

Shallow trapdoors (Fig 9.1(a))

$$\sigma_{18} = \sigma_{81} = 0$$

$$\tau_{18} = \tau_{81} = \tau_{12} = \tau_{21} = \tau_{23} = \tau_{32} = \tau_{34} = \tau_{43} = \tau_{45} = \tau_{54} = 0$$

$$\text{Objective function } -(\sigma_{23} + \sigma_{32} + \sigma_{34} + \sigma_{43} + \sigma_{45} + \sigma_{54})$$

Deep trapdoors (Fig 9.1(b))

$$\sigma_{78} = \sigma_{87} = 0$$

$$\tau_{78} = \tau_{87} = \tau_{12} = \tau_{21} = \tau_{23} = \tau_{32} = \tau_{34} = \tau_{43} = \tau_{81} = \tau_{18} = 0$$

$$\text{Objective function } -(\sigma_{23} + \sigma_{32} + \sigma_{34} + \sigma_{43})$$

The average uniformly distributed stress (q), which is transmitted to the trap door is obtained by numerically integrating the stress terms in the objective function by using Simpson's (1/3)rd quadrature rule. The stability number (N) is then obtained by using the expression as given above.

The necessity of classifying the trapdoors as shallow and deep has been presented in the following section.

9.4 Results and Discussions

To validate and show the effectiveness of the present method the results are obtained for different values of the embedment ratio (H/B) using a HP-9000/850s computer system. These are presented and discussed as follows.

The obtained results are presented in Table 9.1 using the mesh pattern of Fig 9.1(a). It is observed that this mesh pattern remains valid up to embedment ratio 1.25 only beyond which no solution could be obtained. To obtain the stability numbers for other embedment ratios the mesh pattern as shown in Fig 9.1(b) has been adopted. It can be observed from the table that this mesh pattern can not be used for embedment ratios less than 1.25. Hence, it can be concluded that the trapdoor may be considered to be 'deep' if the embedment ratio is greater than 1.25.

TABLE 9.1
Stability numbers for trap door

Mesh pattern	Embedment ratios (H/B)									
	0.4	0.6	0.8	1.0	1.25	1.67	2.5	5.0	10.0	
Fig 9.1	0.50	0.76	1.35	1.75	2.08	-	-	-	-	-
Fig 9.2	-	-	-	-	0.37	3.0	4.0	6.16	7.55	

In Table 9.2 the obtained results are presented with the solutions available in literature. It can be observed that for deep trapdoors the present solutions are either equal or higher than the lower bound solutions given by Sloan et al (1990). It should be noted that the present lower bound solutions for embedment ratios of 5 and 10 are marginally higher than those of

upper bound solutions predicted by them. However, these values being very close may be treated as a true indicator of the exact critical load.

The correctness of the predicted stability numbers by either method can not be commented upon with certainty in the absence of experimental model studies.

TABLE 9 2
Comparison of obtained stability numbers with the reported values

H/B	Davis(1968)*		Gunn(1980)*		Sloan et al (1990)*		Present study
	L B	U B	L B	U B	L B	U B	
0 40	0 40	0 85	-	0 85	0 65	0 65	0 50
0 60	0 80	1 25	0 60	1 28	0 90	0 90	0 76
0 80	1 25	1 65	0 70	1 35	1 50	1 50	1 35
1 00	1 60	2 00	1 40	1 85	1 86	1 86	1 75
1 25	2 00	2 50	1 65	2 45	2 26	2 40	2 08
1 67	3 00	3 35	2 40	3 40	2 66	2 80	2 85
2 50	3 50	5 00	3 25	4 50	4 00	4 26	4 00
5 00	3 95	10 00	4 50	6 40	5 46	6 00	6 16
10 00	4 00	20 00	6 00	9 00	6 66	7 33	7 55

*Read from the graphs

L B Lower Bound, U B Upper Bound

If the stress path dependent stress-strain behavior and the corresponding strength parameters are not properly correlated then two different predictive models, one based on displacement formulation and the other on stress formulation may not give the expected results. For shallow trapdoors ($H/B \leq 1.25$) the present solutions are closer to the corresponding values of Davis (1968) and Sloan et al (1990) as compared to those of Gunn (1980), however for embedment ratio of 0.8 and 1.0 the present solutions are either identical or closer to the upper bound solutions of Gunn (1980) which in turn are also very close to the lower and upper bound solutions of Sloan et al (1990), however, for shallow

trapdoors the later authors predict higher lower bound values as compared to the present solutions

The study reveals that the present approach based on nonlinear programming predicts better results for deep trapdoors as compared to other studies For shallow trapdoors the comparison shows reasonable agreement

As it is impossible to guess a feasible starting point design vector in such analytical problems, the iterations to obtain an optimal solution were carried out starting from a design vector whose all elements are zero The design vector, sigma vector, equality and inequality constraints along with the value of objective function achieved at the optimum corresponding to a deep trapdoor with $H/B=2.5$ are given in Table 9.3 Most of the equality constraints being either zeros or of such a small order of magnitude that for all practical purposes these may be considered to be satisfied

The problems analyzed needed only 0.47 to 1.51 seconds of CPU time to obtain the optimal solution This establishes the computational efficiency of the method

The complete stress field along with the stress-strength ratio is shown in Table 9.4 for a trapdoor with $H/B=2.5$ The ratio close to unity signifies the limiting equilibrium state From this consideration it may be observed that for the chosen mesh pattern many of the nodal points are very near to the limiting state Similar stress fields were obtained for other embedment ratios too However, for the sake of brevity these are not presented herein

(D)Vector

1 3155	0 2965	0 2412	1 4823	1 2620	0 9582	0 9552
0 5735	0 3618	0 3630				

(σ)Vector

0 5655	0 5735	0 3516	0 3630	0 0000	0 0000	0 3745
1 2846	0 3778	1 2867	0 3873	1 2979	0 3964	1 0110
0 3209	0 2965	0 2446	0 0000	0 2412	0 0000	1 3155
1 4029	1 4029	1 4823	1 2620	0 9582	0 9592	0 3630
0 3618	0 0000	0 0000	0 0000			

Interface shear equality constraints

-0 1205E-06	0 7003E-06	-0 9118E-07	-0 8940E-06	0 1464E-06
0 1341E-06	-0 1490E-07	-0 1490E-06	0 4470E-07	-0 7450E-08

Boundary shear equality constraints

0 7450E-08	0 0000	0 1490E-07	0 0000	0 1151E-06
0 3874E-06	-0 3874E-06	-0 3427E-06	0 8270E-06	0 8284E-06

Yield constraints(inequality)

-0 3505E-02	-0 3904E-01	-0 2600E-01	-0 4522E-03	-0 2600E-01
-0 9656E-03	-0 4782E-03	-0 1229E-02	-0 7741E-02	-0 2533E-01
-0 3848E-03	-0 2033E-03	-0 4000E-01	-0 2592E-01	-0 3593E-03
-0 4000E-01	-0 3992E-01	-0 4000E-01		

No-tension constraints(inequality)

-0 5655E 00	-0 5735E 00	-0 3516E 00	-0 3630E 00	-0 3745E 00
-0 1284E+01	-0 3778E 00	-0 1286E+01	-0 3873E 00	-0 1297E+01
-0 3964E 00	-0 1011E+01	-0 3209E 00	-0 2965E 00	-0 2446E 00
0 7450E-08	-0 2412E 00	0 0000	-0 1315E+01	-0 1402E+01
-0 1402E+01	-0 1482E+01	-0 1262E+01	-0 9582E 00	-0 9552E 00
-0 3630E 00	-0 3618E 00	0 5053E-08		

Optimal function value

Optimal function value	5 6038
------------------------	--------

*All values are normalized with γH

TABLE 9 4*

Stress field and the Stress-strength ratios at the nodal points
for a trapdoor (H/B=2 5)

Element no	Nodal point no	σ_x	σ_z	τ_{zx}	Stress-strength ratio
1	1	0 3745	0 5655	0 0000	0 9123
1	2	1 2846	1 3155	0 0000	0 0239
1	3	1 2846	1 4029	0 0000	0 3499
2	1	0 3746	0 5735	0 0010	0 9886
2	3	1 2846	1 4029	0 0000	0 3499
2	4	1 2847	1 4823	0 0000	0 9758
3	1	0 3516	0 2496	0 0853	0 9880
3	4	1 2620	1 1631	0 0851	0 9692
3	5	0 9582	0 9088	0 0863	0 8064
4	1	0 3630	0 3209	0 0567	0 3667
4	5	0 9552	0 8897	0 0939	0 9903
4	6	0 3630	0 2965	0 0940	0 9949
5	7	0 0000	0 0000	0 0000	-
5	1	0 2866	0 3209	0 0567	0 3519
5	6	0 3618	0 2965	0 0940	0 9910
6	8	0 0000	0 0000	0 0000	-
6	1	0 2412	0 2500	0 0000	0 0019
6	7	0 0000	0 0000	0 0000	-

Figs 9 2(a) and 9 2(b) show the variation of the objective function with penalty parameter and number of function evaluations. It is observed that the objective function attains a steady value (5.6038) corresponding to the penalty parameter equal to 1E-06 and 1888 function evaluations.

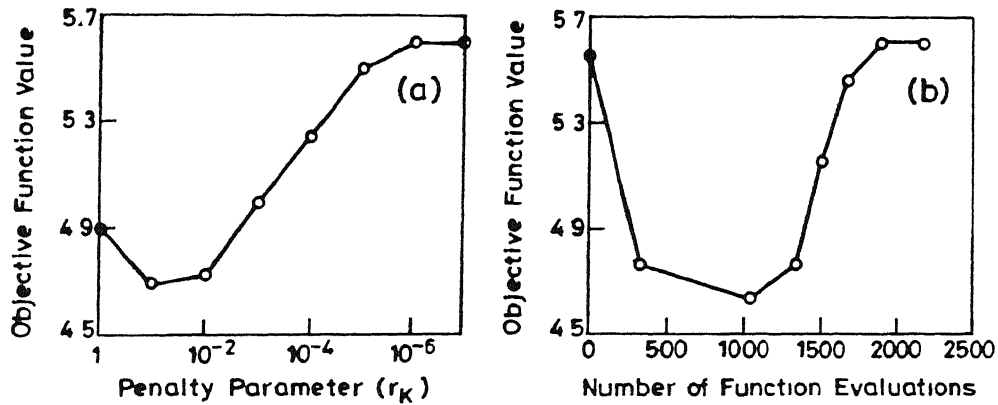


Fig 9 2 Variation of objective function with (a) Penalty parameter and (b) number of function evaluations for a trapdoor ($H/B=2.5$)

To check the effect of number of elements a study was conducted by dividing the soil mass as shown in Fig 9 1(a) into 10 number of elements. The obtained stability number is 1.71 for $H/B=1.0$ as compared to 1.75 obtained by using 6 elements. However, for the sake of brevity the details are not presented herein. For 10 elements the CPU time required to obtain the optimal solution is 0.88 seconds.

9.5 Conclusions

On the basis of the results and discussions the following conclusions can be drawn:

- 1) The Lysmer-Basudhar approach using finite element and nonlinear programming is quite reliable and efficient in predicting the

lower bound stability numbers for a trapdoor in cohesive soil

2)The choice of mesh pattern is important and is different for the deep and shallow trapdoors

3)The obtained stability numbers for shallow trapdoors compare well with the solutions reported in the literature. But for deep trapdoors the predicted values are better than the solutions available

4)Using only a few elements the present approach gives solutions which are close to the solutions obtained by using other reported techniques with large number of elements

CHAPTER 10

GENERALIZED CONCLUSIONS AND SCOPE FOR FUTURE STUDIES

10.1 Conclusions

The conclusions specific to various problems studied are not repeated here and only the generalized conclusions which are common to all are

- 1) Modified Lysmer (Lysmer-Basudhar) approach using discrete element and nonlinear programming has been found to be very successful in predicting the lower bound solutions of various stability problems in geotechnical engineering
- 2) The mesh patterns have significant influence over the obtained optimal solutions. The suggested generalized mesh patterns pertinent to each problem can be used
- 3) Comparison of the obtained solutions with the available theoretical and experimental results shows a good agreement
- 4) Sequential unconstrained minimization of the composite function using Powell's technique for multivariable search and quadratic interpolation for unidirectional search is found to be efficient in isolating the optimal solutions
- 5) The approach is found to be very efficient in terms of economy of computations and takes only few seconds of CPU time to obtain a feasible solution

10 2 Scope for future studies

The following topics are recommended for future studies

- 1 Determination of lower bound solution using present approach and
 - a)considering nonhomogeneous and anisotropic undrained shear strength distribution of soil medium
 - and, b)considering a multi layer soil deposit
- 2 Modification of the present approach to incorporate-
 - a)a nonlinear stress field
 - b)rectangular elements
 - and, c)three dimensional elements
- 3 Consideration of soil slip at the soil-reinforcement interface
- 4 Experimental validation of the obtained results through model studies

REFERENCES

Anderheggen, E and Knopfel, H (1972), "Finite Element Limit Analysis Using Linear Programming", *Int J Solids Struct*, 8, No 12, 1413-1431

Arai, K and Tagyo, K (1985), "Limit Analysis of Geotechnical Problems by Applying Lower Bound Theorem", *Soils and Foundations*, 25, No.4, 37-48

Arai, K and Nakagawa, M (1988), "A New Limit Equilibrium Analysis of Slope Stability Based on Lower Bound Theorem", *Soils and Foundations*, 28, No.1, 1-15

Assadi, A and Sloan, S W (1991), "Undrained Stability of A Shallow Square Tunnel", *Journal of Geotechnical Engineering*, ASCE, 117, No 8, 1152-1173

Azam, G , Hsieh, C W and Wang, M C (1991), "Performance of Strip Footing on Stratified Deposit With Void", *Journal of Geotechnical Engineering*, ASCE, 117, No 5, 753-772

Baker, R and Frydman, S (1983), "Upper Bound Limit Analysis of Soil With Non-linear Failure Criterion", *Soils and Foundations*, 23, No.4, 34-42

Basudhar, P K (1976), "Some Applications of Mathematical Programming Techniques to Stability Problems in Geotechnical Engineering", Ph D thesis, *Indian Institute of Technology, Kanpur, India*

Basudhar, P K , Madhav, M R and Valsangkar, A J (1979), "Optimal Lower Bound of Passive Earth Pressure Using Finite Elements and Nonlinear Programming", *International Journal for Numerical and Analytical Methods in Geomechanics*, 3, 367-379

Basudhar, P K , Madhav, M R and Valsangkar, A J (1981), "Sequential Unconstrained Minimization in the Optimal Lower Bound Bearing Capacity Analysis", *Indian Geotechnical Journal*, 11, 42-55

Baus, R L and Wang, M C (1983), "Bearing Capacity of Strip Footing Above Void", *Journal of Geotechnical Engineering*, ASCE, 109, No.1, 1-14

Belytschko, T and Hodge, P G (1970), "Plane Stress Limit Analysis By Finite Elements", *Journal of Engg Mech Div*, ASCE, 96, 931-944

Booker, J R and Davis, E H (1972), "A Note On A Plasticity Solution to the Stability of Slopes in Homogeneous Clays", *Geotechnique*, 22, No 3, 509-513

Bottero, A , Negre, R , Pastor, J and Turgeman, S (1980), "Finite Element Method and Limit Analysis Theory for Soil Mechanics Problems", *Comput Methods Appl Mech Engg*, 22, 131-149

Bowles, J E (1988), "Foundation Analysis and Design", *McGraw-Hill Company* New York

Britto, A M and Kusakabe, O (1988), "Stability of Axisymmetric Excavation in Clay", *Civil Engineering Practice, Geotechnical/Ocean Engineering*, 3, Chapter 9, 337-363, Eds P N Cheremisinoff et al Technomic Publishing Co Inc Lancaster USA

Brown, B S and Poulos, H G (1981), "Analysis of Foundations on reinforced Soil", *Proc 10th Int Conf Soil Mech and Foundation Engg*, Stockholm, 3, 595-598

Casciaro, R and Cascini, L (1982), "A Mixed Formulation and Mixed Finite Elements for Limit Analysis", *International Journal for Numerical and Analytical Methods in Geomechanics*, 18, 211-243

Chen, W F (1968), "Discussion on Application of Limit Plasticity in Soil Mechanics, by W D Liam Finn", *Journal of Soil Mech Found Div*, ASCE, 94, No SM2, 608-613

Chen, W F (1969), "Soil Mechanics and Theorems of Limit Analysis", *Journal of Soil Mech Found Div*, ASCE, 95, No SM2, 493-518

Chen, W F (1975), "Limit Analysis and Soil Plasticity", *Elsevier*, Amsterdam

Chen, W F (1987), "Stability Analysis of Slopes With General Nonlinear Failure Criterion", *International Journal for Numerical and Analytical Methods in Geomechanics*, 11, 33-50

Chen, W F and Baladi, G Y (1985), "Soil Plasticity Theory and Implementation", *Developments in Geotechnical Engineering*, 38, Elsevier

Chen, W F and Davidson, H L (1973), "Bearing Capacity Determination by Limit Analysis", *Journal of the Soil Mechanics and Foundations Division*, ASCE, 99, No SM 6, 433-449

Chen, W F and Giger, M W (1971), "Limit Analysis of Stability of Slopes", *Journal of the Soil Mechanics and Foundations Division*, ASCE, 97, No SM 1, 19-26

Chen, W F, Giger, M W and Fang, H Y (1969), "On The Limit Analysis of Stability of Slopes", *Soils and Foundations*, 9, No 4, 23-32

Chen, W F and Rosenfarb, J L (1973), "Limit Analysis solutions of Earth Pressure Problem", *Soils and Foundations*, 13, No 4, 45-60

Chen, W F and Scawthorn, C R (1970), "Limit Analysis and Limit Equilibrium Solutions in Soil Mechanics", *Soils and Foundations*, 10, No 3, 13-49

Clemence, P S and Veesaert, C J (1977), "Dynamic Pullout Resistance of Anchors in Sand", *Proc Int Symp on Soil Structure Interaction* Roorkee, 389-397

Cox, A D (1962), "Axially Symmetric Plastic Deformation in Soil-II-Indentation of Ponderable Soils", *Int J Mech Sc*, 4, 371-380

Das, B M (1990), "Earth Anchors", *Developments in Geotechnical Engineering*, 50, Elsevier

Davidon, W C (1959), "Variable Metric Method for Minimization", *Argonne Natl Lab ANL-9990 Rev*, Univ of Chicago

Davis, E H (1968), "Theories of Plasticity and the Failure of Soil Masses", *Soil Mechanics - Selected Topics*, Ed I K Lee, Chapter 6, American Elsevier, New York, 341-380

Davis, E H and Booker, J R (1973), "The Effect of Increasing Strength With Depth on the Bearing Capacity of Clays", *Geotechnique*, 23, No 4, 551-563

Davis, E H, Gunn, M J, Mair, R J and Seneviratne, H N (1980), "The Stability of Shallow Tunnels and Underground Openings in Cohesive Material", *Geotechnique*, 30, NO 4, 397-416

DeBorst, R and Vermeer, P A (1984), "Possibilities and Limitations of Finite Elements for Limit Analysis", *Geotechnique*, 34, No 2, 199-210

DeBuhan, P, Mangiavacchi, R, Nova, R, Pellegrini, G and Salencon, J (1989), "Yield-Design of Reinforced Earth Walls by A Homogenization Method", *Geotechnique*, 39, NO 2, 189-201

De Jong, Josselin G (1980), "Application of the Calculus of Variations to the Vertical Cutoff in Cohesive Friction less Soil", *Geotechnique*, 30, No 1, 1-16

Drucker, D C (1953), "Limit Analysis of Two and Three Dimensional Soil Mechanics Problem", *Journal of the Mechanics and Physics of Solids*, London, 1, 217-226

Drucker, D C, Greenberg, H J and Prager, W (1952), "Extended Limit Design Theorems for Continuous Media", *Quarterly Journal of Applied Mathematics*, 9, 381-389

Drucker, D C and Prager, W (1952), "Soil Mechanics and Plastic Analysis or Limit Design", *Quarterly Journal of Applied Mathematics*, 10, 157-165

Drumm, E C, Kane, W F and Yoon, C J (1990), "Application of Plasticity to the Stability of Sinkholes", *Engineering Geology*, Amsterdam, 29, No 3, 213-225

Fiacco, A V and McCormick, G P (1968), "Nonlinear programming Sequential Unconstrained Minimization Techniques", *John Wiley*, NY

Finn, W D L (1967), "Application of Limit Plasticity in Soil Mechanics", *Journal of the Soil Mechanics and Foundations Division*, ASCE, 93, No SM 5, 101-120

Fletcher, R (1973), "Mathematical Programming Methods- A Critical Review", Optimum Structural Design-Theory and Application, 51-77, Eds R H Gallagher and O C Zienkiewicz John Wiley and Sons Printed in Great Britain

Fletcher, R and Reeves, C M (1964), "Function Minimization by Conjugate Gradients", *Computer Journal*, 7(2), 149-154

Fox, R L (1971), "Optimization Methods for Engineering Design", Addison-Wesley, Reading, Mass

Giger, M W and Krizek, R J (1975), "Stability Analysis of Vertical Cut with Variable Corner Angle", *Soils and Foundations*, 15, No 2, 63-71

Gioda, G and Donato, O D (1979), "Elastic-Plastic Analysis of Geotechnical Problems by Mathematical Programming", *International Journal for Numerical and Analytical Methods in Geomechanics*, 3, 381-401

Graham, J (1968), "Plane Plastic Failure in Cohesion less Soils", *Geotechnique*, 18, 301-316

Graham, J (1979), "Embankment Stability on Anisotropic Soft Clays", *Canadian Geotechnique Journal*, 16, No 2, 295-308

Griffiths, D V (1982), "Elasto-Plastic Analysis of Deep Foundations in Cohesive Soil", *International Journal for Numerical and Analytical Methods in Geomechanics*, 6, 211-218

Gunn, M J (1980), "Limit Analysis of Undrained Stability Problems Using A Very Small Computer", *Proc Symp on Computer Applications to Geotechnical Problems in Highway Engineering*, Cambridge Univ, Engrg Dept, 5-30

Hanna, A M, Das, B M and Foriero, A (1988), "Behavior of Shallow Inclined Plate Anchors in Sand", In Spec Topics in Found, *Geotech Spec Tech Publ No.16*, ASCE, 54-72

Hansen, J B (1961), "A General Formula for Bearing Capacity", *Bulletin No 11*, The Danish Geotechnical Institute

Hayes, D J and Marcal, P V (1967), "Determination of Upper Bounds for Problems in Plane Stress Using Finite Element Technique", *International Journal of Mech Sci*, Pergamon Press Ltd, 9, 245-251 Printed in Great Britain

Heyman, J (1973), "The Stability of a Vertical Cut", *International Journal of Mech Sci*, Pergamon Press Ltd, 15, 845-854 Printed in Great Britain

Kavlie, D and Moe, J (1971), "Automated Design of Frame Structures", *Journal of Structural Division*, ASCE, 97, ST1, 33-61

Koopman, D C A and Lance, R H (1965), "On Linear Programming and Plastic Limit Analysis", *Journal of the Mechanics and Physics of Solids*, London, 13, 77-87

Koutsabeloulis, N C and Griffiths, D V (1989), "Numerical Modelling of the Trap Door Problem", *Geotechnique*, 39, No 1, 77-89

Kusakabe, O, Kimura, T and Yamaguchi, H (1981), "Bearing Capacity of Slopes Under Strip Loads on the Top Surface", *Soils and Foundations*, 21, No 4, 29-40

Lysmer, J (1970), "Limit Analysis of Plane Problems in Soil Mechanics", *Journal of the Soil Mechanics and Foundations Division*, ASCE, 96, SM4, 1311-1334

Maib, A A, Das, B M and Picornell, M (1986), "Ultimate Resistance of Shallow Inclined Strip Anchor Plate in Sand", *Proc Southeastern Conf on Theoretical and Applied Mech (SECTAM XII)*, Columbia, S C, USA

Meyerhof, G G (1951), "The Ultimate Bearing Capacity of Foundations", *Geotechnique*, 2, No 4, 301-332

Meyerhof, G G (1973), "The Uplift Capacity of Foundations Under Oblique Loads", *Canadian Geotechnical Journal*, 10, No 1, 64-70

Meyerhof, G G (1980), "Limit Equilibrium Plasticity in Soil Mechanics", *Application of Plasticity and Generalized Stress-Strain in Geotechnical Engineering* Ed R N Yong and E T Selig, ASCE, New York

Meyerhof, G G and Adams, J I (1968), "The Ultimate Capacity of Foundations", *Canadian Geotechnical Journal*, 5, No 4, 225-244

Mizuno, E and Chen, W F (1983a), "Plasticity Analysis of Slope With Different Flow Rules", *Comp and Strs*, 17, No 3, 375-388

Mizuno, E and Chen, W F (1983b), "Cap Models for Clay Strata to Footing Loads", *Comp and Strs*, 17, No 4, 511-528

Mizuno, E and Chen, W F (1983c), "Plasticity Modeling and its Application to Geomechanics", *Recent Developments in Laboratory and Field Tests and Analysis of Geotechnical Problems* Bangkok

Naylor, D J (1982), "Finite Elements and Slope Stability", *Numerical Methods in Geomechanics*, Ed J B Martin, D Reidel Publishing Company, 229-244

Pastor, J (1978), "Analyse Limite Determination de Solutions Statiques Complètes Application au Talus Vertical", *J de Mécanique Appliquée*, 2, No 2, 167-197

Powell, M J D (1964), "An Efficient Method for Finding the Minimum of A Function of Several Variables Without Calculating Derivatives", *Computer J*, 7, No 4, 303-307

Purushothamaraj, P, Ramiah, B K and Rao, K N V (1974), "Bearing Capacity of Strip Footings in Two Layered Cohesive - Friction Soils", *Canadian Geotechnical Journal*, 11, No 1, 32-45

Rao, S S (1984), "Optimization Theory and Application", Wiley-Eastern Limited

Reddy, A S, Dutt, H H and Jagannath, S V (1989), "Bearing Capacity of Circular Footing in Two Layered Soil", *Indian Geotechnical Journal*, 19, No.2, 167-180

Reddy, A S, Jagannath, S V and Dutt, H H (1990), "Bearing Capacity of Footings on Two Layered Soil", *Indian Geotechnical Journal*, 20, No 3, 161-174

Reddy, A S and Rao, K N V (1982), "Stability of Slopes by Method of Characteristics", *Journal of Geotechnical Engineering Division*, ASCE, 108, No GT9, 1182-1186

Reddy, A S and Rao, K N V (1983a), "Earth Pressures by the Method of Characteristics With Different Adhesion Ratio and Wall Friction Ratio", *Indian Geotechnical Journal*, 13, No 4, 228-248

Reddy, A S and Rao, K N V (1983b), "Bearing Capacity of Strip Footing in Two Layer C- ϕ Soils Exhibiting Anisotropy and Nonhomogeneity in Cohesion", *Indian Geotechnical Journal*, 13(4), 187-210

Reddy, A S and Sridevi B (1990), "Stability Analysis of Axisymmetric Slopes by Method of Characteristics", *Journal of Institution of Engineers(I)*, 71, H3-H9, UDC 624 139 3

Rowe, R K and Booker, J R (1978), "A Method of Analysis for Horizontally Embedded Anchors in an Elastic Soil", *Research Report no R316*, The Univ of Sydney, School of Civil Engineering

Rowe, R K and Davis, E H (1977), "Application of The Finite Element Method to The Prediction of Collapse Loads", *Research Report no R310*, The Univ of Sydney, School of Civil Engineering

Rowe, R K and Davis, E H (1982a), "The Behavior of Anchor Plates in Clay", *Geotechnique*, 32, No.1, 9-23

Rowe, R K and Davis, E H (1982b), "The Behavior of Anchor Plates in Sand", *Geotechnique*, 32, No 1, 25-41

Sabzevari, A and Ghahramani, A (1972), "The Limit Analysis of Bearing Capacity and Earth Pressure Problems in Nonhomogeneous Soils", *Soils and Foundations*, 12, No 3, 33-48

Salencon, J (1977), "Application of the theory of plasticity in Soil Mechanics", *John Wiley*

Sawicki, A (1988), "Plastic Behavior of Reinforced Earth", *Civil Engineering Practice, Geotechnical/Ocean Engineering*, 3, Chapter3, 45-64 Eds P N Cheremisinoff et al Technomic Publishing Co Inc Lancaster USA

Sawicki, A and Lesniewska, D (1987), "Failure Modes and Bearing Capacity of Reinforced Soil Retaining Walls", *Geotextiles and Geomembranes*, 5, 29-44

Sawicki, A and Lesniewska, D (1988), "Limit Analysis of Reinforced Slopes", *Geotextiles and Geomembranes*, 7, 203-220

Schmertmann, G R, Chouery-Curtis, V E, Jhonson, A D and Bonaparte, R D (1987), "Design Charts for Geogrid-Reinforced Soil Slopes", *Proc Geosynthetics Conf*, Los Angeles, 1, 108-120

Seneviratne, H N and Uthayakumar, M (1989), "Computer Aided Bound Solutions in A Cohesive Material", *Computer and physical modelling in Geotechnical Engineering*, Eds Balasubramaniam et al Balkema, Rotterdam

Sloan, S W (1988), "Lower Bound Limit Analysis Using Finite Elements and Linear Programming", *International Journal for Numerical and Analytical Methods in Geomechanics*, 12, 61-77

Sloan, S W (1989), "Upper Bound Limit Analysis Using Finite Elements and Linear Programming", *International Journal for Numerical and Analytical Methods in Geomechanics*, 13, 263-282

Sloan, S W and Assadi, A (1991), "The Stability of A Square Tunnel in A Purely Cohesive Material Whose Strength Increases Linearly With Depth", *Computer methods and advances in Geomechanics*, Eds Beer, Booker and Carter Balkema, Rotterdam

Sloan, S W, Assadi, A and Purushothaman, N (1990), "Undrained Stability of A Trapdoor", *Geotechnique*, 40, No 1, 45-62

Sloan, S W and Randolph, M F (1982), "Numerical Prediction of Collapse Loads Using Finite Element Methods", *International Journal for Numerical and Analytical Methods in Geomechanics*, 6, 47-76

Snitbhan, N and Chen, W F (1978), "Elastic-plastic Large Deformation Analysis of Soil Slopes", *Comput Struct*, 9, 567-577

Sokolovski, V V (1960), "Statics of Soil Media", Butterworth, London

Sokolovski, V V (1965), "Statics of Granular Media", Pergamon press, Oxford

Spencer, A J M (1962), "Perturbation Methods in Plasticity-III Plane Strain of Ideal Soils and Plastic Solids With Body Forces", *Journal of the Mechanics and Physics of Solids*, 10, 165-177

Tamura, T, Kobayashi, S and Sumi, T (1984), "Limit Analysis of Soil Structures by Rigid Plastic Finite Element Methods", *Soils and Foundations*, 24, No.1, 34-42

Tamura, T, Kobayashi, S and Sumi, T (1987), "Rigid-Plastic Finite Element Method for Frictional Materials", *Soils and Foundations*, 27, No 3, 1-12

Terzaghi, K (1936), "Stress Distribution in Dry and in Saturated Sand Above A Yielding Trapdoor", *Proc Int Conf on Soil Mechanics*, Cambridge, Mass , 1, 307-311

Terzaghi, K (1943), "Theoretical Soil Mechanics", John Wiley and Sons , Inc , New York, NY, 66-76

Thamm, B R , Krieger, B and Lesniewska, D (1990), "Full Scale Test of A Geotextile-Reinforced Soil Wall", *Reinforced Soil Conf Glasgow*, 1-11

Turgeman, S and Pastor, J (1982), "Limit Analysis A Linear Formulation of The Kinematic Approach for Axisymmetric Mechanic Problem", *International Journal for Numerical and Analytical Methods in Geomechanics*, 6, 109-128

Vermeer, P A and Sutjiadi, W (1985), "The Uplift Resistance of Shallow Embedded Anchors", *Proc of Eleventh Int Conf on Soil Mechanics and Foundation Engineering*, San Francisco, 3, 1635-1638

Vesic, A S (1971), "Breakout Resistance of Objects Embedded in Ocean Bottom", *Journal of Geotechnical Engineering Division*, ASCE, 96, No SM4, 1311-1334

Vesic, A (1975), "Bearing Capacity of Shallow Foundations", *Foundation Engineering Handbook* Eds Winterkorn and H Y Fang, Van Nostrand Reinhold Company Inc , New York, N Y

Vijayan, C (1981), "Finite Element Analysis of Strip and Circular Plate Anchors", Ph D thesis, *Indian Institute of Technology, Kanpur, India*

Wang, M W and Hsieh, C W (1987), "Collapse Load of Strip Footings Above Circular Void", *Journal of Geotechnical Engg.*, ASCE, 113, No.5, 511-515

Zienkiewicz, O C (1977), "The Finite Element Method", *McGraw - Hill Book Co , Inc , New York, NY*

LIST OF PUBLICATIONS

- 1 Singh, D N and Basudhar, P K , "A Note on the Optimal Lower Bound Pullout Capacity of Inclined Strip Anchor in Sand", To appear in *Canadian Geotechnical Journal* October, 1992
- 2 Singh, D N and Basudhar, P K , "Optimal Lower Bound Solution of Stability Problems in Geotechnical Engineering", Paper accepted for *OPTEC-NS 92* In Press
- 3 Singh, D N and Basudhar, P K , "Determination of the Optimal Lower Bound Bearing Capacity of Reinforced Soil Retaining Walls Using Finite Elements and Nonlinear Programming", Paper accepted for publication in *Geotextiles and Geomembranes* (1992)
- 4 Singh, D N and Basudhar, P K , "A Note on Vertical Cuts in Homogeneous Soils", Accepted for publication in *Canadian Geotechnical Journal* (1992)
- 5 Basudhar, P K and Singh, D N , "A Generalized Procedure for Predicting Optimal Lower Bound Breakout Factors of Strip Anchors", Paper reviewed and submitted to *Geotechnique* (1992)
- 6 Singh, D N and Basudhar, P K , "Effect of Mesh Pattern on the Optimal Lower Bound Bearing Capacity of Embedded Strip Footings", Communicated to *Int J for Numerical and Analytical Methods in Geomechanics* (1992)
- 7 Singh, D N and Basudhar, P K , "A Note on the Stability of A Trapdoor", Communicated to *Int J for Numerical and Analytical Methods in Geomechanics* (1992)
- 8 Singh, D N and Basudhar, P K , "Optimal Lower Bound Bearing Capacity of Strip Footings", Communicated to *Soils and Foundations* (1992)
- 9 Singh, D N and Basudhar, P K , "Lower Bound Bearing Capacity of A Strip Footing Over Underground Openings", Communicated to *Journal of Geotechnical Engineering, ASCE* (1992)

44 11-561

CE 1992-1 - IN-Low